

THE UNIVERSITY OF CALGARY

A Process Based Rainfall-Runoff Relation for a
Small Forested Mountain Watershed

by

Robert O. Hudson

A THESIS

SUBMITTED TO THE FACULTY OF GRADUATE STUDIES
IN PARTIAL FULFILLMENT OF THE REQUIREMENTS FOR THE
DEGREE OF MASTER OF SCIENCE

DEPARTMENT OF GEOGRAPHY

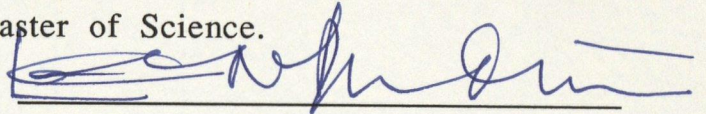
CALGARY, ALBERTA

© Robert Hudson 1986

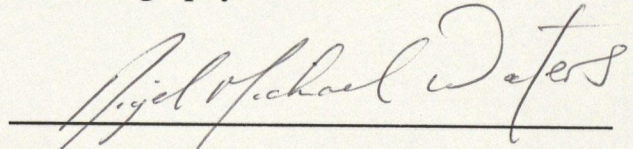
THE UNIVERSITY OF CALGARY

FACULTY OF GRADUATE STUDIES

The undersigned certify that they have read, and recommend to the Faculty of Graduate Studies for acceptance, a thesis entitled "A Process Based Rainfall-Runoff Relation for a Small Forested Mountain Watershed" submitted by Robert O. Hudson in partial fulfillment of the degree of Master of Science.



Dr. L.C. Nkemdirim, supervisor,
Geography



Dr. N.M. Waters, Geography



Dr. I. Muzik, Civil Engineering

September 18, 1986

ABSTRACT

This thesis presents a rainfall-runoff model which predicts the volume of storm runoff produced by a rainfall event in Marmot Creek Basin, a small forested mountain watershed in Southwestern Alberta. It was found that antecedent base flow, an index of antecedent soil moisture and maximum 24-hour rainfall intensity were all significant factors governing the rainfall-runoff relation. These factors were incorporated into the model. The statistical procedure of Multiple Polynomial Regression was used to develop a best fit third order model with an r^2 of over 99% and a mean error of 8.6%.

To develop the model, historical data concerning streamflow, precipitation, net radiation and groundwater were used. A site specific base flow separation method was developed to calculate storm runoff volume with some degree of accuracy. It was found that the water table tended to rise rapidly in response to rainfall. For high flow, high volume events, base flow often rose to more than 50% of the peak of the storm hydrograph. Groundwater data and information concerning infiltration, permeability and basin morphology were used to model the rising limb of the base flow hydrograph, and a base flow recession curve was used for the falling limb. An index of soil moisture was developed by adapting a site specific energy budget method for estimating evapotranspiration.

ACKNOWLEDGEMENTS

I would like to thank my supervisor, Dr. Lawrence Nkemdirim, for his assistance and direction. Without him, none of this would have been possible.

I would also like to thank the rest of the Geography department for their support, in particular, Donna and Joyce and the other ladies in the department office. Special thanks go to my good friends Pam MacQuarrie and Tim Sampson, without whom I would surely have died of a heart attack.

I am indebted to several people in both the governments of Canada and Alberta for their assistance in obtaining data and other information. They are too numerous to mention them all, however I would like to thank Zdenek Fischera and Pierre Bernier of the Canadian Forestry Service, Manfred Drews of the Atmospheric Environment Service and Joe Marciniuk of Alberta Environment, Hydrogeology Branch for the time and efforts which they devoted to my cause.

Finally, my very special thanks go to my wife Pam and my parents for their continued support and faith in my ability to see this project through to a successful conclusion.

TABLE OF CONTENTS

Title page.....	i
Approval page.....	ii
Abstract.....	iii
Acknowledgements.....	iv
List of Tables.....	vii
List of Figures.....	viii

Chapter	page
1 Introduction.....	1
1.1 Review of Literature.....	2
1.1a Theory of Runoff.....	2
1.1b Analytical Rainfall-Runoff Techniques.....	7
1.1c Empirical Models.....	9
1.1d Computer Watershed Simulators.....	10
1.2 The Current Research.....	16
2 The Study Area.....	17
2.1 Instrumentation.....	17
2.1a Precipitation.....	17
2.1b Streamflow.....	21
2.1c Snow Accumulation.....	21
2.1d Net Radiation.....	22
2.1e Temperature and Relative Humidity.....	22
2.1f Wind.....	22
2.1g Groundwater.....	22
2.2 Climate.....	22

2.3 Vegetation.....	25
2.4 Geology.....	25
2.5 Hydrology.....	29
3 Methodology.....	31
3.1 Selection of Events.....	31
3.2 Precipitation.....	35
3.3 Base Flow Separation and Storm Runoff.....	42
3.4 Estimation of Soil Moisture.....	67
3.5 Other Parameters.....	71
4 Analysis.....	75
5 Discussion and Conclusions.....	105
5.1 Discussion.....	105
5.2 Conclusions.....	108
References.....	110

LIST OF TABLES

Table	.page
2.1 Summary of Morphological Factors.....	19
3.1 Some Properties of Soils (after Beke, 1969).....	48
3.2 Some Properties of the Basin at Low and High Flow.....	50
3.3 Summary of Base Flow Time Lags.....	55
3.4 Example of Water Budget Calculation.....	72
3.5 The Data Set.....	73
4.1a Trial 2 nd Order Model of Q_V on P_V , B and S.....	78
4.1b Trial 3 rd Order Model of Q_V on P_V , B and S.....	80
4.1c Trial 3 rd Order Model of Q_V on P_V , B, S and I.....	82
4.2a Selection of Second Order Model From Optimized Data Set for	
Test of Parsimony.....	86
4.2b Selection of Third Order Model From Optimized Data Set for	
Test of Parsimony.....	87
4.2c Third Order Model.....	89
4.3a Identification of Model for $P_V > 250$	92
4.3b Model for $P_V < 250$	94
4.4a Model for $B < 0.2 \text{ m}^3 / \text{sec}$	97
4.4b Model for $B > 0.2 \text{ m}^3 / \text{sec}$	99

LIST OF FIGURES

Figure	page
1.1 Movement of Water on Slopes (after Gerrard, 1981)	4
2.1 Location Map	18
2.2 Hypsometric Curve.....	19
2.3 Instrumentation	20
2.4 Climatograph.....	27
2.5 Vegetation (after Dep't of Forestry of Canada, 1965).....	26
2.6a Surficial Geology (after Stalker, 1973).....	27
2.6b Bedrock Geology.....	28
3.1a Base Flow Recession Curve.....	33
3.1b Determining the End of Snowmelt (an example).....	34
3.2a 4-gauge Network.....	37
3.2b 8-gauge Network.....	37
3.2c 10-gauge Network (1962-65).....	38
3.2d 10-gauge Network (optimum).....	38
3.2e Gauge Network Error.....	39
3.3 Hypsometric and Gauge-elevation Curves.....	40
3.4 Mean July-August Precipitation vs Elevation.....	40
3.5 Groundwater Rating Curves.....	44
3.6 Soil Moisture Sampling Sites (after Beke, 1969) and Water Table Wells.....	46
3.7 Base Flow Separation (an example).....	54
3.8 Graphs of Stormflow Events.....	57
3.9 Graphs for Calculating E (after Storr, 1974).....	69
4.1 Residual Plot for a Trial First Order Model.....	76
4.2a Residual Plot For Table 4.1a.....	79

4.2b Residual Plot for Table 4.1b.....	81
4.2c Residual Plot for Table 4.1c.....	83
4.3 A Graph of Q_V vs I	84
4.4 Residual Plot for Table 4.2c.....	90
4.5 A Quadratic Function of P_V	91
4.6a Plots of Q_V vs P_V and Residuals for Table 4.3a.....	95
4.6b Plots of Q_V vs P_V and Residuals for Table 4.3b.....	95
4.7 A Cubic Function of B	96
4.8a Plots of Q_V vs P_V and Residuals for Table 4.4a.....	101
4.8b Plots of Q_V vs P_V and Residuals for Table 4.4b.....	101
4.9 Q_V vs $Q_{V,est}$	103

CHAPTER 1

INTRODUCTION

The objective of this thesis is to develop a rainfall-runoff relation for Marmot Creek Basin in the lower Kananaskis River Valley of Southwestern Alberta. This relation will be empirically derived using historic data and employing statistical analysis techniques. This rainfall-runoff model will incorporate some measure of antecedent basin storage.

Much research in the field of hydrology has been devoted to modeling the relationships between rainfall and runoff. The goal of such research is to improve our ability to predict the volume and timing of the runoff which is produced by a rainfall event. Rainfall-runoff models have been developed for research watersheds with a wide variety of hydrological and morphological features using various modeling techniques. Several attempts have been made to use existing simulators to predict runoff from Marmot Creek Basin, with varying degrees of success (Cheng and Nemanishen, 1974). The environment of this watershed will be discussed in chapter 2.

There are three main approaches to watershed modeling: deterministic, stochastic and parametric. The deterministic approach is based on the laws of physics. Most models of this type attempt to re-create the actual physical processes which occur within a drainage basin as runoff is being produced. If the initial conditions, boundary conditions and the characteristics of the rainfall input are specified with certainty, it is assumed that the output is known with certainty (Woolhiser, 1971). Thus, the only errors in the output are those which are due to measurement of the input variables and boundary conditions. In the stochastic approach, nothing is assumed about the physical processes which occur within the watershed. The output of the basin is usually modeled using time series analysis, which uses autocorrelation functions to specify the type and order of stochastic process inherent in a given drainage basin. This approach is generally used to generate synthetic hydrological data (DeCoursey, 1971). Since 1970, there has been a trend to

look for a physical basis behind stochastic hydrological processes (Klemes, 1973). The purpose of this research is to predict stochastic functions on the basis of basin morphology.

According to Snyder (1971), the parametric approach to watershed modeling is midway between the stochastic and deterministic approaches. It is an advance towards determinism because it involves more understanding of the physical system than stochastic modeling. On the other hand, the complexity of natural systems makes absolute determinism somewhat suspect. Hydrological models which claim to be deterministic are not capable of precise prediction, suggesting that perhaps such a model does not actually exist yet in Hydrology. The behaviour of man-made systems can be predicted exactly because they are built to meet pre-set criteria. However, natural systems defy precise definition because of their heterogeneity. Therefore, parametric modeling appears to be the most rational approach to predict runoff as a function of rainfall and other physical parameters.

Parametric modeling is defined as the "development and analysis of relationships among the hydrological and physical characteristics of the drainage area..." and utilizes "...historical hydrological data and known physical data..." (Snyder, 1971). This approach will be used to develop a rainfall-runoff model for Marmot Creek Basin.

1.1: Review of Literature

1.1a: Runoff Processes

Runoff is defined as that portion of rainfall drains away from a basin and eventually leaves the system. A large body of research has been conducted to investigate the physical mechanisms by which runoff is produced.

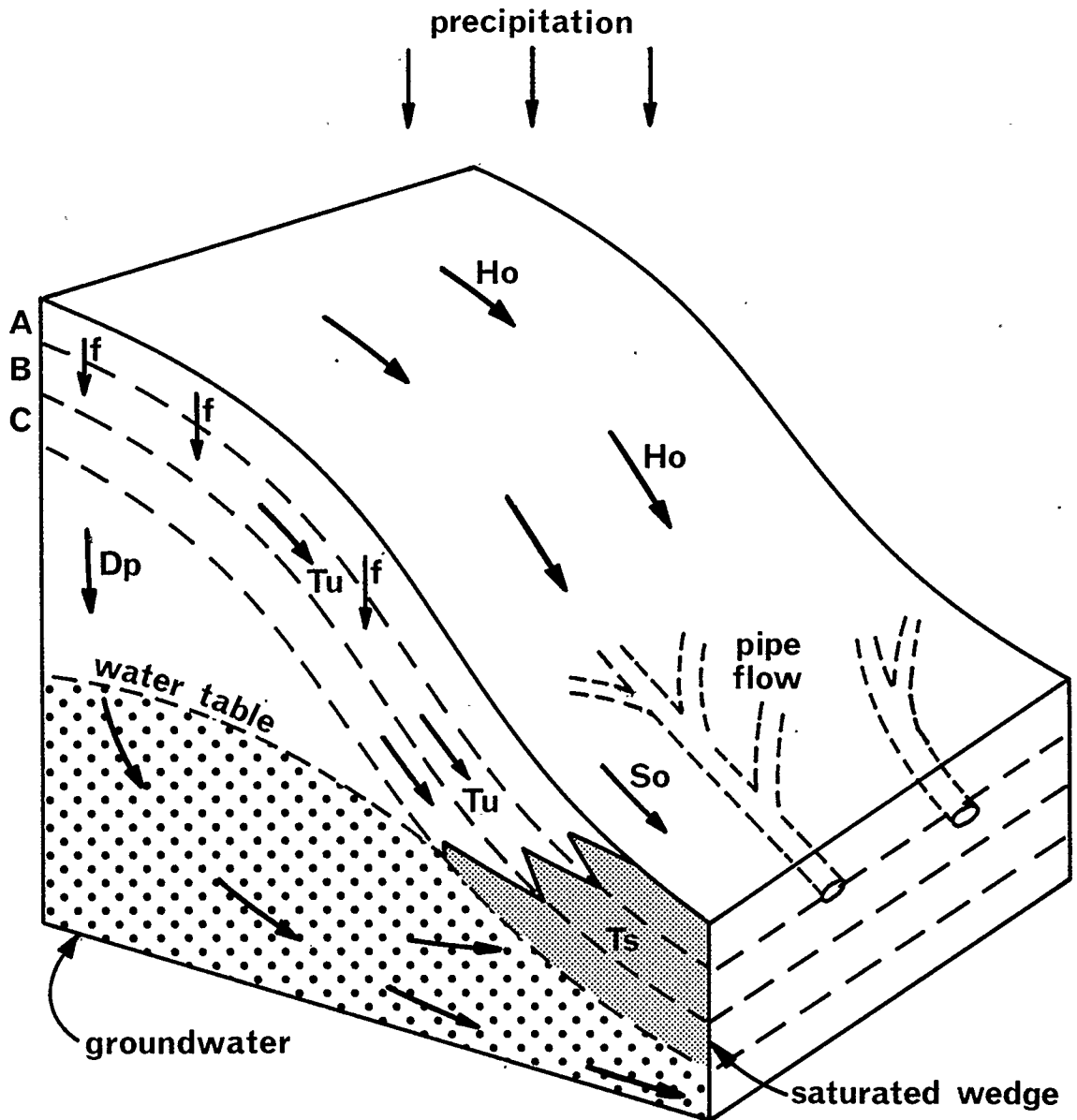
Among the earliest research on rainfall-runoff modeling was that of Horton (1933). He claimed that runoff occurred in the form of overland flow when the intensity of rainfall exceeded the infiltration capacity of the soil. Based on this assumption, average infiltration capacities for large areas were mathematically determined for runoff prediction. Essentially, this involved subtracting total runoff from total rainfall and dividing this difference by the duration of rainfall (Horton, 1937). In an attempt to refine this method, Cook (1946) identified the need to incorporate the effects of

season on the infiltration capacity. He also identified the fact that the infiltration method would be useless wherever subsurface runoff was involved. In the early 1940s, Hursh (1944) suggested that rapid subsurface flow was the primary cause of runoff from forested basins and not overland flow. A large body of research conducted mostly in the 1960s and 70s has shown that this is indeed the case not only in forested basins but also in most well managed agricultural basins.

Horton's concept has proved adequate for most engineering requirements (Bernier, 1982). Consequently it persists even today in many aspects of hydrological analysis, despite overwhelming evidence that Hortonian overland flow is a rare phenomenon in forested and agricultural basins (Hewlett and Hibbert, 1967). It is dominant only in desert, badland (Kirkby and Chorley, 1967) and artificial environments. Thus, new theory has been developed to describe storm runoff from forested upland basins.

Whipkey (1965) states that subsurface stormflow (interflow, throughflow) occurs where land is sloping, the soil surface is permeable, and where there is an impermeable horizon present in the soil and the soil is saturated. This was determined by collecting subsurface seepage from various levels in a soil pit. The percentage of water applied which appeared as seepage depended on the depth within the soil and on the antecedent condition of the soil. In coarse textured soil, water was found to percolate down to an impeding horizon and then to flow laterally along that horizon, the flow rate depending on storm depth.

Many authors refer to a saturated wedge which collects at the base of a slope during storm runoff. Saturated throughflow occurs within that wedge, and in the upslope regions, unsaturated throughflow and pipeflow occur (figure 1.1, Gerrard, 1981). Dunne and Black (1970) were able to induce saturation overland flow artificially in a basin in New England. This occurred at the base of the slope when the saturated wedge rose to intersect the soil surface. However, overland flow was not observed in natural storms even when the saturated wedge was only about one foot from the surface. Kirkby and Chorley (1967) state that overland flow occurs only in valley bottoms and adjacent to streams in forested land. Similar observations were made by Betson and Marius (1969), Weyman (1973), and Pilgrim et. al. (1978). Mosley (1979) observed that even in a high



LEGEND

- Ho Horton overland flow
- So saturated overland flow
- f infiltration
- Tu unsaturated throughflow
- Ts saturated throughflow
- Dp deep percolation

figure 1.1 Movement of Water on Slopes (after Gerrard, 1981)

precipitation basin in New Zealand where mean annual rainfall is 2610 mm, overland flow was rare and occurred only adjacent to streams.

Horton (1933) noted that in some storms, runoff may be confined to part of the catchment only. This principle has since developed into the Partial Area concept (Betson, 1964) and the Variable Source Area concept (Hewlett and Hibbert, 1967). In the Partial Area concept, the valley bottoms are the areas which supply storm runoff to the streams, and the ridge tops are recharge areas. The area in between is a transition zone which may be a source area or a recharge area depending on basin storage and storm intensity (Engman, 1974). This concept arose from the work of Betson (1964) when he attempted to use regression analysis to model storm runoff as a function of rainfall volume and duration, and soil moisture. Part of the basis for this model was the use of an infiltration model. After running the model, he found that the residuals were biased. Adjustment of the infiltration model to account for the spatial variability of infiltration capacity corrected the residual bias. Thus, the model suggested that only part of the basin was contributing storm runoff. Studying several storms, he stated that the source areas were essentially constant for all but exceptionally large storms. For those large storms, the source areas were expanded.

Engman (1981) studied an experimental watershed in Vermont which is divided into ten sub-basins. He calculated source areas within each sub-basin for all storms on record by assuming that all runoff was generated within those areas. Regressing the partial areas on five day antecedent rainfall, rainfall volume, maximum intensity and baseflow, he determined that base flow was by far the major factor in determining the extent of source areas, with an r^2 value of .653.

The Variable Source Area concept (Hewlett and Hibbert, 1967) appears to be a refinement of the Partial Area concept. The source areas are said to expand rapidly during a storm event until after the peak of rainfall, and to shrink gradually thereafter. While the source areas are expanding, the channels also expand as the capacity of the soils within the source areas to transmit water is exceeded. Stormflow was explained as resulting from translatory flow. In this process, water which was temporarily stored in the soil prior to an event is displaced downslope by the addition of new

rainfall, to appear as runoff. Water would move through the capillary pores under Darcian flow before appearing as runoff. Several more recent experiments have shown that this may not be the active mechanism involved in throughflow. Weyman (1973) measured throughflow under natural conditions in a basin with loamy soils. He states that rapid subsurface stormflow occurs as non-Darcian flow through macropores or pipes along distinct soil horizons, rather than through capillary pores. These findings are supported by Pilgrim, Huff and Steele (1978) and by Mosely (1979). Pilgrim et al used measurements of specific conductance to show that interflow consisted mostly of new water as opposed to translatory flow. Mosley used dye tracer tests to show that stormflow appeared in streams too soon to have flowed through the capillary pores of the soil, and concluded that rapid throughflow must have occurred through macropores. In both these studies, throughflow dominated the storm runoff with only a small amount of overland flow occurring near streams. Jones (1971) says that pipe networks are common in the U.K. and U.S. and are hydrologically more important than was previously thought. Pipes are most common in steep loamy soils (Gerrard, 1981).

Betson and Marius (1969) studied a steep agricultural watershed in N. Carolina. They used a network of piezometers to study the actual subsurface response to variable source areas. They found that stormflow volume was not related solely to the saturated area, but also to rainfall intensity and antecedent conditions. In studying two separate storms it was found that the storm which involved the higher hourly intensity yielded a higher runoff volume and a higher flood peak even though the saturated area was lower and overland flow did not occur. Hewlett, Forston and Cunningham (1977) considered 545 storm events on a basin in the Coweeta Hydrologic Laboratory in N. Carolina to determine the effect of storm intensity on stormflow and peak flow. Regressing stormflow volume and peak flow on rainfall, duration, initial baseflow, season and various rainfall intensities, they found intensity to be insignificant regardless of the time base over which it was assessed. Subsequently, Hewlett and Bosch (1984) studied eight basins in South Africa to determine the effects of intensity on stormflow. It was found that intensity was a significant factor in seven of the eight basins. The exceptional basin had average response factor

and stormflow volume about ten times the means of the other seven basins. (Response factor is equal to the volume of stormflow divided by the volume of precipitation, Hewlett and Hibbert, 1967). They concluded that the lower the response factor and the smaller the stormflow, the greater the effect of rainfall intensity.

From the foregoing literature, it is evident that stormflow from forested land is dominated by rapid subsurface flow which originates over a small saturated area of the drainage basin. Some of it may also flow from upland areas through macropores or pipes along relatively impermeable horizons. Antecedent basin storage either within the soil or below the water table clearly influences the volume of stormflow. The intensity of rainfall may also have an effect, depending on the hydrological characteristics of the catchment.

In sections 1.1b and 1.1c, several types of runoff models and rainfall-runoff relations are reviewed. According to the definitions given earlier, all appear to be essentially parametric in nature due to their reliance on historical data.

1.1b: Analytical Rainfall-Runoff Techniques

The unit hydrograph is a runoff model developed by Sherman (1942). It has proved quite successful for modeling flood peaks and volumes in large humid areas and is still used extensively today. The unit hydrograph of a drainage basin is defined as the storm hydrograph which results from one inch of excess rainfall of a given duration over that particular basin. Excess rainfall was defined by Horton (1933) as that rainfall which is in excess of the infiltration capacity. The Unit Hydrograph is developed by averaging the hydrographs of several such storms in the basin in question. It involves the following assumptions (Chow, 1964):

1. The excess rainfall is of uniform intensity within its specified duration.
2. The excess rainfall is of uniform spatial distribution.
3. For a given duration of excess rainfall, the time base of the runoff hydrograph is constant.
4. To reproduce the ordinates for a hydrograph of a given time base, the ordinates of the unit hydrograph of the same time base are multiplied by the total depth of direct runoff. This is the application of the principle of linearity.

5. The unit hydrograph of a basin reflects the physical characteristics of that basin.

The S curve method is used to convert the unit hydrograph of one time base to a unit hydrograph of a different time base (Bruce and Clark, 1966). Using this method unit hydrographs of any duration can be synthesized. A storm runoff event can thereby be reconstructed by dividing the rainfall into sections of uniform intensity. The corresponding hydrographs are then lagged and accumulated. Sangal (1986) has derived formulae to replace the S curve method. Despite its utility in engineering hydrology, several of the above assumptions are questionable. The term excess rainfall, while it accounts for antecedent soil moisture, is based on the principal of Horton overland flow, which has been shown to be rare in most drainage basins. The first assumption accounts for rainfall intensity, but the requirement of uniformity cannot be met under natural conditions regardless of the time base. Gupta, Wang and Waymire (1980) have questioned the assumption of linearity for small basins. The unit hydrograph does not account for the antecedent base flow, which has been shown to be an important factor for upland basins. There is a certain error involved in the generation of a unit hydrograph. In humid areas where storms usually contain more than one inch of excess rainfall, the error is reduced when the hydrograph is scaled down. In dry areas such as the prairies, storms generally contain much less than one inch of excess rainfall. In scaling the hydrographs up to one inch equivalent, the error is correspondingly increased, usually to an unacceptable level (E. Caligiuri, pers. comm.). Therefore, it is of great value to develop rainfall-runoff relations which avoid these problems.

Later, coaxial models were developed to predict storm runoff volume (Linsley, Kohler and Paulhus, 1982). These are graphical models which usually consist of four quadrants. Basin recharge is predicted as a function of quantity and duration of rainfall, the week of the year and API (antecedent precipitation index). Basin recharge is assumed to be the difference between rainfall and runoff. API is a type of water budget which assumes that evapotranspiration depletes the soil moisture by a constant percentage each day. The week of the year was introduced to adjust the API for seasonal variations in evapotranspiration. Thus, the coaxial model accounts for a seasonally adjusted index of soil moisture prior to the storm event, but does not account explicitly

for groundwater storage. Usually, a different model is developed for each drainage basin. Miller and Paulhus (1957) developed a variant of the coaxial model for a small basin, in which storm runoff is determined directly. Because basins of 15 mi² or less have low response times, the model uses hourly increments of rainfall and hourly API to predict hourly increments of storm runoff. It was suggested that the model could be applied to all small basins in the same physiographically homogeneous area.

These types of coaxial model could only deal with continuous rainfall. If attempts were made to predict runoff volume from discontinuous rainfall, the forecast would be too high because it would not account for the interception and retention losses incurred each time rainfall began. Sittner, Schauss and Monroe (1969) developed an incremental coaxial type model to deal with this problem. Because the model was to be used over fixed increments of time, the storm duration parameter was eliminated. In its place, a retention index was incorporated to account for initial losses at the start of each increment of rainfall. Essentially, the retention index is a short term API. The model yields 6-hour increments of runoff in inches which are plugged into a 6-hour unit hydrograph, thereby reconstructing the streamflow series.

Another graphical approach to calculate storm runoff was proposed by Linsley and Ackermann (1942). They developed curves to determine the quantity of water lost to soil moisture and interception/retention. The field moisture losses are a function of cumulative pan evaporation less intervening rainfall and the surface losses are expressed as a function of rainfall. The two losses are subtracted from rainfall to give runoff in inches.

1.1c: Numerical Models

Since the late 1960's there has been a shift in emphasis from graphical to numerical models due to the advent of statistical methods. Betson, Tucker and Haller (1969) converted the standard coaxial model into a pair of equations, in which the equations and contributing variables simulate the quadrants and curves of the coaxial model with slightly better results. Hewlett, Cunningham and Troendle (1977) used the R index (response factor) to predict stormflow. Non linear least squares analysis was used to generate the following equation:

$$Q_{est} = .4P^{1.5}R(1+I^{0.25})$$

R = Q/P (averaged for each basin)

P = rainfall (inches)

I = initial base flow

Eleven small basins in the eastern United States with a range of morphological factors were used. Although the variables slope and area were considered in the model, they were not significant. Thus, R is a characteristic of a particular basin which incorporates such factors as basin morphology and infiltration and I accounts for the average extent of the source areas for the storm in question.

Another type of statistical model is one developed by Bonell, Gilmour and Sinclair (1979) to model storm runoff in a tropical rainforest catchment in Australia. This is quite a different hydrological environment from any in North America with average annual rainfall of 4175 mm and high intensities. Daily rainfalls are often in excess of 250 mm. The top 10 cm of soil has very high permeability but below 20 cm, permeability is very low. Thus, during heavy rain saturation overland flow develops quickly and dominates stormflow. This means that the response time is very fast and the shape of the runoff series closely resembles that of the rainfall series. Cross correlation between the two series was used to identify the response time, which is equal to the lag position, k, in cross correlation where the correlation coefficient is optimum. Then, simple lagged regression was used. Instantaneous runoff, Q_t , was regressed on rainfall, P_{t-k} , to predict the runoff series as a simple function of the rainfall series.

1.1d: Computer Watershed Simulators

In the past two decades, a lot of research has been done to develop computer runoff simulators. These simulators attempt to recreate mathematically the physical processes which occur during a rainfall or snowmelt event. They are essentially deterministic in nature even though they are as yet imprecise. A great many such models are available, and most are in a constant state of development. The following is a discussion of some of the simulators which have been attempted or are being developed for Western Canada.

The most common simulators are of two types: the water balance or the analytical type. Some incorporate elements of both types. Each watershed model consists essentially of up to three components (Lawson, 1974):

1. A precipitation-runoff relation to predict the volume of runoff.
2. Some method to predict the shape and timing of the runoff hydrograph.
3. A technique to route the hydrograph further downstream. On some models, this is an integral part of the watershed model. Other watershed simulators consist of only the first two parts, with the routing section separate.

In the most common simulators, the precipitation-runoff relation can be either in the form of soil moisture and other indices (analytical type) or water balance computations. Many of the models divide the watershed spatially into homogeneous segments and model the response of each segment individually. The relevant hydrological and geometric parameters for each segment are then required as input into the model, as well as meteorological data. The individual responses are then combined to give total basin outflow.

Some of the water balance type models currently in use and development in Canada are the Stanford IV model (Crawford & Linsley, 1966) or variants of it, the TANK model (Sugawara et al, 1984) the UBC model (Quick & Pipes, 1974) the SACRAMENTO model (Lawson & Shiau, 1977) and the MARMOT model (Lawson, 1974). Most of these models divide the watershed into vertically distributed storage zones with a similar structure. For purposes of this description it is convenient to use four reservoirs: interception storage, upper soil storage, lower soil storage and groundwater. The reservoirs are linked to each other and to the stream by a series of transfer functions. Each reservoir has an upper limit of storage at which overflow will occur into the next reservoir, and another storage limit above which runoff will occur from that zone. These threshold values must be specified for each zone for the watershed in question. It is generally assumed that the interception storage will supply channel interception, upper soil zone will supply surface runoff, lower soil zone will supply interflow and groundwater will supply base flow. Evapotranspiration may occur from any or all of these zones. The models vary in complexity and

behaviour of the various reservoirs and transfer functions. In using simulators to model a particular watershed, the user must be familiar with the behaviour of the various models to select the one which best represents the physical system of that basin. If this is not possible, a new model must be developed.

The Stanford IV model was the first digital simulator. The model contains five storage zones including an inactive groundwater zone in addition to the four mentioned earlier. Infiltration curves govern the transfer of water to the upper zone. Water which fails to infiltrate runs off. The overland flow rate depends on surface detention storage and Manning's n . Part of the infiltrated water is diverted to lower soil storage and groundwater, the apportionment being a function of lower zone storage. Of the water which remains in the upper zone, the quantity over and above the runoff threshold goes to interflow storage, which directly governs the rate of interflow. Base flow is proportional to the groundwater storage and inflow to the active groundwater reservoir. A fixed portion of that inflow goes on to inactive groundwater which does not contribute to streamflow or evapotranspiration. Evapotranspiration from all other reservoirs is assumed to occur at the potential rate.

The basin is divided into segments of homogeneous surface features and infiltration rates. The instantaneous outflow from each segment is the sum of overland flow, interflow and base flow. The time-area histogram concept is used to reconstruct hydrographs. There is also a routing program. A drawback of the Stanford IV model is that it relies heavily on the concept of Horton overland flow. Perhaps for this reason, Cheng & Nemanishen (1974) found it to be more applicable to the plains than to upland basins. Several modified versions have appeared since the original documentation (Lawson, 1974).

The TANK model is similar in structure to the Stanford IV model but contains simpler transfer and outflow functions. Water storage zones are represented as a series of tanks stacked vertically. Each tank behaves exactly like a barrel of water with a hole in the bottom and one in the side. Water from rainfall or snowmelt enters the top tank and infiltrates to lower tanks through the bottom outlet. Evapotranspiration occurs only from the upper tank. Runoff from each tank occurs

through the side outlets. The top tank contains the soil moisture structure. The bottom outlet has a 'pipe' which raises its overflow level. This creates a dead water zone at the bottom of the tank which represents soil moisture storage. The side outlet is above that level. Whether runoff is generated from any tank depends on the height of the side outlets, the volume of water added to the system and the rate at which it is added. Outflow through any outlet at time t is assumed to be a function of the head over the outlet at time t , and each outlet has a flow coefficient which is characteristic of the basin in question. Thus, the outlet coefficients and the outlet heights become fixed parameters of a given basin. Originally, the model was calibrated by trial and error, but an automatic calibration technique is now available. This simulator has proved to be one of the most accurate, and is currently being calibrated for use by the Water Survey of Canada.

Other models have structure similar to the Stanford IV, and appear to be site or area specific modifications of existing models. The SACRAMENTO model was originally developed by the U.S. National Weather Service and the State of California (Lawson & Shiau, 1977). It uses only two subsurface storage zones of more complex structure than Stanford IV. It is a lumped rather than distributed model. The MARMOT model is a snowmelt simulator which was developed by Dr. W.T. Dickinson for the Northern Forest Research Center, Edmonton (Lawson, 1974).

The UBC model was originally developed to simulate snowmelt runoff in the Fraser River but has since been adapted for use in the South Saskatchewan River headwaters (Quick & Pipes, 1974). It is a water balance model of a different structure from those previously discussed. It is not vertically distributed, but divided into a series of homogeneous elevation bands. Certain fixed parameters are specified which relate to a basin's physiographic features. The hypsometry is required to divide the basin into bands. Historic hydrometeorological data is required to calibrate the fixed parameters, which are:

1. The constant of an elevation-precipitation relation.
2. Maximum daily percolation rate.
3. Decay constant affecting actual evapotranspiration.
4. Maximum portion of each elevation band which acts as a source area of direct runoff.

5. A decay constant for shrinkage of the source areas. These latter two parameters embody the Variable Source Area Concept.

6. Constants specifying unit hydrograph ordinates.

The basic input of the model is daily temperature and precipitation. The model uses a daily water accounting procedure for each separate elevation band. Daily water input is the sum of snowmelt and rainfall. The condition of the soil is calculated for any day based on the previous day's soil moisture and the evapotranspiration and water input for the current day. The excess water is divided between surface and subsurface runoff by a function of soil moisture. Stream flow is synthesized by separate surface and subsurface unit hydrographs. The model was used to simulate runoff at Marmot Creek. It was very good at capturing the general shape and timing of the hydrograph, but there was considerable error in estimating the peaks of individual events.

Another type of simulator is classed by Lawson (1974) as analytical. Examples of this type are the SSARR model (U.S. Army Engineer Division, 1972) and the USDAHL-74 model (Holtan et. al, 1975). The SSARR model consists of three components: a watershed model, a routing model and reservoir regulation model. The watershed component uses stored tables which represent curves of various indices, instead of using water balance computations. A daily input of water from rainfall and/or snowmelt is divided into soil moisture and runoff using a soil moisture index (SMI). A relationship between SMI and runoff as a percentage of input is used. This relationship may have rainfall intensity as a parameter. A continuous account of SMI is maintained by subtracting evapotranspiration and adding soil moisture input. The initial value of SMI must be specified before the start of the simulation. Runoff is then divided into direct runoff and base flow. A relationship between base flow infiltration index (BII) and percent of runoff to base flow is stored in the program. BII must be specified for the basin in question. Direct runoff is divided into surface and subsurface runoff by a separation curve which must be specified for a given basin. The three flow components are converted to streamflow by routing them through a specified number of storage increments using the standard routing equation. Each routing increment is treated as though it were a small reservoir.

Cheng & Nemanishen (1974) have used SSARR to simulate flows at Marmot Creek. Its success is similar to that of the UBC model, both of which are suitable for modeling upland basins. They state that the required input parameters are such that a hydrologist who is familiar with the basin can easily estimate initial trial values. However, Lawson (1974) maintains that the calibration technique is excessively time consuming and subjective.

The USDAHL-74 model relies heavily on soil and crop survey information and so would not be of use in remote areas, since there is no calibration procedure. The watershed is divided into homogeneous zones for which computations of infiltration, evapotranspiration and overland flow are made. Runoff cascades from one zone to the next until it eventually cascades into the stream. At each zone it is subject to further infiltration. Subsurface storages within each zone are classed according to soil horizons. Subsurface flows also cascade from zone to zone. Holtan, Ormsby & Fisher (1977) applied this model to a watershed in Maryland which contained a variety of land use types including extensive urbanization, agricultural land (including crop and pasture fields and golf courses) and woodlands. The basin was zoned using Landsat imagery. The resulting simulations were excellent at reproducing stormflow peaks, but grossly underestimated the low flows. This occurred because too much emphasis was placed upon overland flow, and subsurface flows were underestimated.

More recent simulation efforts have attempted to recreate the Variable Source Area Concept and its response to rainfall input. The latest in this series appears to be that of Bernier (1982). In this highly complex model, the basin is divided into segments running up slope away from the stream to the drainage divide. The side boundaries run perpendicular to the contours. As rainfall begins, the source areas are assumed to expand up the slope at right angles to the stream. Flow occurs through the upper 2 to 5 metres of soil. The soil is divided into layers, and each layer into increments such that the soil mantle is represented by a matrix of elements. A finite difference solution to a partial differential equation is used to calculate vertical and lateral flow rates through each soil element as a function of the soil moisture content of each element. Water flows from one element to the next until it reaches the stream.

This simulator is reasonably successful at capturing the general shape of the storm hydrograph in the test basin in Georgia, but requires further improvement. Because of the inherent complexity of the model, refinements may prove very costly in terms of computer time. At its current stage of development, it tends to overestimate stormflow volumes for smaller events and underestimate larger events. An attempt to apply this simulator to Marmot Creek Basin was abandoned in the early stages, because the basin was assumed to be unsuitable (Bernier, pers. comm).

1.2: The Current Research

It has been shown that stormflow volume depends on the volume of rainfall and on antecedent basin conditions, and perhaps also on rainfall intensity. It has also been shown that various regression techniques have been effective in modelling storm runoff. The author proposes to develop a model to predict the volume of storm runoff produced by a rainfall event for Marmot Creek Basin, using the historic data for that basin (Water Survey of Canada, 1962-1980). Multiple regression of an appropriate order will be used. The primary parameters which will be considered are precipitation, antecedent base flow and some index of soil moisture. Rainfall intensity will also be considered if necessary.

CHAPTER 2

STUDY AREA

Marmot Creek Basin is located in the lower Kananaskis Valley of Southwestern Alberta (figure 2.1). The 9.4 km² basin is on the west side of the valley, it is largely east facing (Water Survey of Canada, 1980) and ranges in elevation from about 1600 m at the main wier to 2814 m at the peak of Mount Allen. It occupies the subalpine-alpine zone, with 56.4% or more of the basin being alpine in character (Fischera, 1974). The basin was selected in 1962 for conducting research projects concerning the hydrology of sub-alpine forests, and in particular, to determine the effects of various timber harvesting techniques on water yield and quality.

A hypsometric curve of the basin area is given in figure 2.2. Table 2.1 contains a list of the morphological factors which contribute to the hydrology of the drainage basin.

2.1: Instrumentation

Instrumentation of the basin began in the summer of 1962. By the mid 1970's the basin was very heavily instrumented. Figure 2.3 depicts some of the instrumentation maintained at Marmot Creek Basin at that time. Because of the map scale, not all the instrumentation sites are shown with absolute accuracy. Priority is given to show the raingauge locations correctly. The meteorological boundaries on the map are not intended to demark the sub-basins. These boundaries are merely arbitrary lines used by the Canadian Forestry Service for naming the meteorological sites. In the interests of conserving space, only the instrumentation which was used in this study is shown. All information regarding instrumentation is taken from Water Survey of Canada (1980) except where indicated.

2.1a: Precipitation

Up until 1975, precipitation gauges were maintained by Atmospheric Environment Service. During the snow free period, up to 33 standard rain gauges were used to measure weekly rainfall. Some of these were also read daily. The gauge at CON 5 was read daily every summer until 1977. In some years, CON1, CON3 and CAB 5 were also read daily, but this was not done consistently.

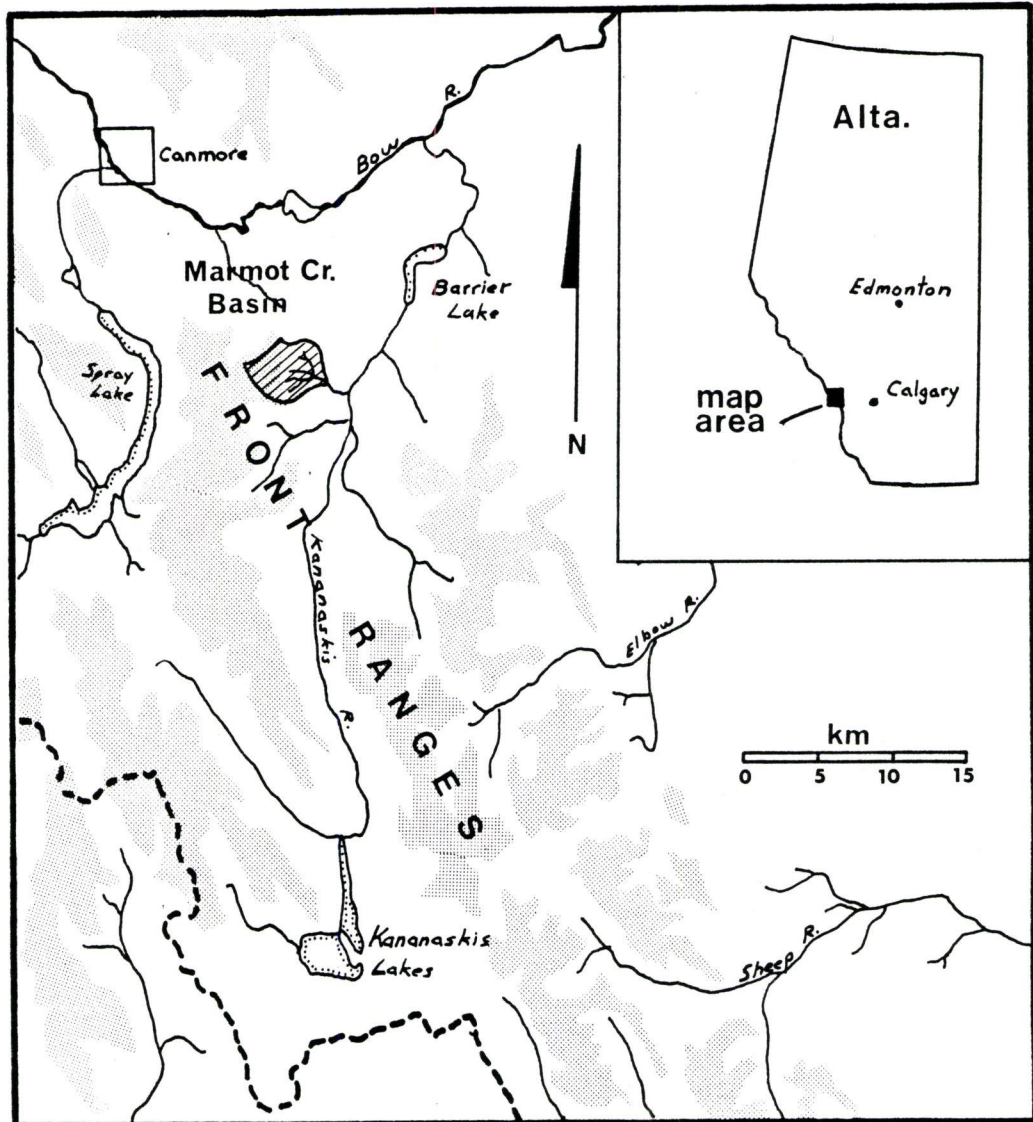


figure 2.1 Location Map

Table 2.1: Summary of Morphological Factors

Factor	Value
Basin area	9.4 km ²
Bifurcation ratio	2.71
Average drainage density	1.06 km/km ²
Average length of overland flow	508 m
Average land slope	34.6%
Average channel slope (root mean square)	17.4%
Form factor	0.34

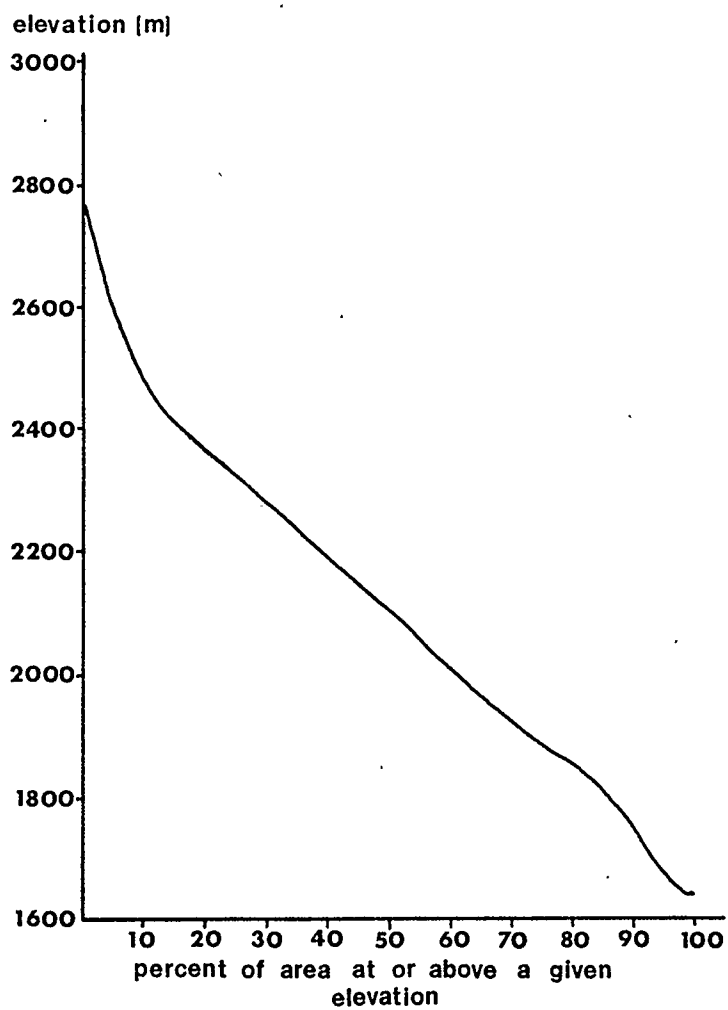


figure 2.2 Hypsometric Curve

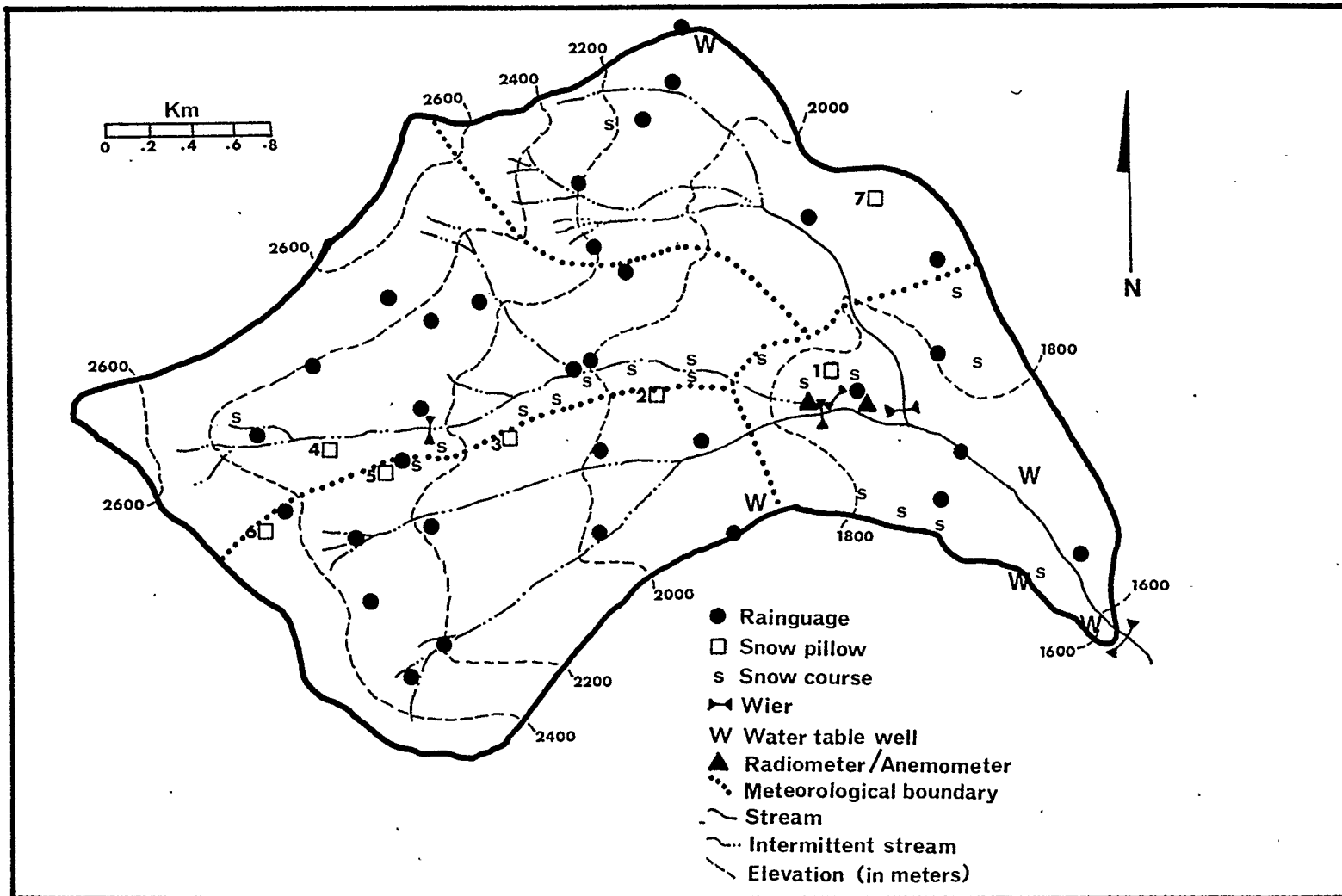


figure 2.3 Instrumentation

At some sites, Taylor and Small Orifice Gauges were also used to measure weekly rainfall. Rainfall intensity was measured by M.S.C. tipping bucket gauges at CON4, CON5 and TWIN1. Selected intensities (usually only extremes) are reported intermittently in the records. Monthly and annual precipitation has been measured using Sacramento, Leopold & Stevens and Fisher-Porter recording gauges. After 1976, A.E.S. pulled out of Marmot Creek Basin and subsequently, maintenance of all precipitation gauges was left up to Mr. Z. Fischera of the Canadian Forestry Service. Due to lack of time and manpower, most of the gauges in the upper parts of the basin were gradually abandoned or monitored irregularly. Since 1981, all precipitation measurements are taken by a network of four Fisher-Porter recording gauges at CON5, CAB5, TWIN1 and TWIN3 (Z. Fischera, pers. comm).

2.1b: Streamflow

Marmot Creek Basin is divided into sub-basins and each is gauged separately. The only stream gauge which is used here is the main wier at the basin outlet. This is a concrete, four foot head, 120 degree sharp crested V-notch wier. Continuous measurement of stage is recorded by a float actuated Stevens A-35 stage recorder. Twin and Middle Fork Creeks are gauged by 90 degree V-notch wiers, and Cabin Creek uses an H-flume. Another H-flume is used to measure the outflow from the cirque in Middle Fork Creek sub-basin.

The main wier was calibrated once after its construction. Because it is a sharp crested wier, the discharge can be calculated as a function of the head over the wier crest, which is determined from the stage.

2.1c: Snow Accumulation

Up to 22 10-point snow courses and eight snow pillows have been used to measure snow accumulation. The snow pillows are equiped with float actuated recording gauges to maintain a continuous record of snow accumulation and ablation.

2.1d: Net Radiation

A C.S.I.R.O. all-wave net radiometer was installed on an 18.3 metre mast near CON5 in May 1963. In July 1967 a similar net radiometer was installed on a 45.7 metre tower at TWIN12. The site near CON5 was discontinued in September 1967.

2.1e: Temperature and Relative Humidity

Hygrothermographs have been used to measure temperature and humidity at CON 1,2, 3, 4 and 5, CAB 1, 5, 62 and 64 and TWIN 1. Thermistors have been used to measure temperature at CON 2 and CON 5. Currently, only the sites CON 5, CAB 5 and TWIN 1 are in use.

2.1f: Wind

Wind is measured at two sites; TWIN 1 on a nine metre mast and TWIN 12 on the same mast as the net radiometer. Mean daily and peak hourly wind speeds are reported in miles per hour. Wind was measured at two other sites which have since been discontinued.

2.1g: Groundwater

Originally, a dense network of 18 water table wells and 15 piezometers was installed in the basin. Most of these were in the lower parts of the basin. After spring runoff in 1970, all but the five water wells shown in figure 2.2 were discontinued. Those five wells were fitted with monthly stage recorders and are maintained by the Alberta Research Council. The five wells were found to be representative of the hydrogeologic environment at Marmot Creek.

2.2: Climate

The climate of the Kananaskis has been described as transitional between a cordilleran and a prairie climate (Cote, 1984). This is reflected in complex temperature and precipitation regimes. Marmot Creek Basin is no exception to this.

A climatograph for Marmot Creek is given in figure 2.4. Mean monthly temperature and mean monthly precipitation are given for four representative sites. Recorded Mean annual temperature ranges from 1.6°C at CON 1 (elev. 1656 m) to -1.4°C at TWIN 1 (elev. 2287 m). Mean annual precipitation is estimated at 782 mm. This is an approximation since the records are of unequal

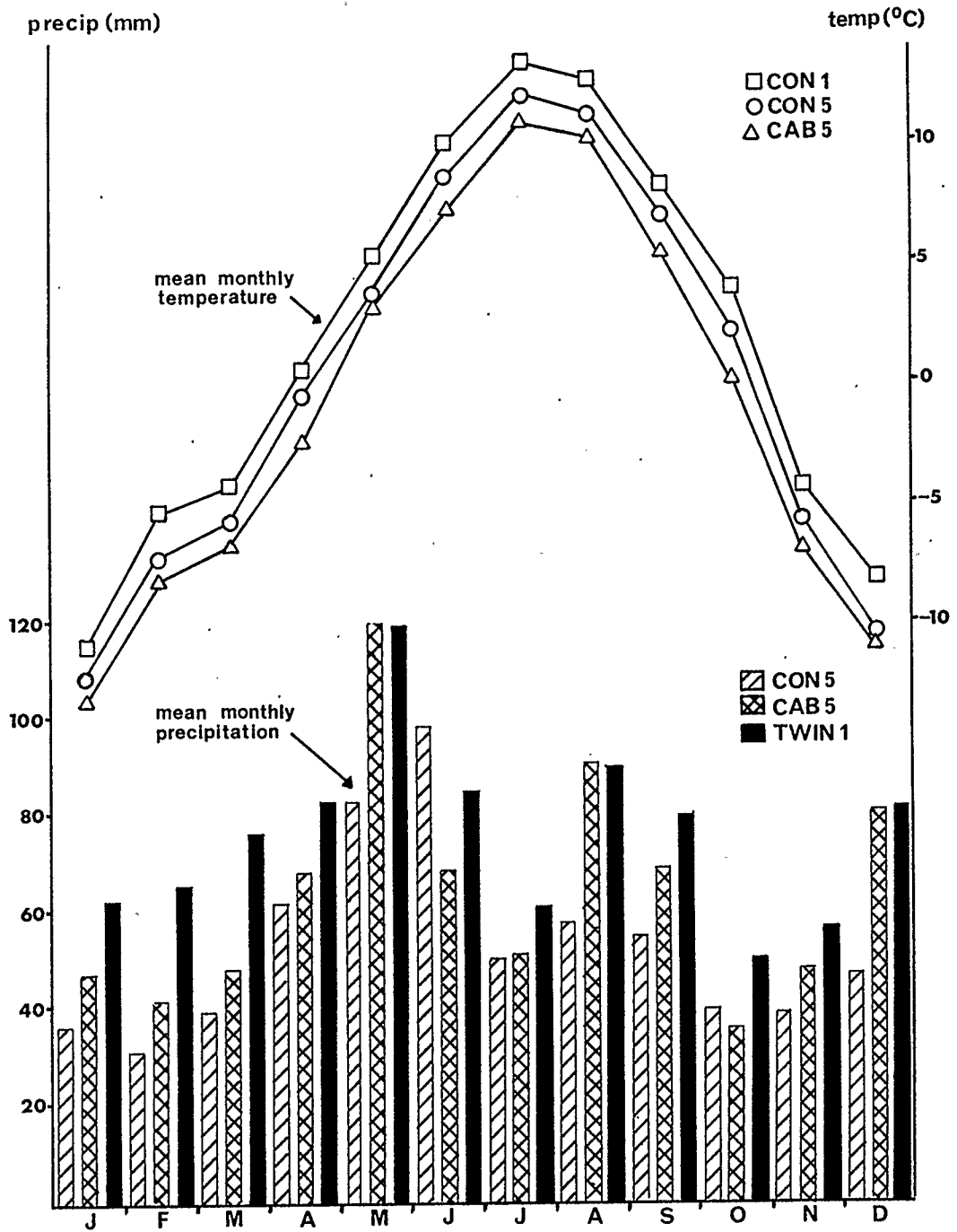


figure 2.4 Climatograph

length at the four sites that have measured annual precipitation. Annual precipitation at Marmot Creek Basin has shown a downward trend since the basin was established in 1962.

Mean annual precipitation at Marmot Creek is quite low for a mountainous region, and this can be attributed to continentality. The peak of precipitation occurs in May at higher elevations and in June at lower elevations. This peak occurs when the Mid-latitude Storm Track is located over the area. Later in the summer, rainfall is caused by convection. The dip in precipitation in July has been attributed to the heat sink of surviving snow packs in and near the basin which inhibit convection (Cote, 1984). The low precipitation months of October and November reflect the continental regime. Generally in the Kananaskis, the highest snowfall month is April, whereas for the Southern Canadian Rocky Mountains it is January. This difference is probably due to the more frequent influxes of moist Pacific air to the Kananaskis in the spring coupled with temperatures which are still low (Cote, 1984).

Chinooks are frequent in the Kananaskis and their importance is that they tend to ablate the snowpack in the winter months. Cote (1984) has given an analysis of Chinook frequency based on temperature alone, but admits that this may be misleading because of the relationship between temperature and elevation. 'Chinook days' were defined as days from December to February when maximum temperatures exceed 4°C. This definition suggested that while on the average 27 Chinook days per season were recorded at Kananaskis Research Center, only 11 were recorded at CON 5. However, another feature of Chinooks is that they are accompanied by strong dry winds, which are very effective at ablating the snow pack even if temperatures are not above 4°C.

At TWIN 1 and TWIN 12 the highest frequency of winds is westerly. However, the highest mean annual wind speeds by direction are southwesterly at speeds of about 14 and 10.5 km/h respectively, suggesting the influence of Chinooks. Wind speeds at TWIN 1 are consistently higher than at TWIN 12, reflecting the ridge top position of TWIN 1. Mean annual speeds from all directions for TWIN 1 and 12 are 12.1 and 7.7 km/h, respectively.

2.3: Vegetation

A vegetation map is given in figure 2.5. The subalpine zone extends to the forest line at about 2300 m. The lower part of the basin is occupied by a fire regeneration stand consisting mostly of *Pinus contorta* (Lodgepole pine) with some *Picea glauca* (White spruce) and *Populus tremuloides* (Aspen) each with typical associated understories. Above this a mature forest extends to the forest line consisting of *Picea glauca* with *Pinus contorta* at lower elevations and merging to *Picea engelmannii* (Engelman spruce) and *Abies lasiocarpa* (Alpine fir) at higher elevations, all with associated understory. The high subalpine zone from about 2100 m to the forest line at 2300 m elevation consists of *Larix lyalii* (Alpine larch) and *Pinus albicaulis* (Whitebark pine).

Above this is the alpine zone. Between the forest line and the tree line there is a Krumholtz forest consisting of isolated clumps of stunted trees, mostly *Larix lyalii*, interspersed with grasses and herbs. The trees get shorter with increasing altitude to the tree line. Above this is the scrub zone which consists of lichens, and mosses and herbs growing in small patches of soil.

2.4: Geology

The surficial geology of Marmot Creek Basin is described by Stalker (1973, figure 2.6a). The lower part of the basin, below 1890-1980 m elevation is covered by a thick mantle of glacial till. Starting near the junction of Cabin Creek and extending to the basin outlet, the stream bed and adjacent area contains coarse fluvial deposits of sand and gravel. Above the till zone, and extending upward in elevation for about 150 m, is a band of mass wasting debris, consisting of poorly sorted fragments of rock, sand and silt. Above this is exposed bedrock. The basin is covered with a variable soil mantle which will be discussed in a later section.

The bedrock geology (figure 2.6b) consists of shales and well cemented sandstones, and has been described in detail by Stevenson (1967). The Spray River formation underlies most of the confluence area part of Cabin Creek. It consists of dark grey, carbonaceous pyritic shales. Along the north bank of Marmot Creek in the confluence area, a cliff of brown flaggy siltstones is

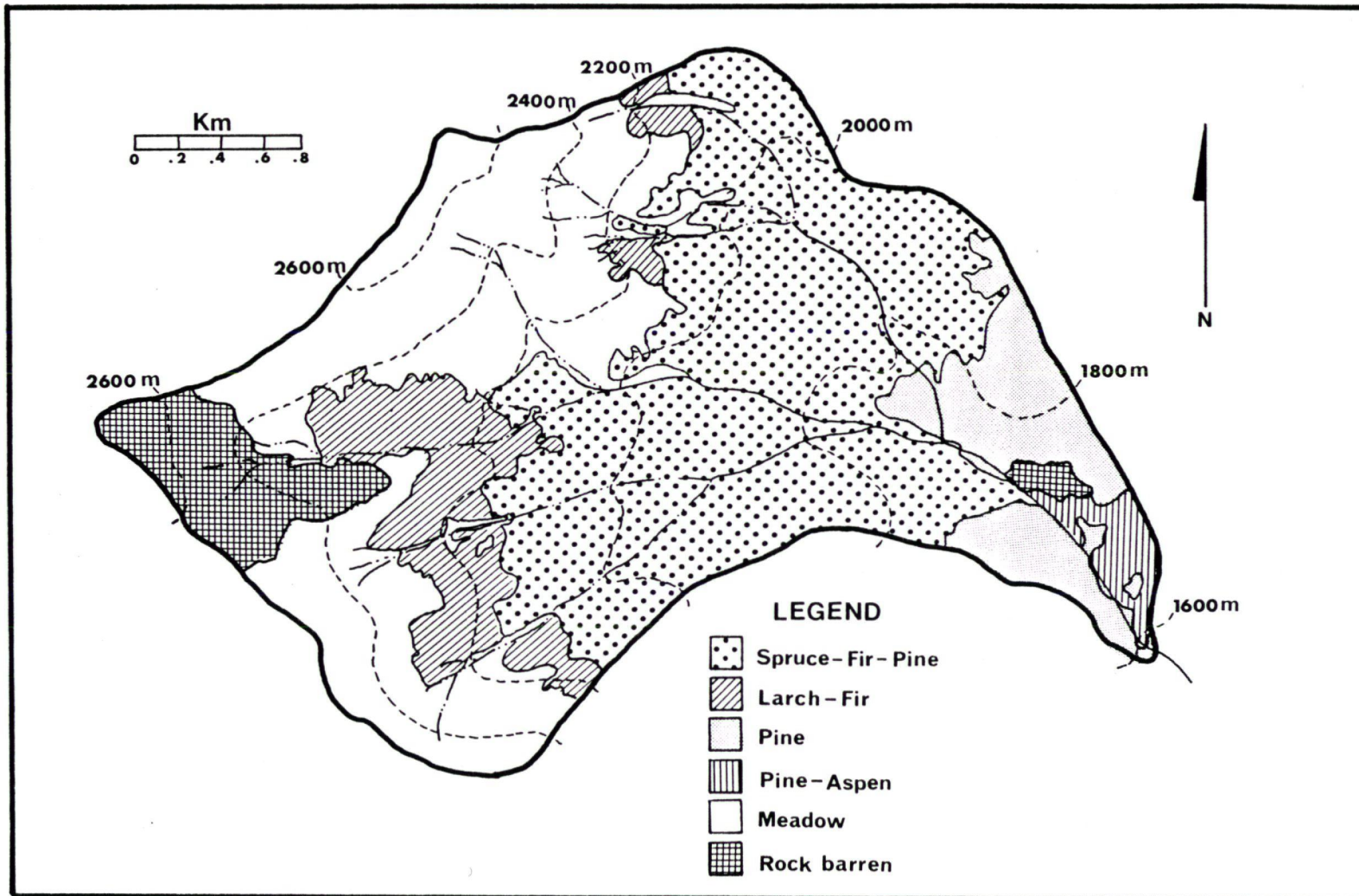


figure 2.5 Vegetation (after Dep't of Forestry of Canada, 1965)

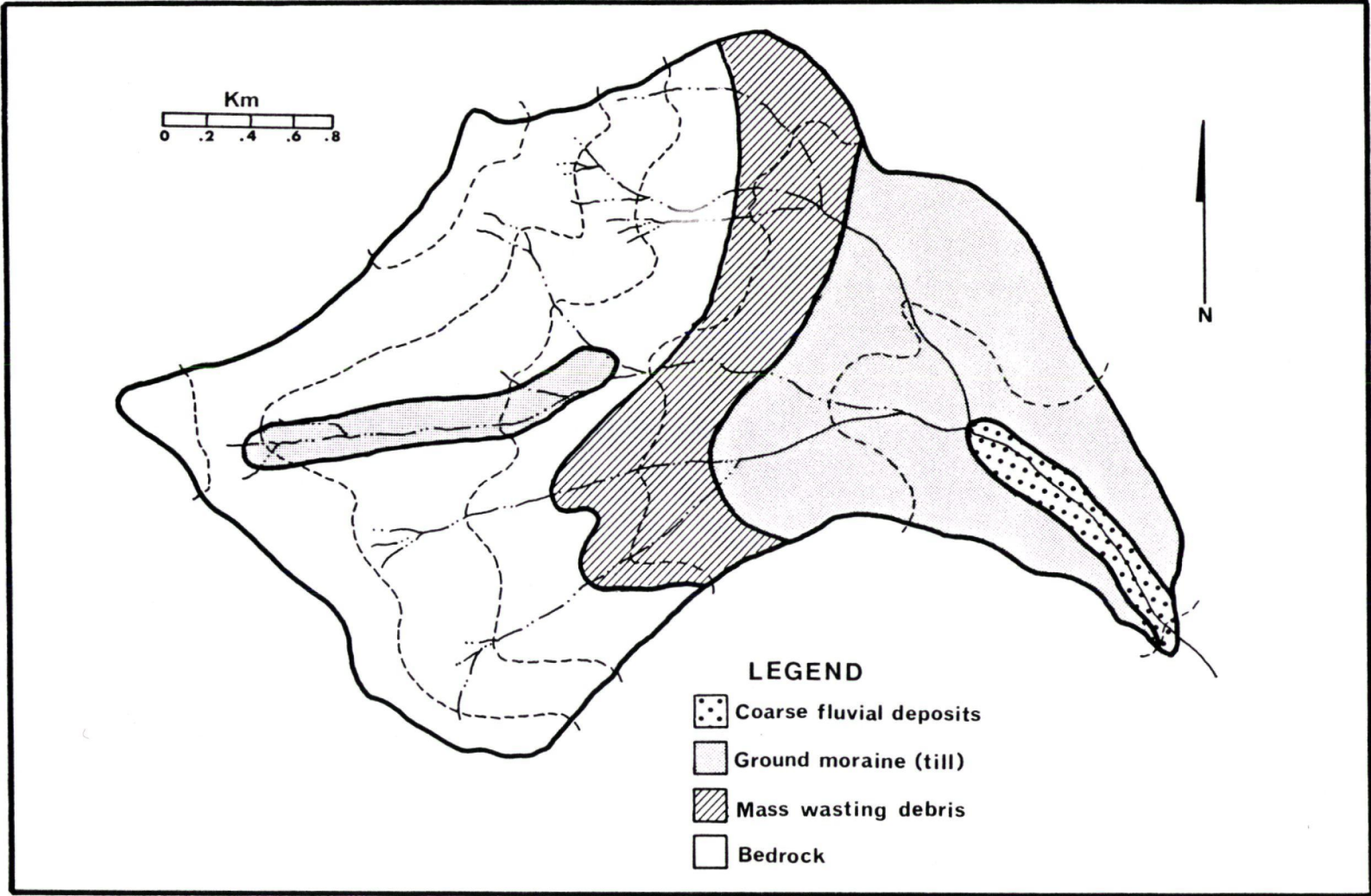


figure 2.6a Surficial Geology (after Stalker, 1973)

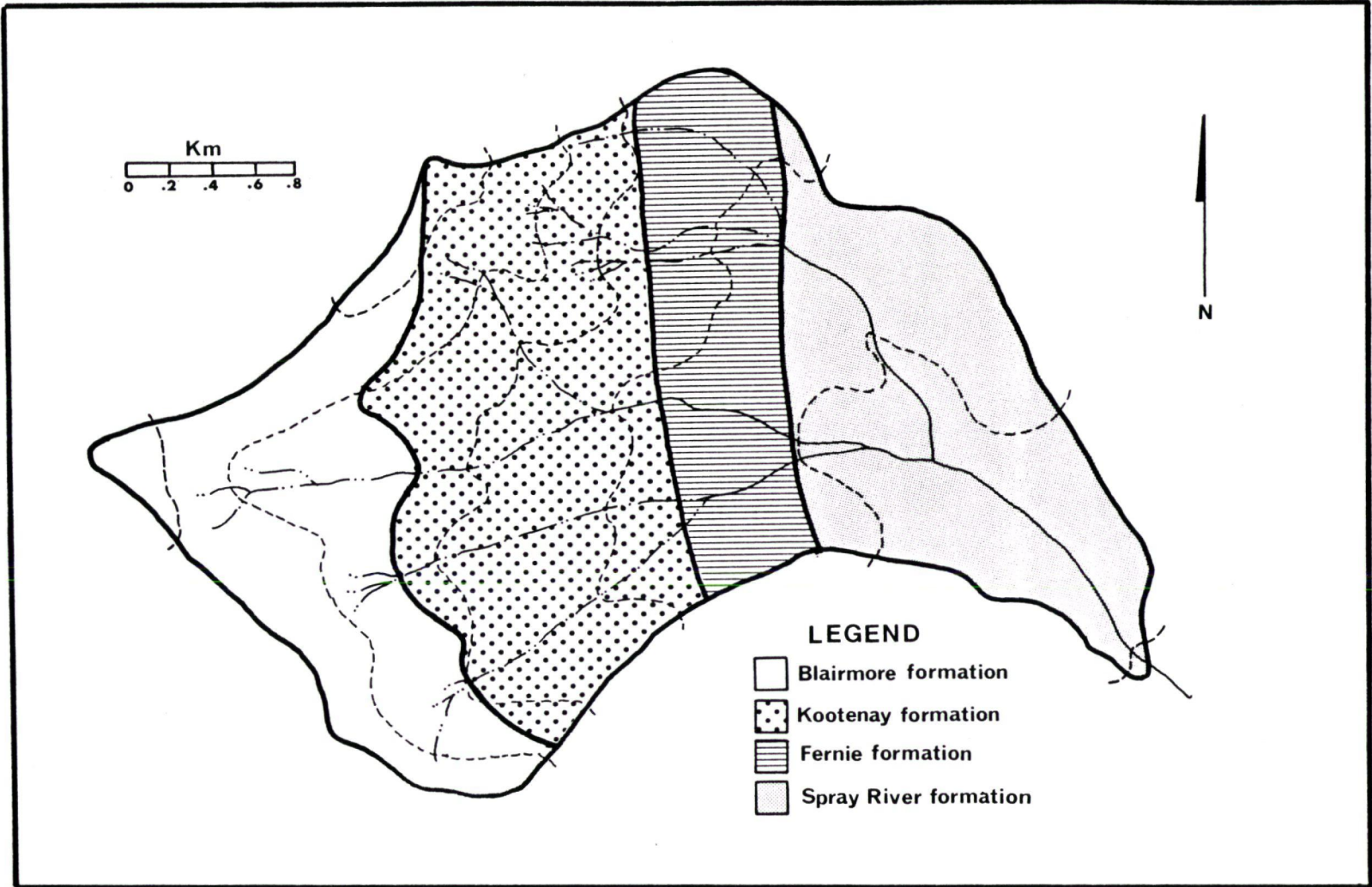


figure 2.6b Bedrock Geology

exposed. Near the outlet of the basin, the stream has cut through the Spray River formation to expose the impermeable quartzite Rocky Mountain formation.

Above the Spray River formation, around the middle of the basin is the Fernie formation. The lower part of this formation, the Rock Creek member, consists of poker chip shales. This is overlain by the Pigeon Creek member which crops out near the junction of the Cabin Creek streams, consisting of 37 m. of blocky, calcereous sandstones.

The Fernie formation is overlain by the Kootenay formation. The lower part of this is a shale-coal sequence with argillaceous sandstone beds dividing the shale beds. The upper part of this formation is a thick jointed sandstone bed which lies under most of the alpine zone. The Kootenay formation is capped by the resistant sandstone and conglomerate beds of the Blairmore formation.

There is some subsurface leakage through the sandstone beds between sub-basins, but the basin as a whole is water tight (Stevenson, 1967).

2.5 Hydrology

From 1963 to 1980, total annual flows have varied between 2447700 m³ in 1979 to 5252100 m³ in 1965. The peak of mean daily discharges occurs anywhere between the end of May and the end of June. This peak discharge has shown a wide variation between 0.46 m³/sec in 1977 and 2.18 m³/sec in 1971. The maximum instantaneous discharge on record is 2.39 m³/sec, occurring at 0400 MST on June 6, 1971.

The minimum mean daily flow in any year varies between 0.01 and 0.02 m³/sec. It normally occurs around middle to late March. However, it has been known to occur as early as December 12 and as late as April 21.

The information presented in this chapter provides some clues to the type of hydrological regime which might be expected at Marmot Creek Basin. The bifurcation ratio is below average, the average drainage density and the average channel slope are high, the average land slope is very high and the basin area is small. These factors would tend to produce high, sharp flood peaks if rainfall events are of sufficient volume and intensity. The basin has an elongated shape. As

suggested by the low form factor, this may tend to moderate the flood peak somewhat. The soils are deep and coarse, tending to promote rapid vertical and horizontal drainage. Because the basin will tend to drain quickly, it is expected that a large proportion of a rainfall event will go to basin recharge, particularly towards the end of the season. Because rainfall at Marmot Creek Basin is low for a mountainous region, large stormflow volumes and high flood peaks will likely be rare. However, given wet antecedent conditions coupled with large intense rainfall events, it is expected that the flood hydrograph will rise rapidly and have a sharp peak.

CHAPTER 3

METHODOLOGY

As was discussed in the introduction, the rainfall-runoff model will be generated to predict the volume of storm runoff resulting from individual events. Here, an event is defined as storm runoff of known duration. The duration is the interval of time during which streamflow exceeds base flow (streamflow which results from groundwater only). At Marmot Creek, such events may result either from a single storm or from several consecutive storms. Since rainfall data are given as daily totals, it is not possible to determine exactly when a storm began or when it ended. Several consecutive days of rainfall could have resulted from a single storm or from several discrete storms. Thus, some of the stormflow events will be single hydrographs and others will be composite hydrographs.

This chapter is divided into five subsections. They will deal with (a) the selection of events, (b) precipitation, (c) stormflow, (d) estimation of soil moisture and (e) other parameters.

3.1: Selection of events

Using the Hydrometeorological Record for Marmot Creek Basin (Water Survey of Canada, 1962-1980), rainfall events which appear to have produced a rise in the hydrograph of Marmot Creek at the main weir are selected. The stormflow hydrograph is the difference between the streamflow and baseflow hydrographs. The stormflow event will be expressed in terms of volume of water (in m^3) and is equal to the area under the stormflow hydrograph. The stormflow event is the product of a rainfall event which, as discussed above, is the result of one or more discrete storms.

The events so described are restricted to those produced by rainfall. Events in which snowmelt might play a role are excluded. Thus, events can only be selected during the time interval between the end of snowmelt runoff and the accumulation of new snow. This normally occurs between mid to late June and mid to late September at Marmot Creek. Since the greatest frequency and magnitude of rainfall events are received in June at Marmot Creek, it is crucial to specify the time at which the snowpack is deemed to have fully melted and snowmelt runoff

ceased. This assessment was made by using snow course and snow pillow data from the basin, and a base flow recession curve.

The first snow pillow was installed in 1969 at an elevation of 1790 m, (chapter 2). The number of snow pillows was increased to 7 by 1980, covering the range of elevations up to 2454 m. The increase in numbers assures better spatial and topographic coverage, both essential in evaluating snow and snowmelt in mountain regions. In later years it is easy to determine approximately when snowmelt ends by referring to the snow pillow data for the higher elevation snow pillows, (in particular, snow pillow #6, figure 2.3), assuming that snow at high elevations is the last to melt. In the earlier part of the record this assessment becomes somewhat more subjective. Generally, it takes about one month longer for all the snow to melt at snow pillow #6 than it takes at snow pillow #1. Although this time differential may vary from year to year depending on weather conditions, it provides a first approximation for the timing of the end of the snowmelt season during the early parts of the record. Prior to 1969 when snow pillow data were not available, the end of snowmelt season was estimated from snow course data, with a further decrease in accuracy. Since snow course measurements are made at irregular intervals averaging about one month, they can only give very rough estimates.

Following the estimation of the approximate timing of snowmelt, a base flow recession curve was prepared in order to specify the date when snowmelt runoff ceased for each year of record. The base flow recession curve is a graph of base flow vs. time. It is determined by assembling sections of the streamflow hydrograph for intervals of time, between runoff events, which do not involve precipitation. This curve is shown in figure 3.1a. It also proved to be quite useful in later phases of the methodology. The recession limb of the streamflow hydrograph is steeper than the base flow recession curve until runoff from either snowmelt or rainfall has left the basin. When runoff ends and when channel storage has left the basin, the hydrograph becomes coincident with the base flow recession curve. Thus, for each year the date of the cessation of snowmelt runoff was determined by comparing the curve to the streamflow hydrograph around the approximate timing of snowmelt (figure 3.1b).

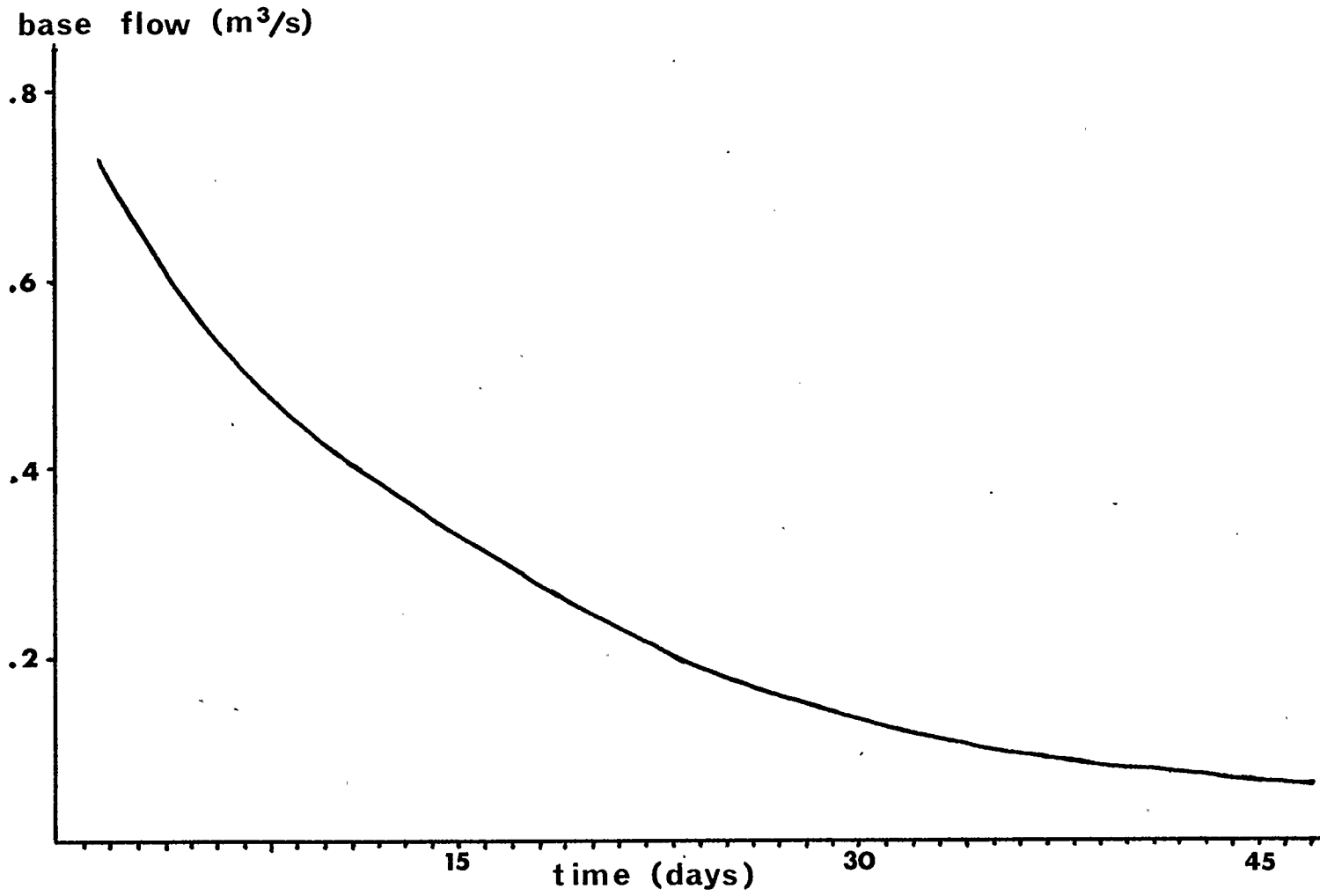


figure 3.1a Base Flow Recession Curve

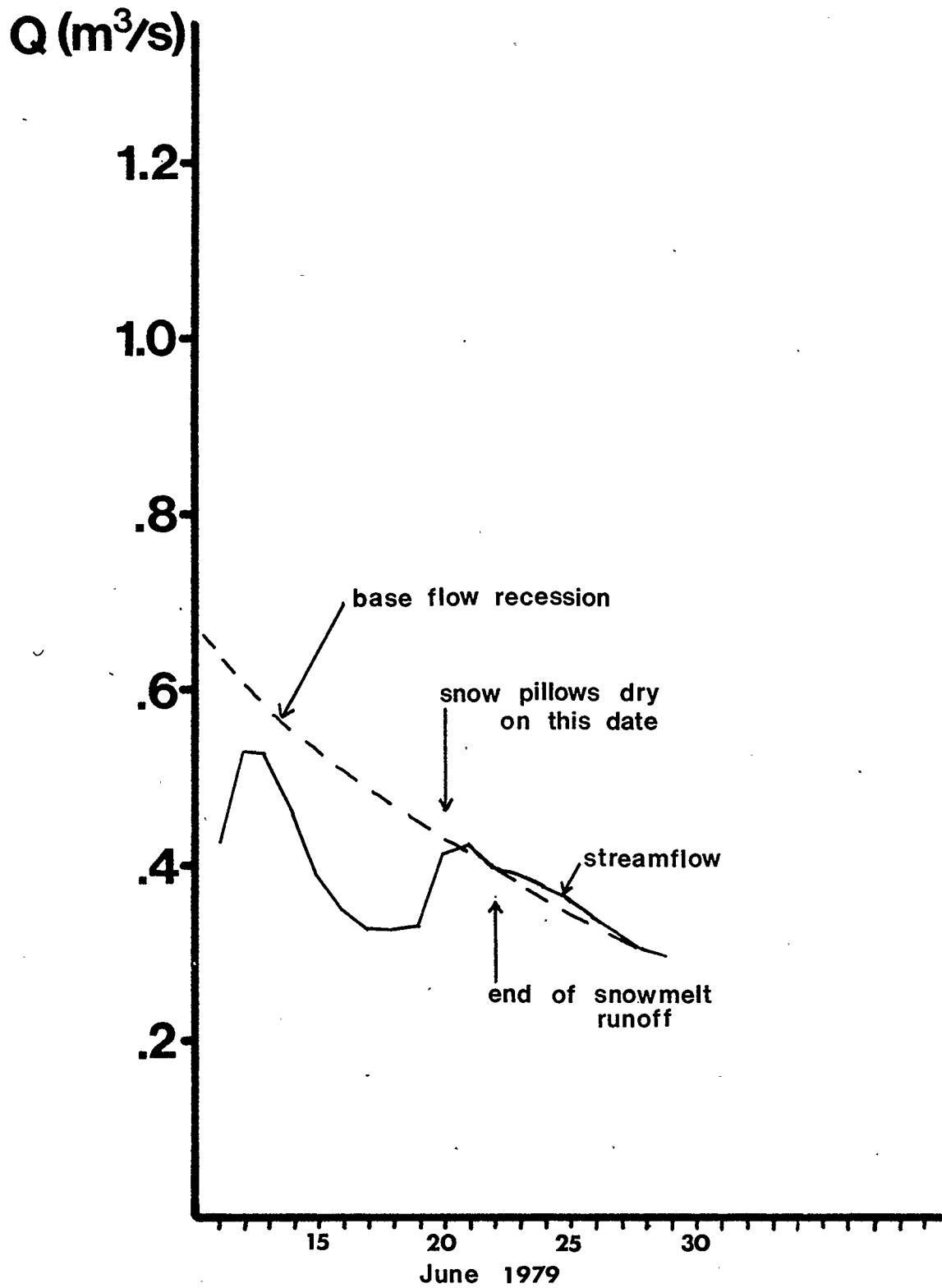


figure 3.1b Determining the End of Snowmelt (an example)

The runoff events can be divided into two groups: those which are entirely the product of rainfall, and those which involve snowmelt. The second group is divided into subgroups as follows:

1. Runoff events which begin before the end of the snowmelt season are not included in the data set. Unfortunately, many of the high volume events were eliminated on this basis.

2. Frequently, in the summer, precipitation may fall in the form of snow, particularly at higher elevations. Occasionally, if a heavy snowfall occurs, it may accumulate and persist for more than one day. An example of such an event occurred on 18-19 July 1972, and cannot be included in the data base even though it produced a significant rise on the hydrograph.

3. Events which fall under subgroup 2 occur only rarely. The summer snowfalls usually are not heavy enough to accumulate and melt as they fall from the heat conducted from the ground and ambient temperature. Events in this category are treated as rainfall.

4. Direct observation and experience (Z. Fischera, pers. comm.) revealed that even when all snow courses and snow pillows are dry, a small amount of snow remains trapped in gullies above the tree line and may take up to a month to melt completely. This was considered a normal part of the environment at Marmot Creek Basin. Events which involved this type of snowmelt were used in the data set since this remaining snow only occupies a negligible proportion of the basin, and would therefore add only a negligible quantity of melt water to a runoff event.

Having taken the above considerations into account, a preliminary list of events was produced. However, that list was later redefined in light of additional information extracted from precipitation and base flow.

3.2: Precipitation

As many as 33 rain gauges have been used to measure weekly rainfall at Marmot Creek Basin, some of which are also read daily (2.1a). Since it was felt that 33 gauges comprise an unnecessarily dense network (3.5 gauges / square km) it was necessary to select an optimum gauge network to estimate weekly basin averages of rainfall. The criteria used are as follows.

In 1971, weekly basin average precipitation was calculated using a 33 point Thiessen polygon method (Thiessen, 1911). According to Storr (1977) the raingauge elevation curve must match the hypsometric (area-elevation) curve as closely as possible to minimize the error in estimating areal rainfall (figure 3.3). In effect this amounts to selecting gauges such that there is a reasonably even distribution of gauges across the basin, and ensuring that each elevation class is properly represented wherever possible. On this basis, Thiessen polygons were constructed with densities of 0.43, 0.85 and 1.06 gauges / square km (4, 8 and 10 gauges respectively). These gauge networks are shown in figure 3.2. For each gauge density, weekly totals of precipitation throughout the 1971 season were calculated and then compared to the weekly basin averages of precipitation as given for the 33 gauge network. A graph of network error, expressed as the mean percentage deviation from the basin average using the 33 gauge network is given in figure 3.2e.

A gauge network which is too sparse will tend to undercatch considerably because the eye of the storm is often missed. A network which is unnecessarily dense might not improve the estimate of weekly basin average rainfall, because of natural variability. Figure 3.2e shows that the change in network accuracy is minimal past the 10 gauge level. Thus, the 10 gauge network is considered optimum because it is the least dense network which closely matches the 33 gauge network. Any deviation between the 10 and 33 gauge networks can be attributed to natural variability. The average deviation of weekly basin average rainfall between these two networks is 1.4%, which is negligible. The percentage deviation for individual storm totals should increase, but it is assumed that this would also be negligible.

While it is generally accepted that the isohyetal method is more accurate than the Thiessen polygon method (Linsley, kohler & Paulhus, 1982), it is usually necessary to have control gauges outside the basin to draw realistic isohyets. Since these are not available at Marmot Creek Basin, the isohyetal method would involve considerable subjectivity. Therefore, it was decided that the Thiessen polygon method would be used to calculate weekly basin averages of precipitation. Storr (1977) states that the two methods give very similar results.

Because of changes in instrumentation throughout the period of record, it was not always

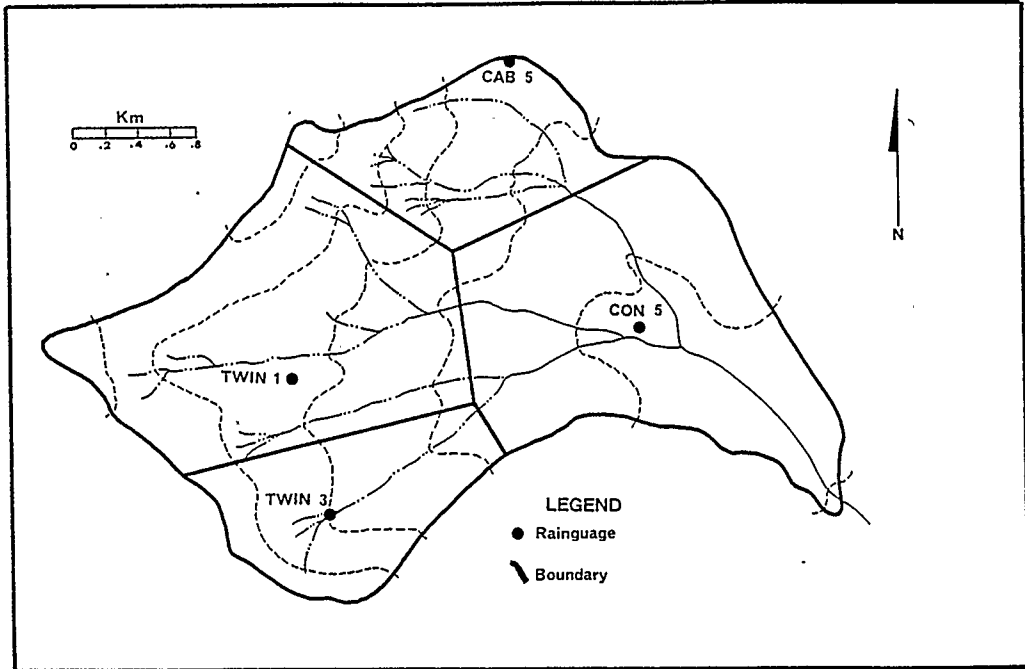


figure 3.2a 4-gauge Network

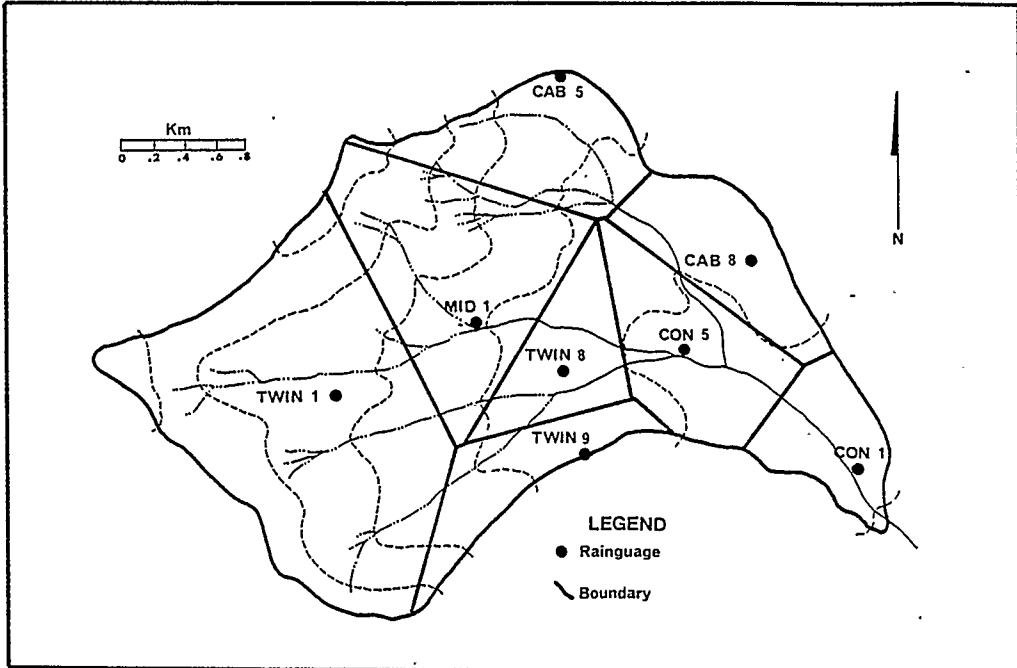


figure 3.2b 8-gauge Network

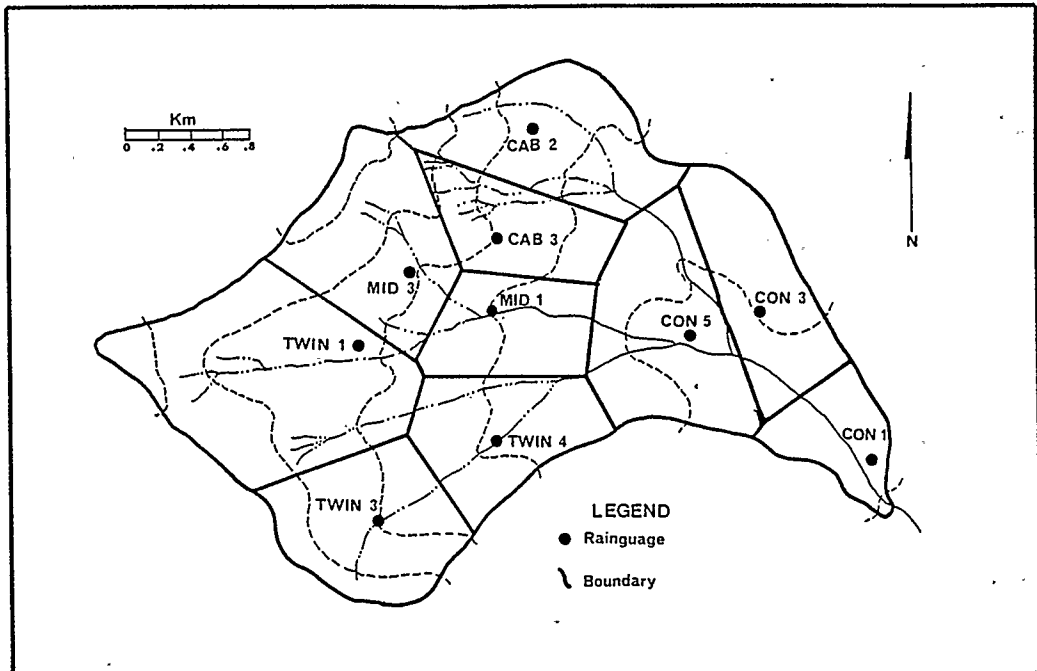


figure 3.2c 10-gauge Network (1962-65)

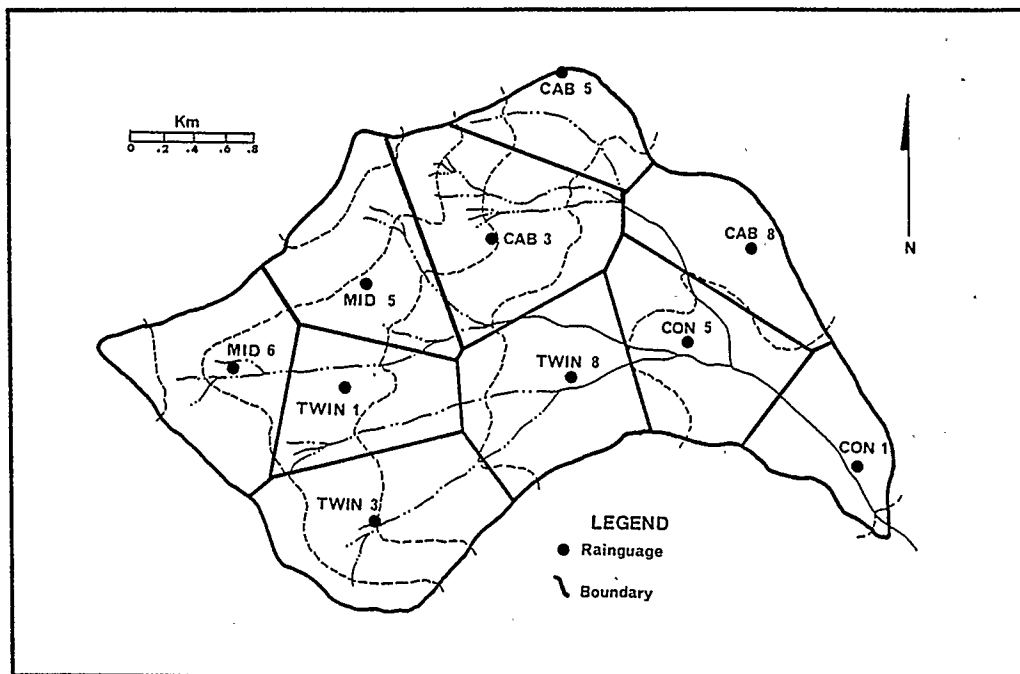


figure 3.2d 10-gauge Network (optimum)

% deviation of weekly average precip.
from that of 33 gauge network

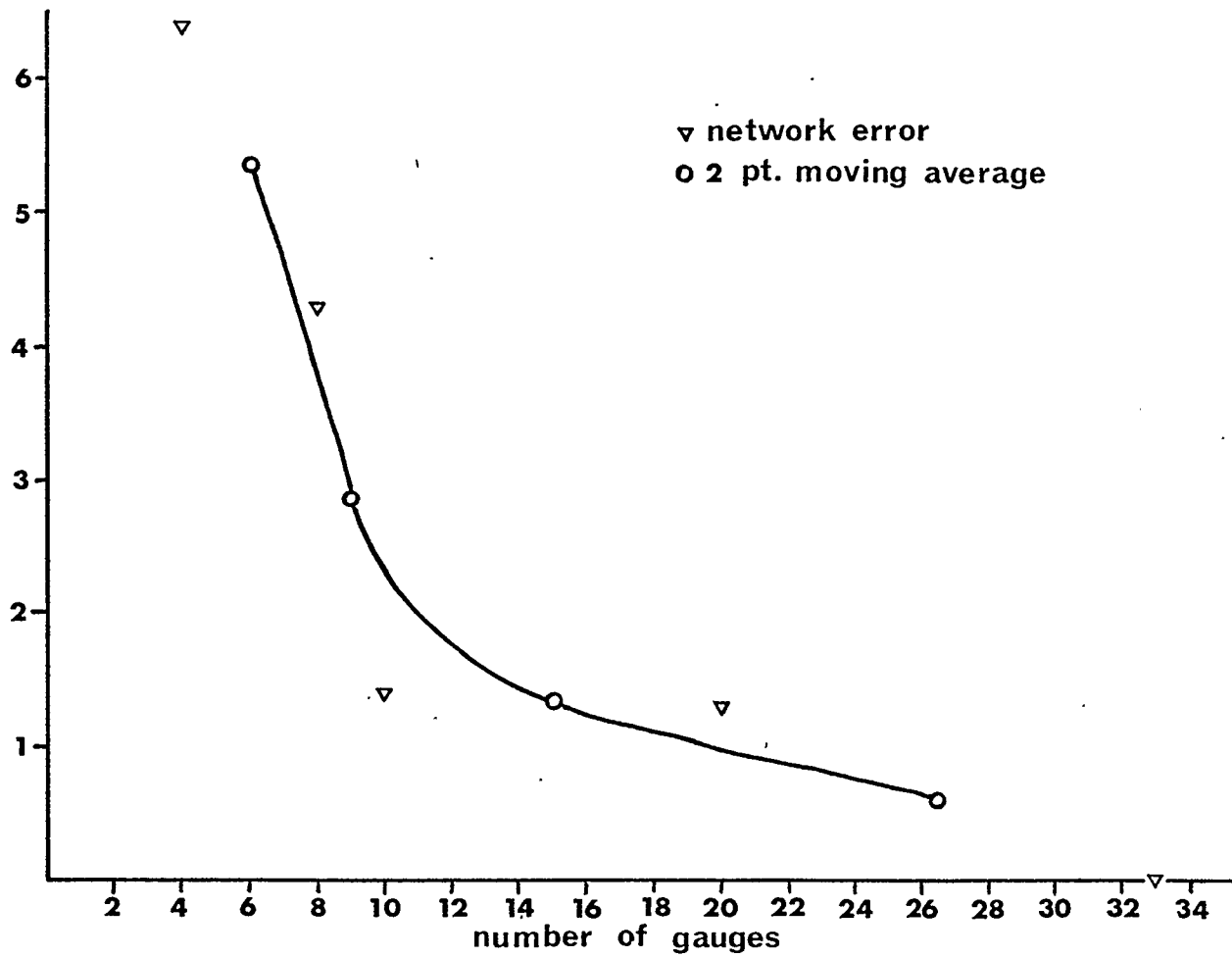


figure 3.2e Gauge Network Error

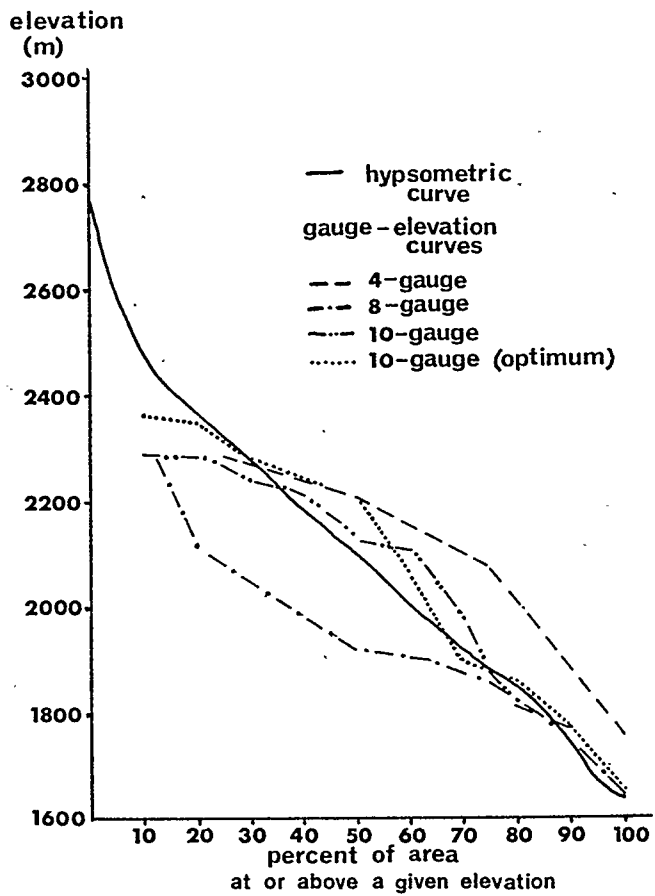


figure 3.3 Hypsometric and Gauge-elevation Curves

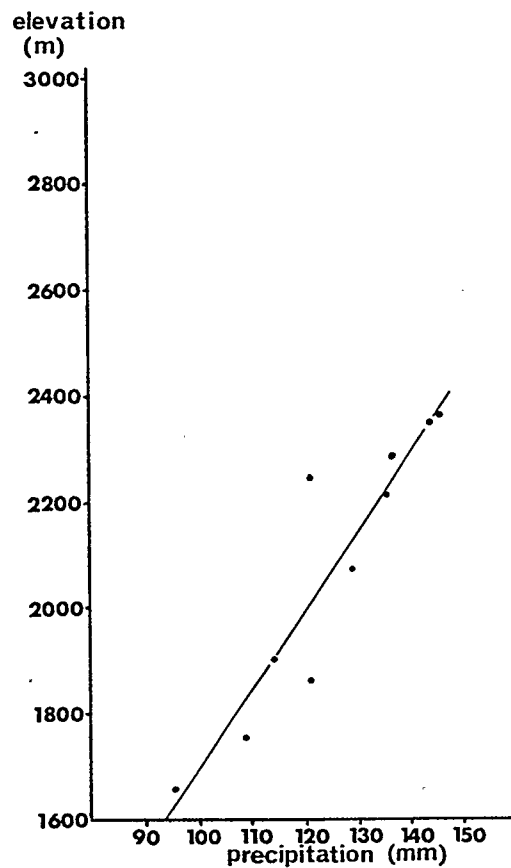


figure 3.4 Mean July-August
Precipitation vs Elevation

possible to use the optimum network shown in figure 3.2d. In order to minimize the number of changes to the network while maintaining the best possible density, three networks have been used. From 1966-1977, the 'optimum' network was used. Prior to 1966, the network as shown in figure 3.2c was used; the upper parts of the basin were more sparsely gauged than optimum, as shown in figure 3.3. After the end of the 1976 season many of the higher elevation gauges were abandoned, and many of the middle elevation gauges were monitored irregularly. For this period of record, the best possible network was found to be the 8 gauge network as shown in figure 3.2b. Note that the part of the basin above 2000m elevation (more than 55% of the basin area) is only represented by three gauges. However, rainfall generally increases with elevation (figure 3.4). Increasing the network to 10 gauges would not increase the accuracy of the basin average since the upper elevations would still be under-represented. The accuracy of the weekly basin averages depends greatly upon the accuracy of the record at TWIN 1 and MID 1 gauges; however, these are the least accurate as they were only read intermittently over periods of 1-3 weeks after 1977. Consequently, weekly values had to be estimated from the totals given. Thus, basin averages calculated after 1977 were less accurate than those calculated before that time, with an error of 4.3%.

Since discharge will be given as daily averages, it is necessary to have estimates of daily rainfall in order to judge accurately the volume of rainfall and the kinds of rainfall intensities involved in each of the storm runoff events. Of all the rain gauges in operation at Marmot Creek Basin, only CON 5 consistently gives both daily and weekly precipitation. Therefore the record at CON 5 was used to estimate daily rainfall. It was assumed that the percentage of the weekly rainfall represented by the daily rainfall at CON 5 was representative of the whole basin. In other words, it was assumed that the basin is meteorologically homogeneous. This is reasonable due to the small size of the basin. Also, CON 5 provides a good meteorological control since it is situated at the bottom of the main creek valley. Mathematically, the method can be formulated as follows. If P_i represents daily rainfall and P_w represents weekly rainfall, then:

$$p = (P_i(\text{CON 5})) / (P_w(\text{CON 5})) \quad (3.1)$$

$$P_i \text{ (average)} = p (P_w \text{ (average)}) \quad (3.2)$$

By consistently applying this method, a daily average rainfall series was synthesized to correspond to each of the storm runoff events.

There were discrepancies between the daily rainfall and the corresponding weekly totals reported at CON 5 in some of the records. Wherever possible, these discrepancies were resolved by referring to the original data sheets kept at Atmospheric Environment Service in Edmonton. However, a few events had to be discarded either because the discrepancies could not be resolved, or because precipitation was not reported.

At this point it is possible to synthesize a daily rainfall series which approximately corresponds to each storm runoff event. However, any rain which falls after storm runoff has ended cannot be included in the event. Thus, it will not be possible to specify with precision how many days of rainfall gave rise to each stormflow event until an acceptable method of base flow separation has been found.

3.3: Base Flow Separation and Storm Runoff

Base flow is defined as the streamflow which is contributed entirely by ground water; base flow occurs in a stream at times when there is no precipitation falling and no storm runoff within the basin.

There are several methods of separating base flow from a hydrograph (Linsley, Kohler & Paulhus, 1982). If a model is to be produced which accurately predicts the volume of storm runoff which results from a rainfall event, then it is crucial to the validity of that model that the base flow be represented as accurately as possible. It is therefore considered that arbitrary methods are incompatible with the purpose of this research. The methods described by Linsley, Kohler and Paulhus all involve some arbitrary element, and were developed in research basins in the Eastern United States and Europe, usually humid, and of low relief. There is no reason to suppose that such methodology can be successfully applied to a small mountainous basin in a region of low precipitation such as Marmot Creek Basin. Site specific methods should be developed wherever possible.

Since base flow is the result of groundwater entering the stream, there must be a relationship between base flow and the average elevation/depth or slope of the water table. This relationship can be established when there is no precipitation occurring and no storm runoff in the stream, as long as detailed groundwater data is available which shows the actual daily fluctuations of the water table. Using the data reported for the five water table wells operating in the basin, weighted average water table slopes and arithmetic averages of water table elevation were calculated for days which meet the above criteria. These were plotted against streamflow. While the relationship between water table slope and base flow was inconclusive, there was a good relationship between average water table elevation and baseflow. A graph of this relationship is shown in figure 3.5, and is called a groundwater rating curve. The graph was linearized with a square root transformation of base flow. Note that the slope of the line changes at a groundwater elevation of about 1767.2 m. This appears to be a characteristic of the basin, and it is not known why this should occur. Also note that after 1975, the slope of the relationship changes. The change corresponds to the cutting of 50% of the harvestable timber from Cabin Creek sub-basin, and this appears to have resulted in a generally higher water table in that area. The curves appear as a set of parallel lines; the actual intercept of the graph may change from year to year. There is apparently no physical reason why this should occur. It is believed to be due to two factors; firstly, the wells were periodically modified (Z. Fischera, pers. comm.); secondly, different government agencies were responsible for reporting the data at different times, and each reports somewhat different ground elevations for the five wells. Alternately, this could possibly be an indicator of basin leakage; however, if this is the case, the leakage only occurs in isolated years and at a non-constant rate. The variable intercept is not considered a serious problem, it just means that base flow must be used as an index of water table height during the analysis phase.

Ground water data is reported in the records up to 1976, in terms of mean geodetic elevations. The remaining data was supplied by the Groundwater Division of the Alberta Research

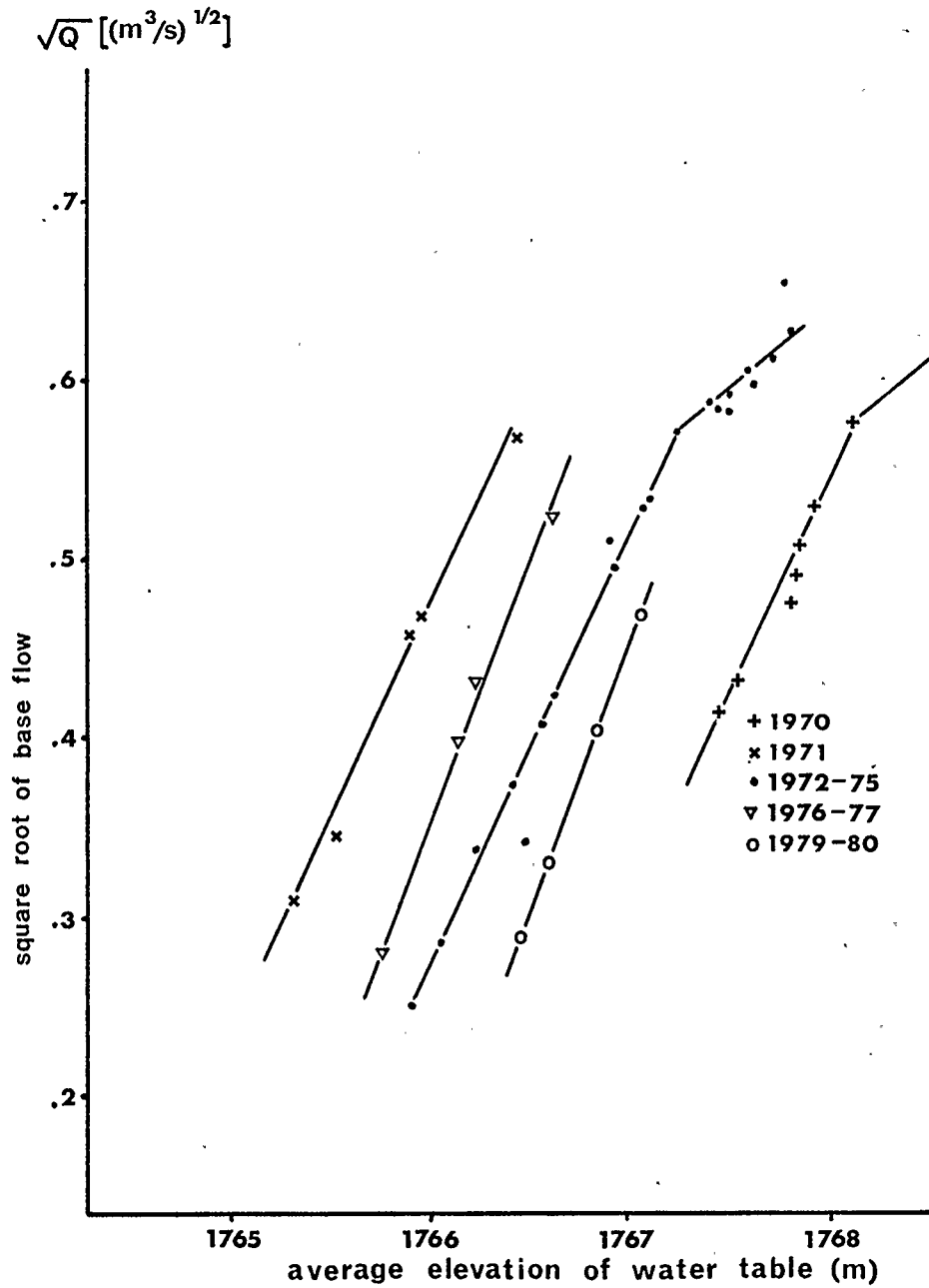


figure 3.5 Groundwater Rating Curves

Council. These data cover the period from 1975 to 1980, and is given in terms of depth below the surface. The data in the overlapping period were used to calculate the surface elevations of the wells. The location of the five wells is shown in figure 3.6 with their surface elevations.

Direct observation of groundwater data reveals that the water table rises in direct response to rainfall events. This was also noted by Stevenson (1967). The groundwater rating curve was used to verify this fact. Initially it was thought that the base flow during a storm event could be assessed by calculating the average water table elevation on each day of the event, and using the groundwater rating curve to convert these elevations to base flows. A preliminary data set was prepared for use in the early stages of analysis using this method to separate base flow. However there are two problems with this procedure. First, during some years the daily water table fluctuations were not reported; instead, indications of the general trends were given. For these years, consistent ground water rating curves could not be prepared. Second, and more important, this method failed to account for the time lags between the changes in water table elevations and the response of the stream to those changes. However, the method was useful in indicating the general characteristics of the base flow when applied to selected events.

The results of the above analysis showed that for events in which the initial base flow exceeded $0.2 \text{ m}^3/\text{sec}$ the base flow hydrograph rose generally as the streamflow hydrograph rose. The peak of the base flow hydrograph (expressed as a percentage of the streamflow peak) increased as the initial base flow increased, often exceeding 50% of that peak where rainfall volume is high. This agrees with research conducted by Sklash & Farvolden (1979) and Traynor (1981) in which oxygen isotope analysis showed that groundwater supplied up to 50% of the streamflow peak. This was expected to be the case at Marmot Creek due to the steep slopes, high drainage density, small size of the basin and the coarse textured soils (Beke, 1969, Stalker, 1973). When the initial base flow was below $0.2 \text{ m}^3/\text{sec}$, the groundwater rating curve failed to show a consistent pattern, probably due to the large time lags and the increased variability involved when the water table is low.

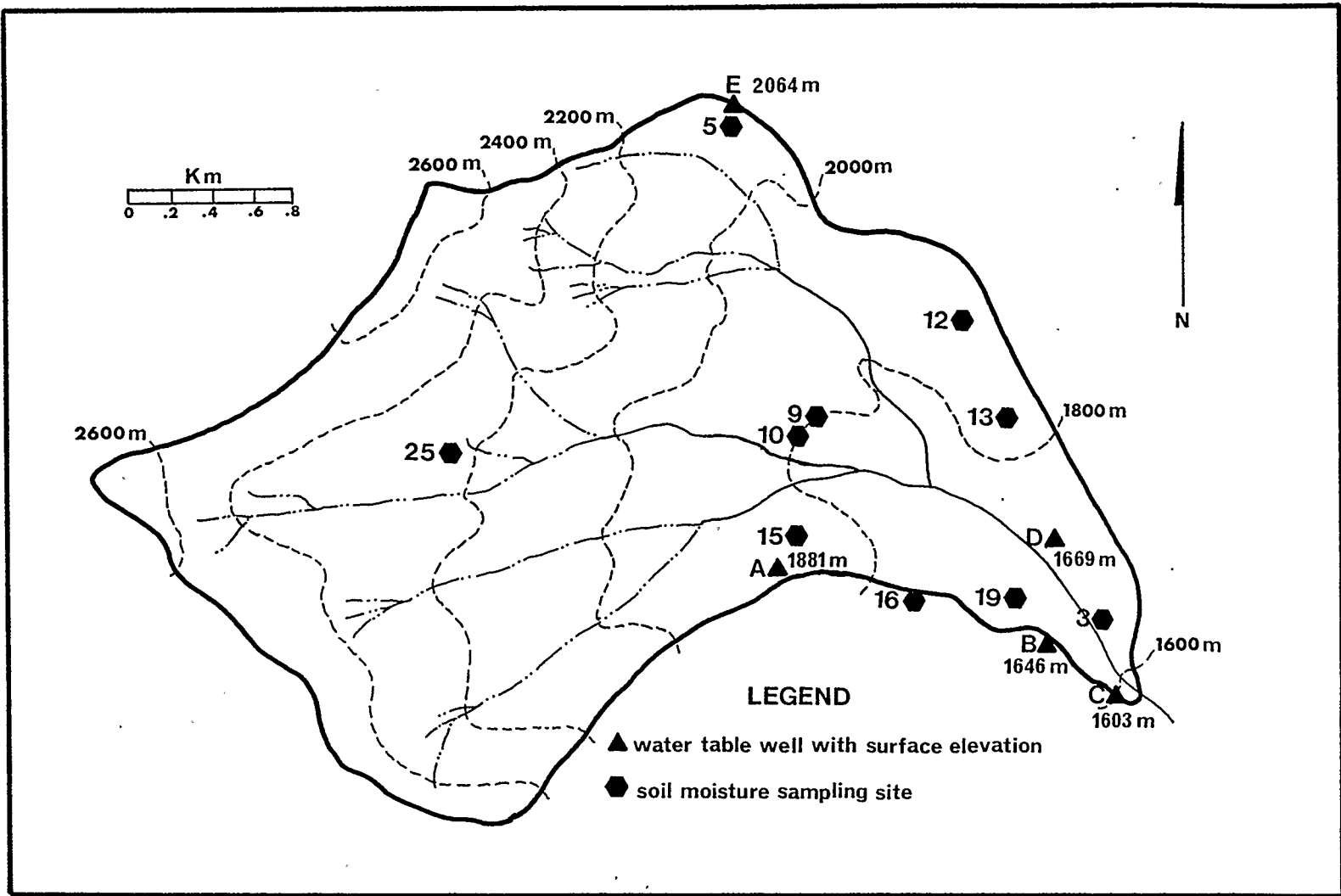


figure 3.6 Soil Moisture Sampling Sites (after Beke, 1969) and Water Table Wells

These results indicate that a method described by Linsley, Kohler & Paulhus (1949,1982) is appropriate, where the base flow recession curve is traced backwards under the streamflow hydrograph to a point some time after the streamflow peak. It is still necessary to refine that method by determining the way in which the timing of that peak and the rise of the base flow hydrograph vary according to the level of the water table.

Hewlett and Hibbert (1967), Hewlett (1982) and Bernier (1982) describe the variable source area theory, which states that only a small proportion of a drainage basin supplies direct runoff to a stream. The initial source areas are adjacent to the stream courses. They expand rapidly during the storm until the peak rainfall intensity is reached, then gradually shrink again thereafter. This is in part a function of the depth of the water table (Engman, 1981). The water table is highest adjacent to stream courses and the soil there contains the most moisture due to drainage down slope and capillary action. Therefore, these areas will supply runoff to the streams sooner than areas further away from the stream where the water table is lower. It follows that a similar effect would result from storm to storm where the initial base flow differs, the result, perhaps, of differences in average source area for each event. When rain percolates down through the soil, the water which was stored in the soil from previous events is flushed down to the water table. It is this pre-event water below the permanent water table which supplies base flow to the stream. Thus, for a situation where the water table is high, the base flow would rise, and peak, sooner than it would for a situation where the water table is low. The time lags involved are a function of the depth of the water table, the distance water must flow to reach a stream and the hydrological properties of the medium through which the water must move.

Beke (1969) presents a survey of some of the hydrological properties of the soils of Marmot Creek Basin. The relevant properties are summarized in Table 3.1. The locations of the sampling sites along with the locations of the water table wells are shown in figure 3.6. The soil sites are divided into two groups; those near permanent stream courses and those farther away from streams. The average minimum infiltration rates of each group are given. Stream courses found at elevations in excess of 2000 m are normally intermittent.

Table 3.1: Some Properties of Soils

group 1:

site	minimum infiltration rate (cm/hr)	group average (cm/hr)	depth to impeding horizon (cm)
M15	6.0		28
M19	9.0		10
M9	8.0	5.7	18
M3	4.8		10
M10	0.5		25

group 2:

site	minimum infiltration rate (cm/hr)	group average (cm/hr)	depth to impeding horizon (cm)
M25	17.8		76
M12	11.5		76
M16	7.2	11.4	25
M5	13.3		76
M13	7.0		28

(after Beke, 1969)

Let us consider two situations which approximately represent the extremes of base flow (and therefore water table level) experienced in the data set: June 18, 1970 and Aug 22, 1973. In the following discussion these will be referred to as case (a) and case (b) respectively. Several of the basin parameters and properties of the water table vary from high flow to low flow (Table 3.2).

When rain falls on a drainage basin, some is absorbed by the soil, some flows laterally through the soil to appear as runoff (interflow) and the remainder percolates down toward the water table. Horton type overland flow rarely if ever occurs at Marmot Creek Basin since maximum recorded rainfall intensities do not exceed the minimum infiltration rates except at soil site M10. Some of the water may reach an impermeable horizon eventually to appear as saturated throughflow. As interflow moves down slope towards the stream a saturated wedge begins to form at the base of the slope (Gerrard, 1981). When that wedge reaches the soil surface, saturated overland flow will occur from a small area which expands as the wedge expands (Hewlett & Hibbert, 1967). Saturated overland flow may also occur at high elevations where the soil is thin over bedrock and the slopes are very steep.

Infiltration does not equal percolation but the two are closely linked (Linsley, Kohler and Paulhus, 1982). Lee (1980) states that percolation rates limit infiltration rates since the permeability of the surface of undisturbed forest soils is always higher than the permeability of lower horizons. This is true because during the soil forming process fine materials such as clay are washed down to be deposited in a lower horizon (Gerrard, 1981). When water percolates through the upper horizon(s) and reaches a deeper horizon of lower permeability, the percolation rate will be reduced and this in turn will limit the infiltration rate at the surface. Thus, minimum infiltration rates can be used to indicate the maximum percolation rate through the soil. The actual percolation rate obviously depends on rainfall intensity; however, if the maximum percolation rate and the depth of the water table are known then the minimum time required for water to reach the water table can be calculated.

It is useful to divide both the water table wells and the soils into two groups: those near or adjacent to the perennial streams and those farther away (ie, upslope) from the streams. The two

Table 3.2: Some Properties of the Basin at Low and High Flow

	case (a)	case (b)
bifurcation ratio (B_i)	2.71	2.45
drainage density (D)	1.34 km/km ²	0.78 km/km ²
average length of overland flow (L_o)	373.3 m	642.5 m
slope of water table	0.1276	0.1260
rate of flow along w. t.	261.6 m/day	258.3 m/day
flow time along w.t. to stream (t_s)	1.4 days	2.5 days
depth of well C	16.8 cm	230.2 cm
percolation time to w.t. at valley bottom (t_b)	1.5 hours	40.4 hours
average depth of wells A, B, D and E	291.2 cm	786.4 cm
percolation time to w.t. at ridge top (t_r)	25.5 hours	69.0 hours

groups of soils are as shown in Table 3.1. The wells as shown on figure 3.6 are similarly grouped; well C is located in a lowlying area near the main wier and wells A, B, D and E are all located on ridges. As expected, the average minimum infiltration rate of soil group 1 is lower than that of group 2. This is because finer particles are washed down slope, thereby reducing the permeability of the soils in the valley bottoms. The water table is always closer to the surface at the valley bottom than on the ridges. Therefore, water will reach the water table sooner at the valley bottom despite the lower percolation rate (Table 3.2). The effect of this is to decrease the slope of the water table. Since the flow rate along the water table depends on its slope, one would expect the base flow to continue to decline while this process is occurring. However, the raising of the water table in the valley bottom will tend to moderate this effect since it is that part of the water table which feeds the stream. As a result of these two factors, the base flow will continue to decline at a reduced rate even after the streamflow hydrograph has begun to rise. When water which falls at the top of the slope has percolated to the water table, the slope of the water table will begin to increase again. At this time, base flow will begin to rise.

The following formulae can be used to calculate the time taken for water to percolate to the water table. The time, in discrete units, is a function of the average minimum infiltration rate and the depth of the water table at that point in time:

$$t_b = d_b / I_1 \quad (3.3)$$

where t_b = time to water table at the base of the slope (hours)

I_1 = average min. infiltration rate of soil group 1 (cm/hr)

d_b = depth of water table at the valley bottom (cm)

$$\text{and } t_r = d_r / I_2 \quad (3.4)$$

where t_r = time to water table at the top of the slope (hours)

I_2 = average min. infiltration rate of soil group 2 (cm/hr)

d_r = average depth of the water table at the ridge tops (cm)

The values of t_r and t_b have been calculated for case (a) and case (b) for the ridge tops and valley bottoms and are summarized in Table 3.2. The value of d_b is obtained from well C and d_r

from the average of wells A, B, D and E. Since streamflow is given in terms of daily averages, it is appropriate to express time lags in terms of days also.

To summarize, base flow will decline until time t_b after streamflow has begun to rise. After this, base flow will decline at a reduced rate until time t_r , and then it will start to rise. The magnitudes of the time lags depend on the base flow prior to the stormflow event. Since water which percolates to the water table is supplied by gravity, it is assumed that the soil above the water table should be above field capacity during percolation. Therefore if rainfall continues, water will be displaced rapidly downwards to the water table. Since the percolation rate is greater at the ridge tops than at the valley bottoms, the slope of the water table will continue to increase as its average elevation rises. Thus, groundwater and hence, base flow, will rise until the critical rainfall intensity has ended. Because it takes time for water to flow along the water table to the nearest stream course, there will be a time lag between the end of intense rainfall and the peak of the base flow hydrograph. This can be calculated using the following formula (Linsley and Franzini, 1979) which gives the actual flow rate of water through a permeable medium:

$$v = \frac{ks}{p} \quad (3.5)$$

where v = flow rate in m/day,

k = permeability in $m^3/day/m^2$,

s = slope of the water table, and

p = porosity.

The soils of Marmot Creek Basin consist entirely of tills (Beke, 1969 and Stalker, 1973). Furthermore, it is shown that even in case (a), the water table exists almost entirely below the level of any impeding horizons (Tables 3.1 and 3.2). Since tills consist mostly of angular pieces of gravel and coarse to medium sand, it can be assumed that its average hydraulic properties are similar to those of gravel and sand. Linsley, Kohler & Paulhus (1982) give typical values of permeability and porosity for gravel and sand as $410 m^3/day/m^2$ and 0.2, respectively. Using equation (3.5), flow rates along the water table were calculated for case(a) and case(b) (Table 3.2).

The following formula gives the average time it takes water flowing along the water table to reach a stream course:

$$t_s = L_o / v \quad (3.6)$$

where t_s = time to a stream course (days), and

L_o = average length of overland flow (m).

This is an approximation, but a good one since the distance along the water table must be very close in value to L_o . Since the drainage density varies between high and low flow, L_o also varies because it is a function of drainage density. Using equation (3.6) values of t_s are calculated and are given in Table 3.2. The water table is in a constant state of flux, and base flow consists of pre-event water. Once peak rainfall intensity has passed, base flow will begin to subside again since it is assumed that all pre-event water has been flushed down to the water table. It is therefore assumed that the time lag t_s is numerically equal to the time lag between the end of peak rainfall intensity and the peak of the base flow hydrograph. This will be termed t_p . It is also appropriate to give these values in terms of days. The time lags t_b , t_r and t_p are summarized in Table 3.3. The base flow is broken up into three classes which can be thought of as high, middle and low flows. To give time lags for the middle flow class it was assumed that they would be mid way between those for the high and low flow classes.

These time lags facilitate the systematic separation of base flow. Base flow recession is extended to a point t_r days after the streamflow hydrograph began to rise. For middle and high flows, the end of storm runoff occurs when the base flow recession curve and the streamflow hydrograph coincide and the recession curve is extended back under the hydrograph to a point t_p days after the end of intense rainfall. The values of t_r and t_p depend on the base flow which existed immediately before storm runoff began. An example of the separation of base flow is shown in figure 3.7. For simplicity, the rising limb of the base flow hydrograph is assumed to be a straight line, except for situations when a storm of high volume and intensity occurs while the base flow is rising. For this type of event, it is assumed that the slope of the base flow rising limb increases at the time of that storm.

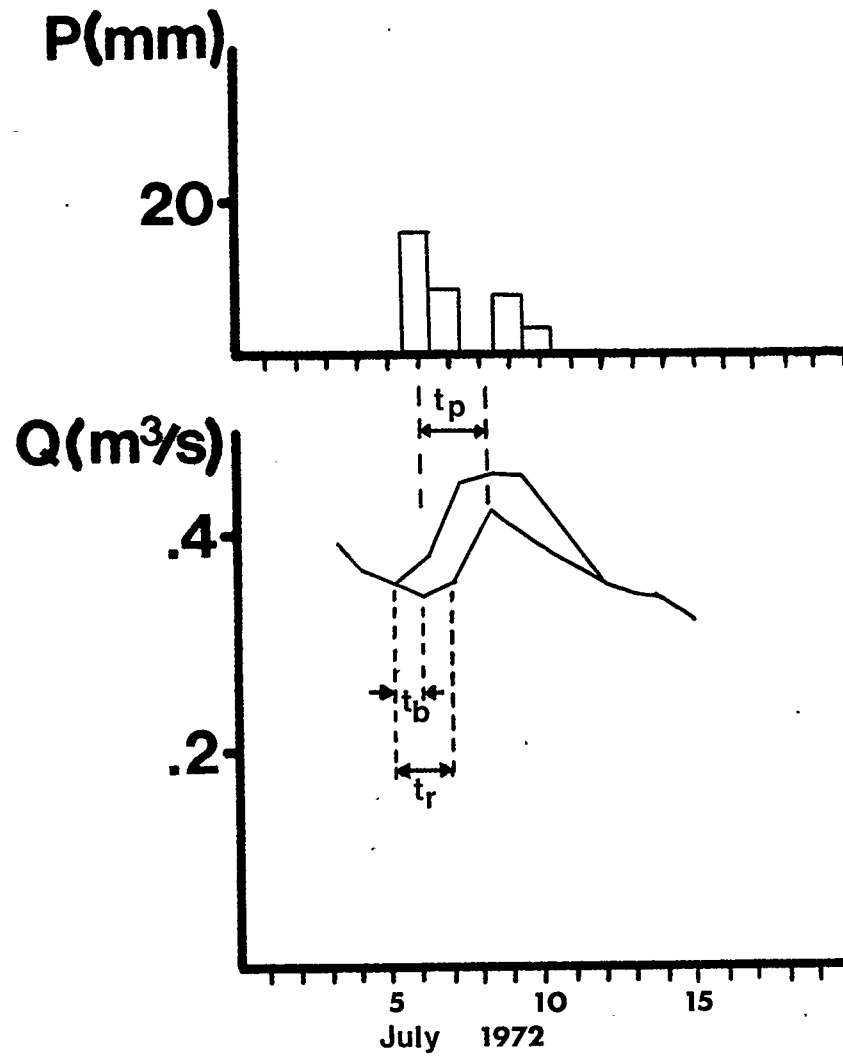


figure 3.7 Base Flow Separation (an example)

During a low flow situation where the initial base flow is below $0.2 \text{ m}^3/\text{sec}$ the falling limb of the streamflow hydrograph is usually the same as the base flow recession curve after the peak of base flow, and sometimes it is even of a smaller slope. Thus, at low flow the recession curve is not actually extended back under the hydrograph, but the base flow rises to peak at a point on the falling limb of the hydrograph. Also note that the time lags t_b and t_r are based on minimum infiltration rates. At low flows, rainfall is usually of low volume and of an intensity much less than the infiltration rate. Since infiltration is governed partly by rainfall intensity, it is often necessary to extend the time lags t_b and t_r by one or even two days. While the author has attempted to make the separation method as objective as possible, it is still necessary to exercise a certain amount of judgement in applying the procedure.

Table 3.3: Summary of Base Flow Time Lags

Base flow range	t_b	t_r	t_p
0.4 - 0.6 m^3/sec	0 day	1 day	1 day
0.2 - 0.399 m^3/sec	1 day	2 days	2 days
0.0 - 0.199 m^3/sec	2 days	3 days	3 days

t_b = time between rise of streamflow hydrograph and decrease in base flow recession.

t_r = time between rise of streamflow hydrograph and rise of base flow hydrograph.

t_p = time between peak rainfall and peak of base flow hydrograph.

At low flow and adjacent to stream courses it is difficult to distinguish storm flow from groundwater flow on a conceptual basis. The separation method which is described above assumes that true base flow is derived from pre-event water which flows along the water table from a higher elevation, and is distinct from the saturated wedge which forms at the base of the slope as a result of interflow, as described by Gerrard (1981), (figure 1.1).

The above separation technique has been applied to each event. The complete set of events is shown graphically in figure 3.8. Since both streamflow and base flow are expressed in terms of average daily discharge, it is appropriate to calculate the daily averages of storm runoff by taking the difference between the average streamflow and average base flow for that day in m^3/sec and multiplying by 86400 seconds/day. Mathematically the total stormflow volume for each event can be expressed as follows:

$$Q_v = 86400 \sum^n (q_i - B_i) \quad (3.7)$$

where Q_v = storm runoff volume in m^3 ,

q_i = average discharge, day i in m^3/sec ,

B_i = average base flow, day i in m^3/sec , and

n = time base of event in days.

Now that the time base of each event is known, the number of days of rainfall which resulted in each event is also known. It is now convenient to give the total rainfall volume of each event. Daily rainfall is given as an average depth over the basin in mm. This can be converted to a volume by multiplying by the area of the basin:

$$\text{Basin area} = 9.4 \text{ km}^2 = 9.4 \times 10^6 \text{ m}^2$$

$$\text{One mm of rain} = 10^{-3} \text{ m.}$$

Therefore, one mm of rain over the basin contains 9400 m^3 of water. Total rainfall for each event is given as:

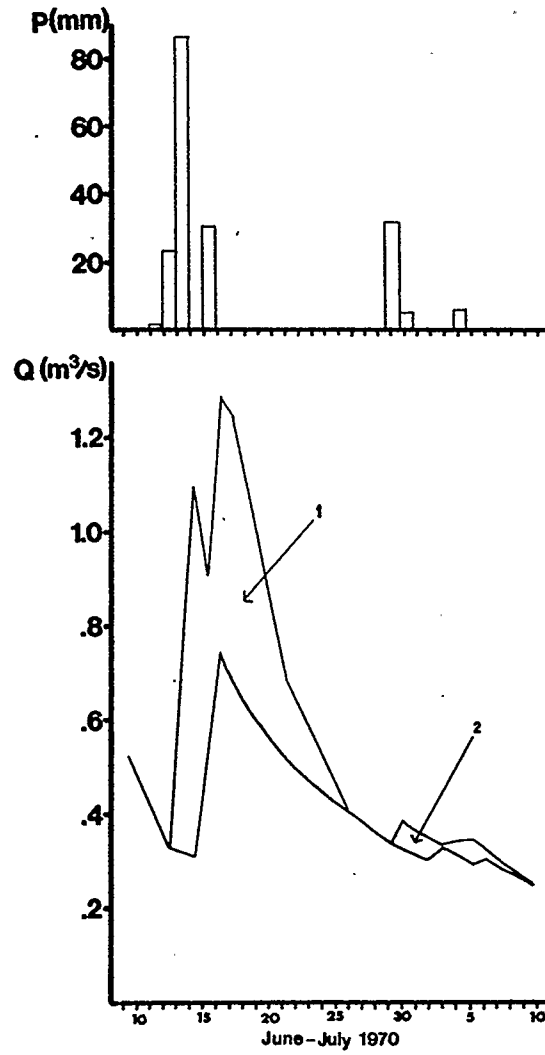
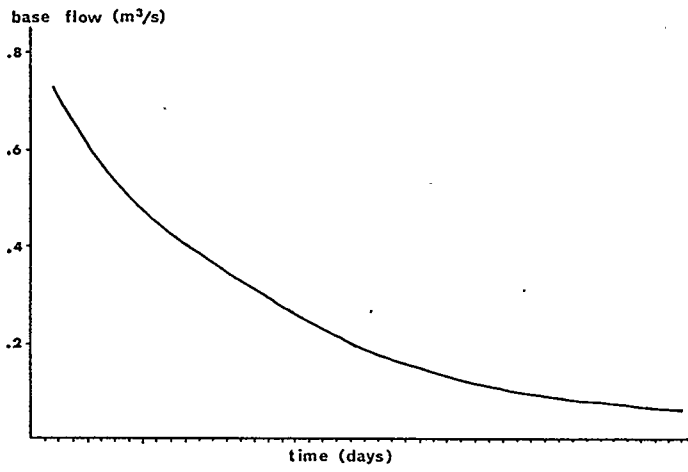
figure 3.7: Graphs of Stormflow Events

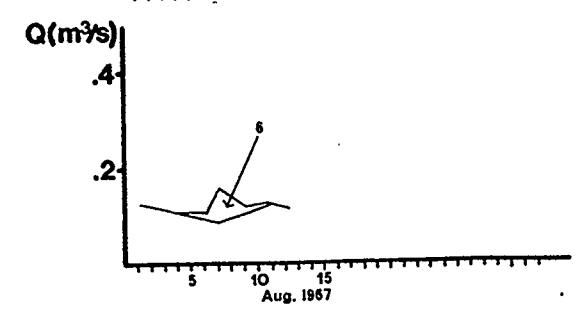
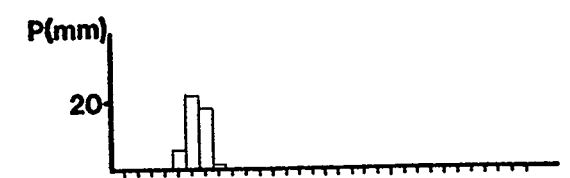
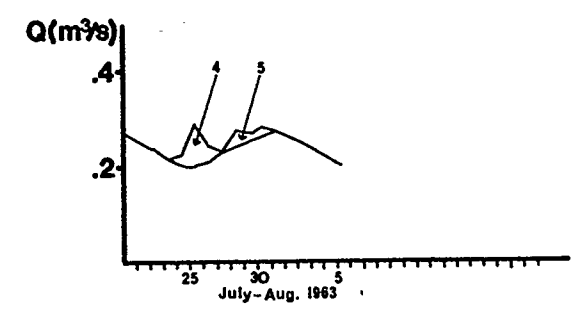
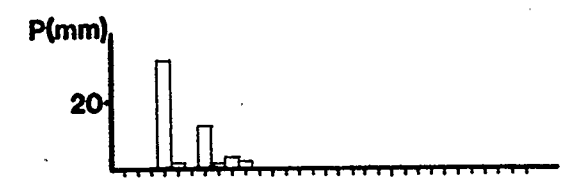
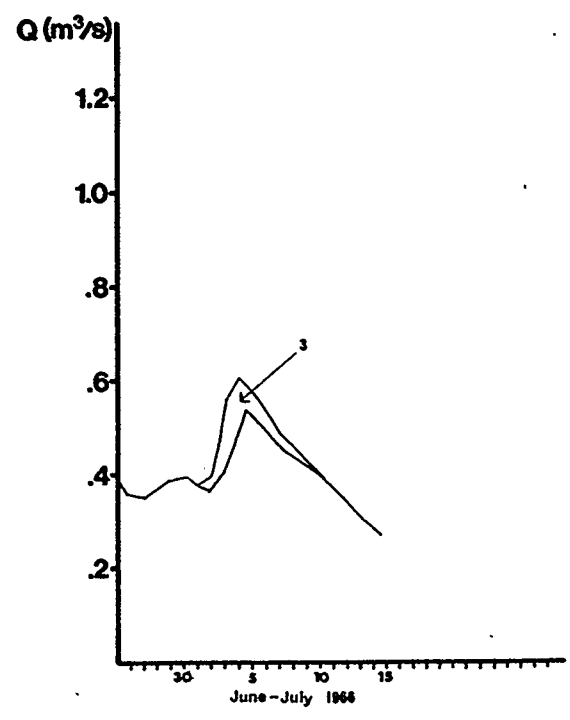
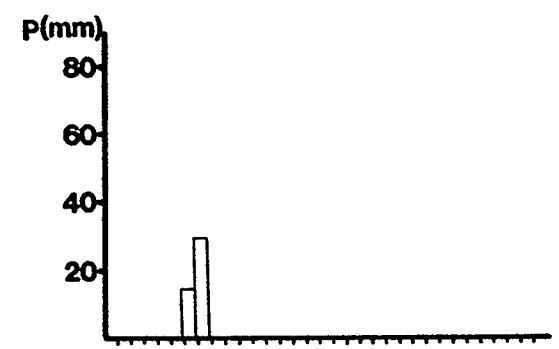
The following nine pages contain graphical representations of the stormflow events and the rainfall events which produced them. The following variable names are used:

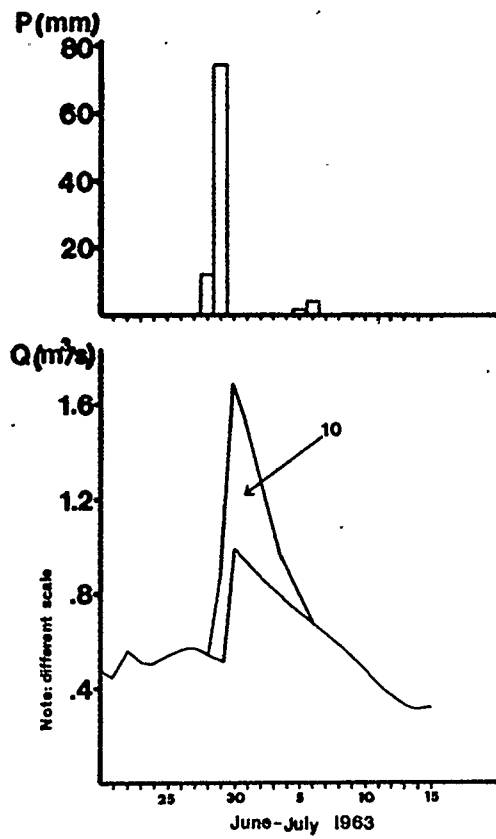
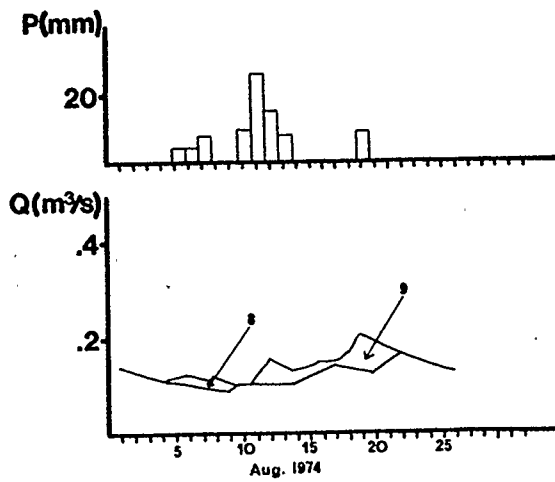
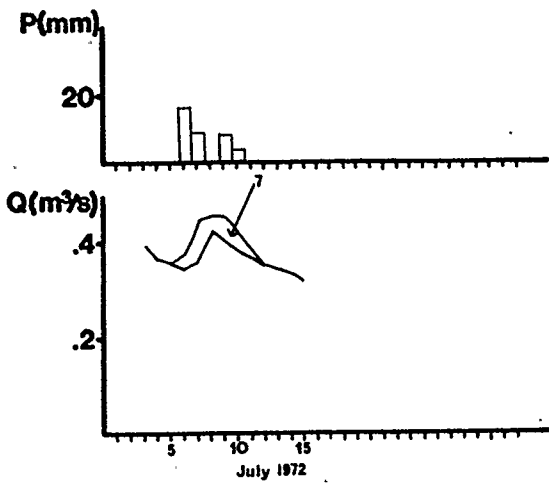
P = daily basin average precipitation

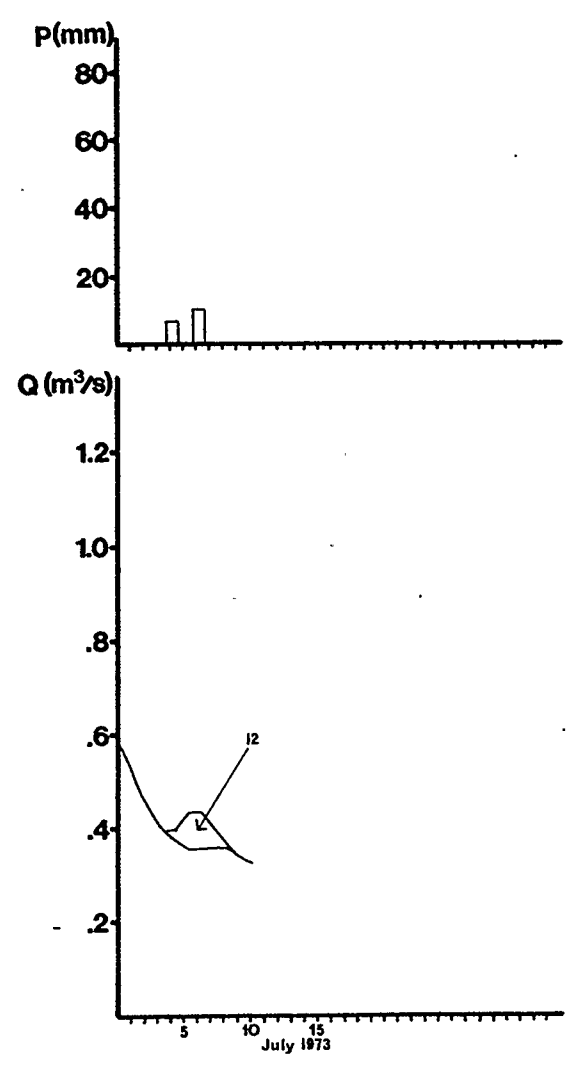
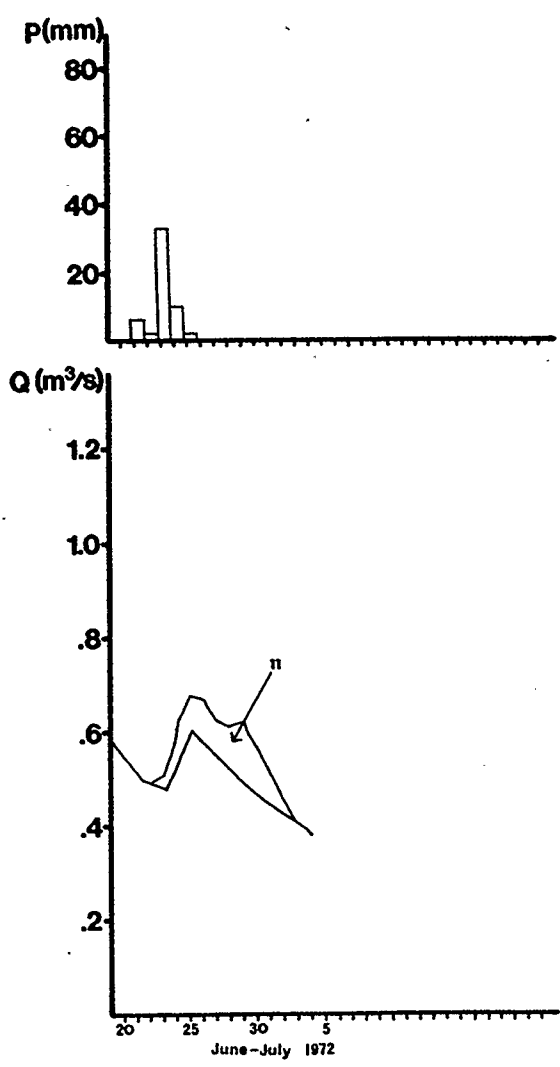
Q = daily mean discharge.

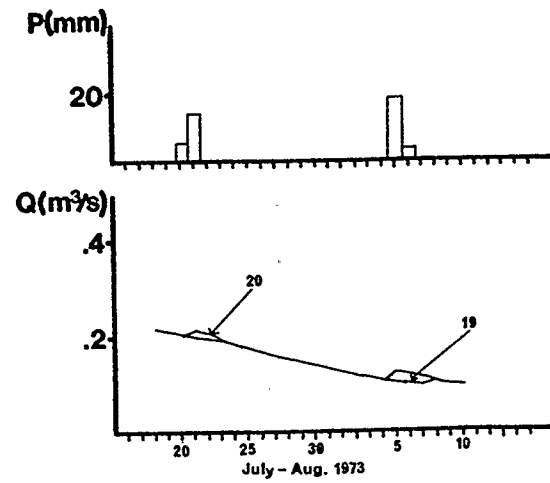
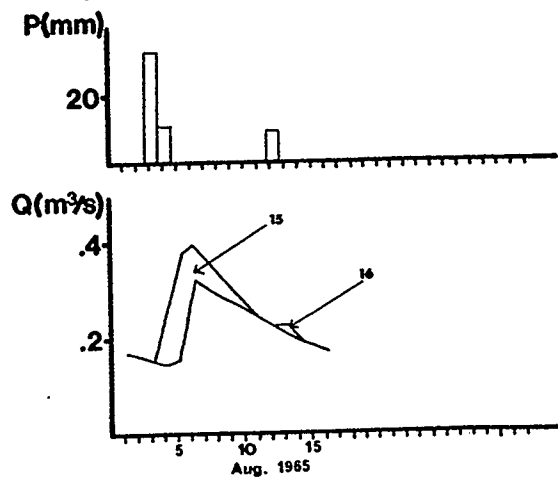
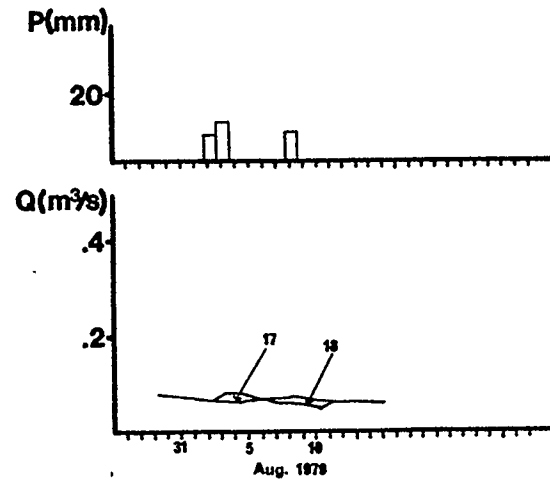
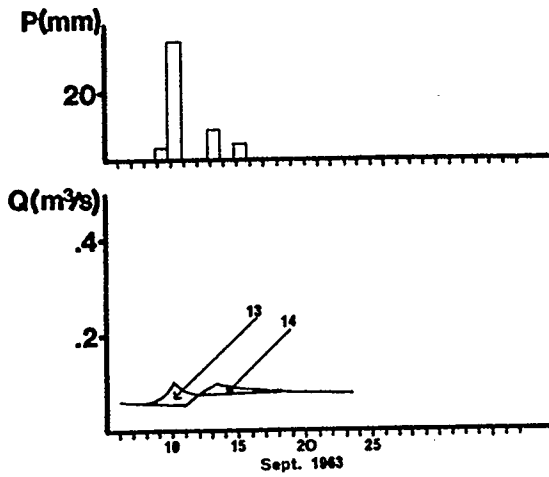
On the hydrographs, the upper line represents streamflow, and the lower line represents base flow. The area between the two lines is equivalent to the volume of storm runoff.

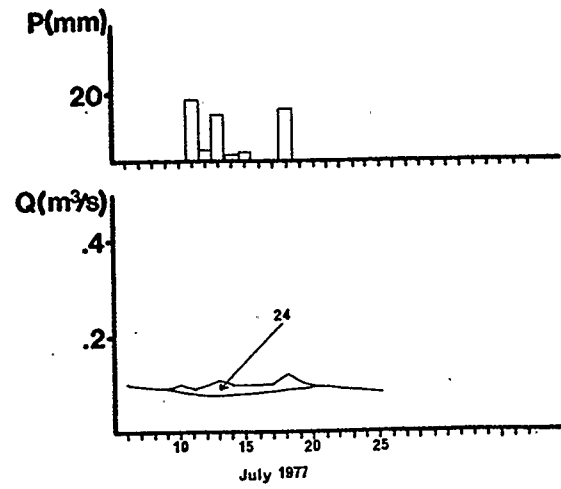
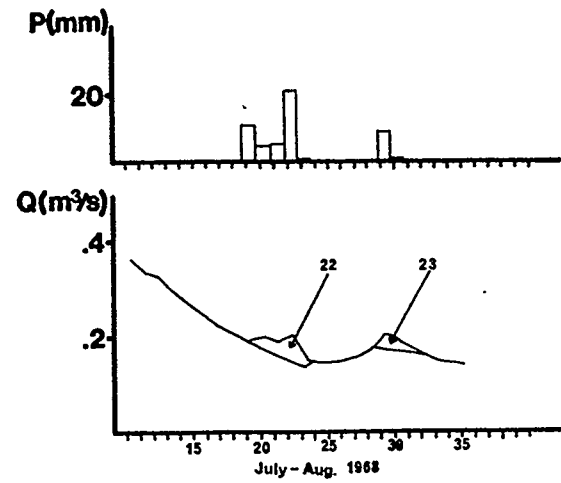
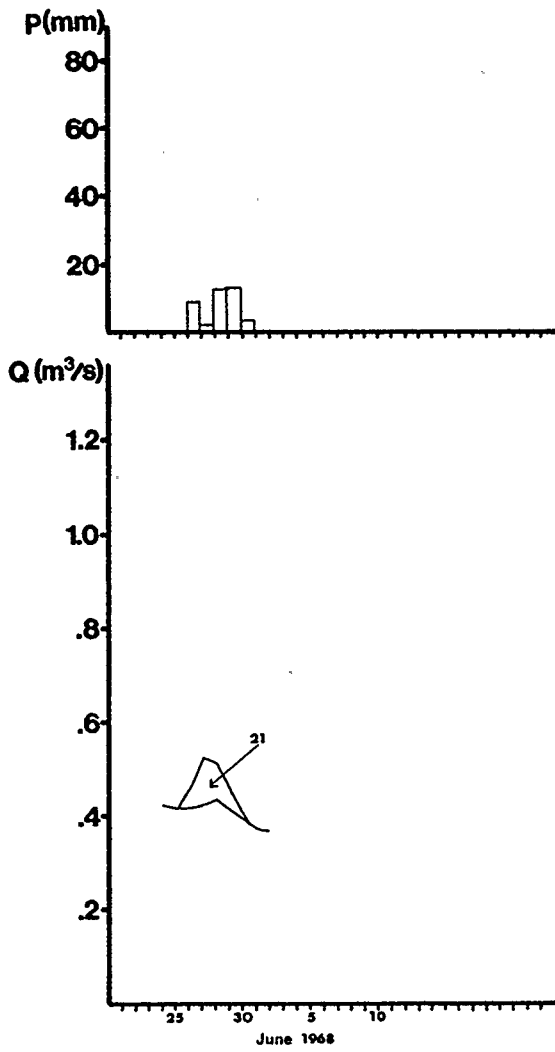


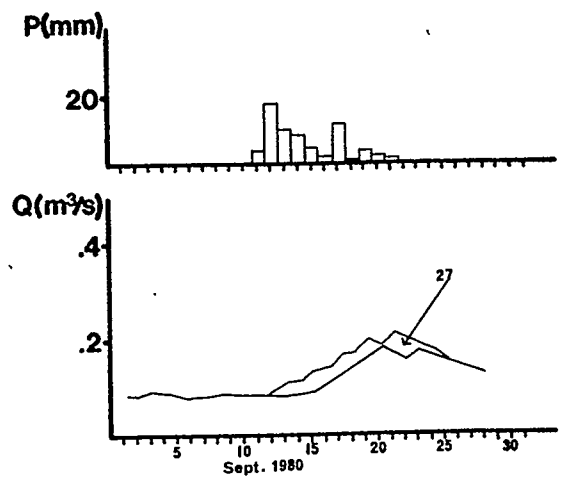
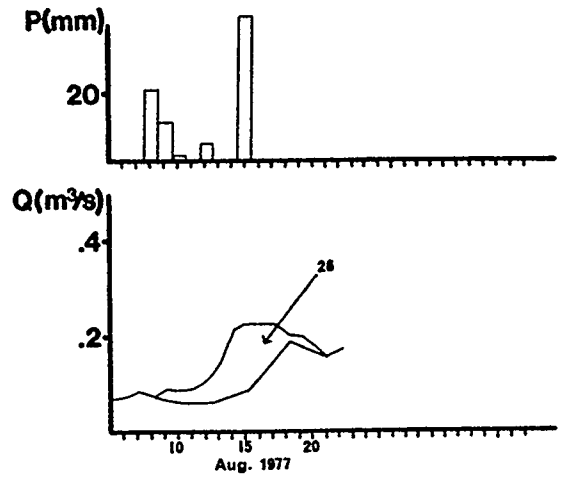
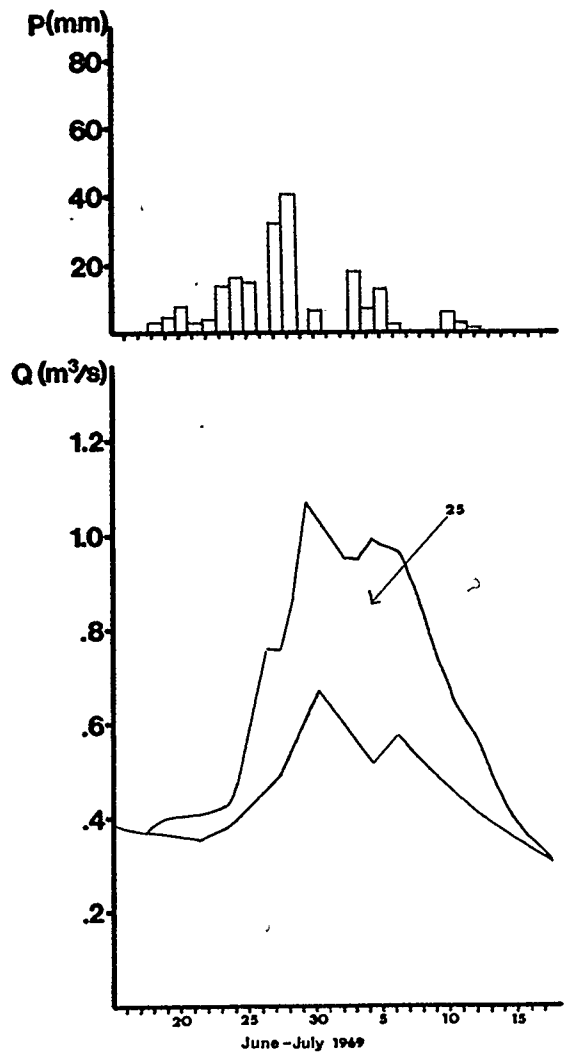


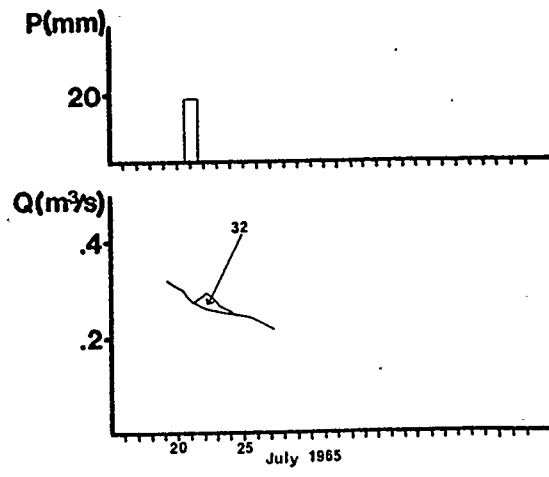
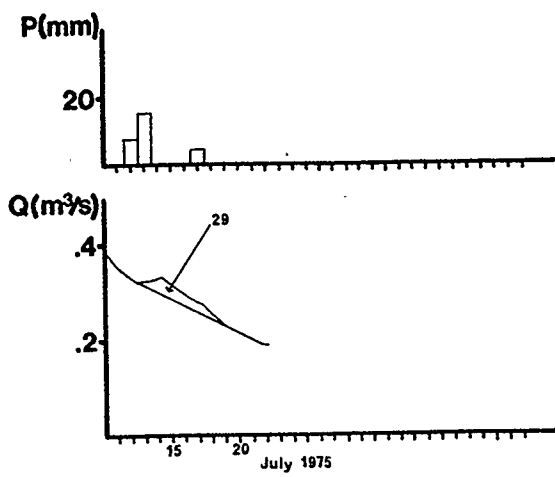
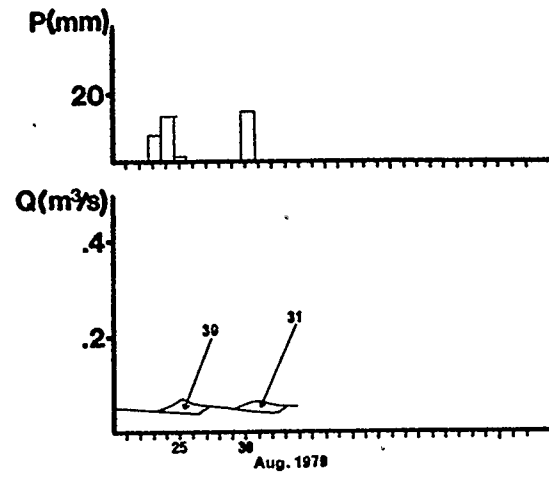
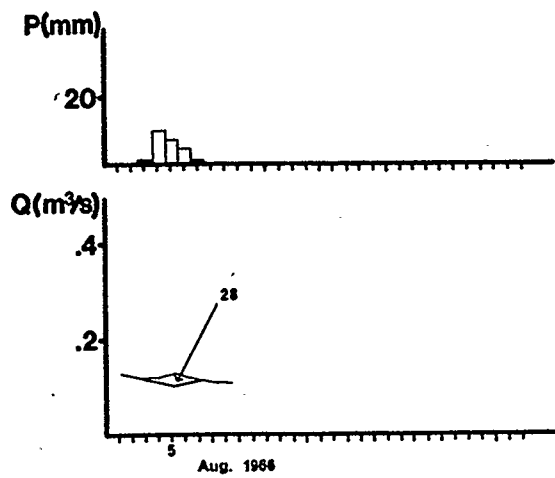


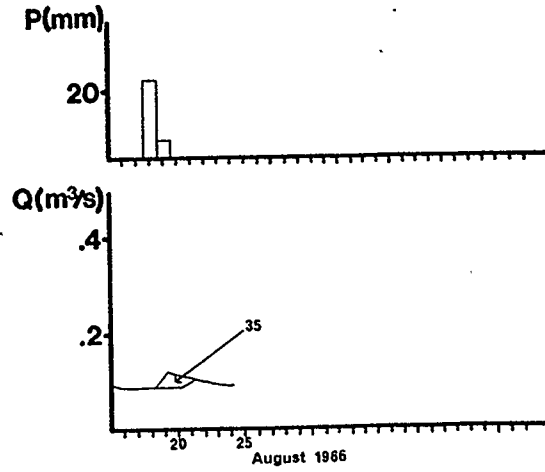
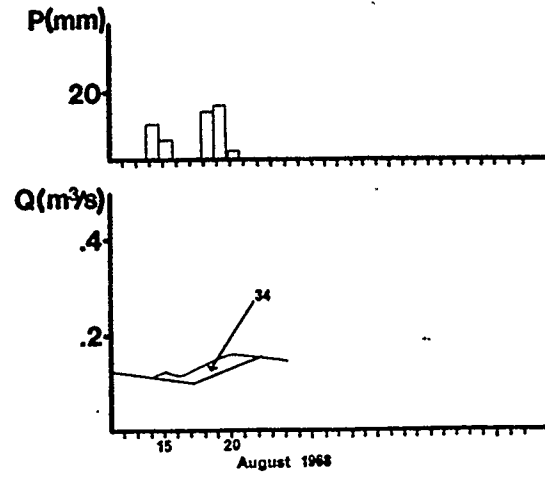
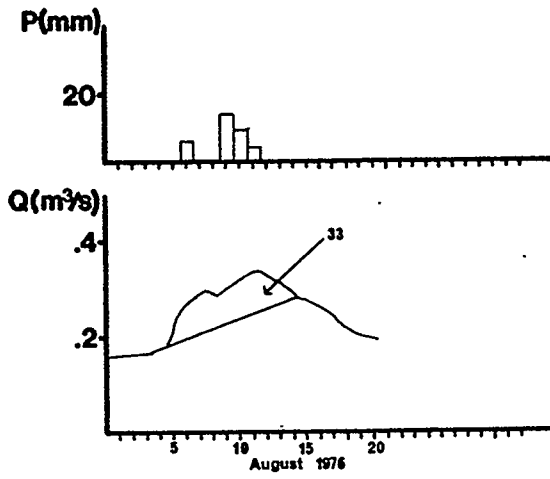












$$P_v = 9400 \sum^m P_i \quad (3.8)$$

where P_v = total rainfall volume in m^3 ,

P_i = rainfall on day i in mm, and

m = time base of rainfall in days.

Rainfall and runoff volumes are given in Table 3.6 following calculation of the remaining parameters.

3.4 Estimation of Soil Moisture

Since soil moisture data was collected only on rare occasions and not reported in the records, it was necessary to estimate the average soil moisture in the basin prior to each event indirectly. To do this, daily water budgets were constructed for each season, starting with the end of snowmelt runoff and using estimates of actual evapotranspiration based on the energy budget method.

The total holding capacity and available moisture for each soil plot is given by Beke (1969) and shown in Table 3.2. Available moisture is the difference between the water stored in the soil at field capacity and at the wilting point. Since we are concerned with the average moisture holding characteristics of the entire soil mantle as a single unit, it is appropriate to use the averages of these values. The average total soil moisture capacity is 191 mm and the average available moisture is 56 mm. For the average soil about half of the soil moisture capacity is gravity water, 25% is available to plants and the remainder is unavailable (Foth & Turk, 1972). If the proportion of gravity water for till were set at about 60% and the remainder divided equally between available and hygroscopic water, this would give an average field capacity of 76 mm and an average wilting point of 20 mm. The exact day on which snowmelt runoff ended had been determined in section 3.1. It is now assumed that the soil was at field capacity yearly on that date.

Actual evapotranspiration for any day can be calculated using the energy budget method as described by Storr (1974a), which gives energy budget calculations specific to Marmot Creek Basin. The energy budget is as follows:

$$Q^* - Q_H - Q_G - Q_F - Q_P - Q_E = 0 \quad (3.9)$$

where Q^* = net radiation,

Q_H = turbulent heat flux to atmosphere,

Q_G = heat flux to the soil,

Q_F = heat to the biomass,

Q_P = energy used in photosynthesis, and

Q_E = energy to evapotranspiration.

Q_G , Q_F and Q_P are subtracted from Q^* and the Bowen Ratio (B) is used to divide the remainder between Q_H and Q_E as follows:

$$B = Q_H / Q_E \quad (3.10)$$

To calculate Q^* , Storr gives factors to convert measured net radiation to effective net radiation, a quantity which accounts for variability of land slopes, albedo and shading. This factor is shown in figure 3.9a. Net radiation is divided into two portions: positive and negative. The positive portion occurs during the day when incoming all-wave radiation exceeds outgoing radiation; the negative portion occurs at night. Both positive and negative portions are multiplied by the factor of figure 3.9a to give $+Q^*$ and $-Q^*$. Since Q_P , Q_G and Q_F only occur during the day these quantities can be expressed as percentages of $+Q^*$ (see figure 3.9b; Q_P is 2% of $+Q^*$ in June and August and 3% in July) and subtracted from $+Q^*$. Then, $-Q^*$ is subtracted from this and the remainder is $Q_H + Q_E$. Q_E can be calculated from the following expression:

$$Q_E = (Q_H + Q_E) / (1 + B) \quad (3.11)$$

To do this, Storr gives estimates of mean monthly Bowen ratios as shown in figure 3.9c. Once Q_E is found then evapotranspiration (E) can be calculated as follows:

$$E = Q_E / L_e \quad (3.12)$$

where L_e = latent heat of vaporization.

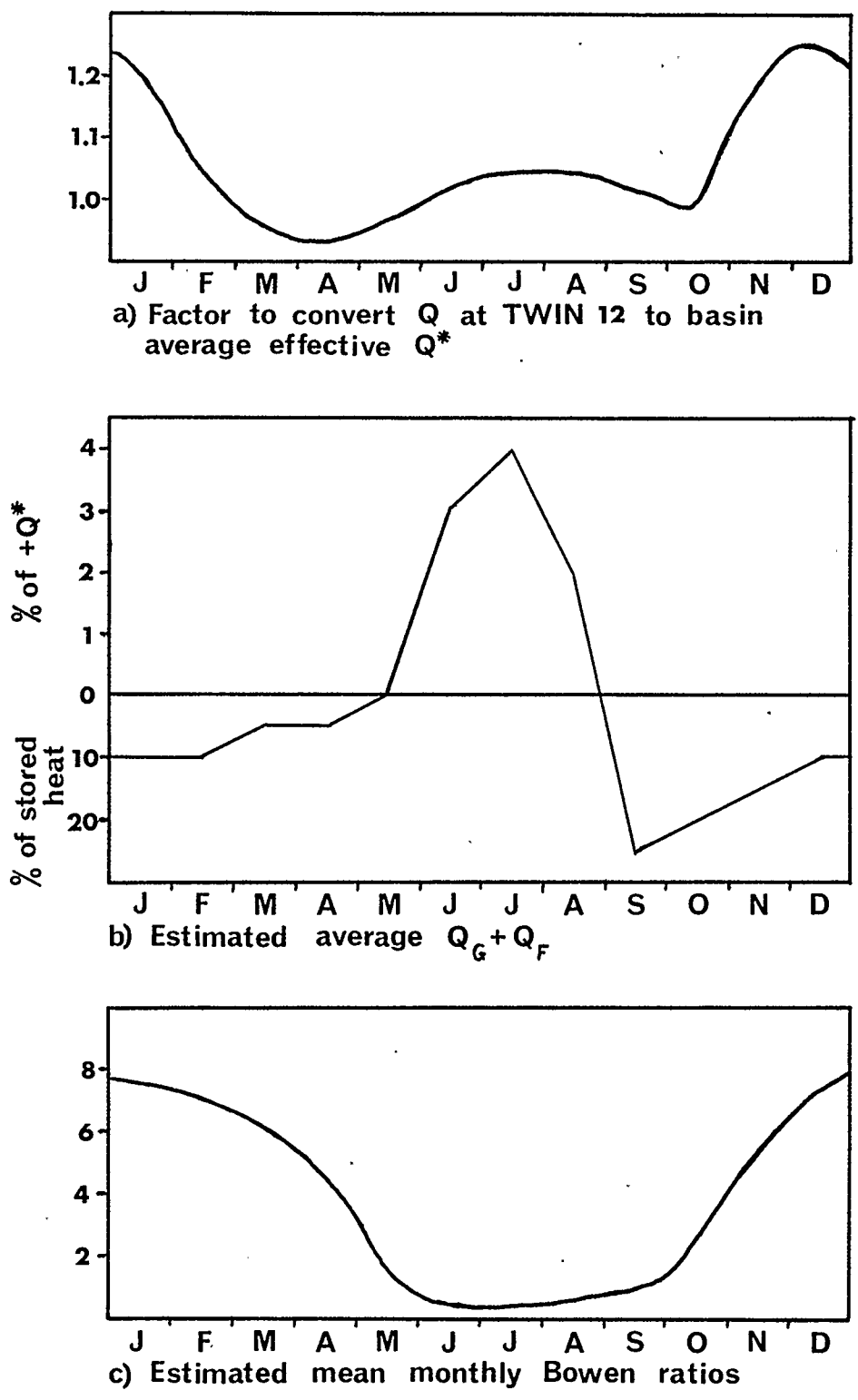


figure 3.9 Graphs for Calculating E (after Storr, 1974)

L_e varies with mean daily temperature as follows:

$$L_e = (597.3 - .564 T) \text{ cal/g} \quad (3.13)$$

where T = mean daily temperature in $^{\circ}\text{C}$

Thus, E is calculated in cm.

Although this method was developed to calculate monthly E , Storr (1974b) also used it successfully to calculate daily E . The main drawback to this is that Bowen ratios are given as estimated monthly means and do not represent the variability of Bowen ratios from day to day. Measurements of temperature and relative humidity must be taken at two levels in the atmosphere to calculate Bowen ratios. Such data is not available at Marmot Creek Basin. B will be higher than average during dry periods and lower than average during moist periods. Thus when soil is dry, E will be too high and when soil moisture is high E will be too low. The errors will be smoothed out partially by the length of time over which water budgets are calculated (Storr, 1974b). Since water budgets begin at field capacity the estimated soil moisture will be exaggerated where soil moisture is high. Estimates will be more accurate for events where soil moisture is low because errors will tend to cancel out. For events where the soil is dried to the wilting point and then partially recharged prior to the event, the estimated soil moisture will be too low given that evapotranspiration will proceed at a reduced rate under less than optimum conditions. It is assumed that tree roots are evenly distributed through the soil profile.

To give optimum accuracy, the graphs of figure 3.9 were interpolated for each day. Direct application of this method proved to be very time consuming and so it was decided that a simpler approach could be developed in the form of a linear equation which expresses E as a function of $+Q^*$ and $-Q^*$. The graphs of figure 3.8 show that values for $Q_G + Q_F$ and Q_P rise to a maximum on or about July 15 and then decline thereafter. Thus a separate equation should be found for each period. The energy budget method was used to calculate daily E for two periods which represented the range of net radiation normally experienced during those periods: July 1-14, 1968 and July 15- Aug 3, 1968. Since E is a function entirely of $+Q^*$, $-Q^*$ and T , E was regressed

on those quantities to produce equations for the estimation of E. Since T was found to be insignificant in both cases, the results of regression are as follows:

June 15 to July 15:

$$E_{\text{est}} = -0.372 + .0133(+Q^*) - .0075(-Q^*) \quad (3.14)$$

$$r^2 = 99.7\%, s = .0622 \text{ (mm)}, n=15$$

July 16 on:

$$E_{\text{est}} = -0.114 + .0103(+Q^*) - .0103(-Q^*) \quad (3.15)$$

$$r^2 = 99.8\%, s = .0627 \text{ (mm)}, n=20$$

Since daily E typically varies between 3 and 5 mm during the summer months, the r^2 and s values given above indicate a high degree of accuracy. However, it must be noted that the values of E which were calculated using the energy budget method are only estimates of daily evapotranspiration, because the calculations employed estimated values of the Bowen ratio. Therefore, the value of E_{est} obtained using equation (3.14) or (3.15) is an estimate of an estimate. The error in equations (3.7) and (3.8) is very low. Because E_{est} is used to calculate water budgets over several days, the errors will be smoothed out to yield a result which is virtually identical to that which would be obtained using E. Thus, if Storr's method is accepted, then the water budgets calculated using E_{est} provide a valid first approximation of the average soil moisture on any given day.

An example of a water budget is given in Table 3.4. This method was used to estimate soil moisture one day before each storm runoff event.

3.5 Other Parameters

The other parameters used in the model were base flow prior to the rise of the hydrograph and maximum 24 hour rainfall intensity during the event. Base flow is expressed in terms of m^3/sec . Maximum intensity (I_m) was taken from the rainfall series for each event.

The data set to be entered into the modelling phase is now complete and is presented in Table 3.5.

Table 3.4: Example of Water Budget Calculation

In 1974, snowmelt runoff ended on June 29.

date	E (mm)	P (mm)	S (mm)
June 29			76.00 (field capacity)
30	5.40	0.00	70.60
July 01	4.11	9.46	75.95
02	5.31	0.00	70.64
03	3.78	0.00	66.86
04	3.19	2.27	65.94
05	5.60	0.00	60.34
06	5.56	0.00	54.78
07	4.14	5.68	56.32
08	1.86	1.14	55.60
09	4.53	0.00	51.07
10	5.84	7.04	52.27
11	1.57	1.04	51.74
12	7.67	0.00	44.07
13	6.25	0.00	37.82
14	7.03	0.00	30.79
15	4.72	3.39	29.46
16	4.89	0.00	24.57
17	3.36	0.00	21.21
18	3.55	0.00	20.00 (wilting point)
19	2.31	0.24	20.00

E = evapotranspiration, P = precipitation, S = estimated average soil moisture.
 On day i , $S_i = S_{i-1} + P_i - E_i$. S is obtained on any day desired.

Table 3.5: The Data Set

event	runoff volume (x1000 m ³)	rainfall volume (x1000 m ³)	antecedent baseflow (m ³ /sec)	est. soil moisture (mm)	maximum intensity (mm/24 hr)
1	361.878	1346.61	0.3226	76.00	87.12
2	27.874	387.58	0.3255	28.56	31.50
3	35.308	408.30	0.3962	60.80	28.96
4	11.419	317.55	0.2264	22.85	32.26
5	5.868	293.67	0.2321	46.22	12.95
6	12.959	427.38	0.1019	23.65	21.84
7	18.950	334.26	0.3538	28.49	16.00
8	5.624	119.38	0.1075	20.00	7.11
9	32.276	606.45	0.1047	20.13	25.56
10	218.105	886.70	0.5349	76.00	74.68
11	65.162	463.19	0.5037	76.00	32.51
12	8.827	143.26	0.3905	76.00	9.40
13	7.702	350.98	0.0566	20.00	34.29
14	4.988	116.99	0.0736	51.70	8.38
15	50.810	642.26	0.1520	20.00	35.81
16	1.467	83.57	0.2239	48.43	8.89
17	4.157	71.91	0.0651	20.00	10.92
18	3.179	78.79	0.0623	20.00	8.38
19	4.646	210.11	0.1019	20.00	18.29
20	2.543	174.30	0.2009	20.00	13.57
21	25.796	339.04	0.4160	76.00	12.32
22	9.047	391.57	0.1783	20.00	21.08
23	5.722	83.57	0.1755	23.30	8.38
24	16.138	498.46	0.0877	39.10	17.78
25	534.259	1793.09	0.3622	76.00	40.64
26	60.884	737.77	0.0736	20.00	42.16
27	31.053	584.96	0.0821	24.83	17.78
28	3.448	210.75	0.1132	20.00	9.65
29	9.536	263.95	0.3283	76.00	15.56
30	4.157	207.72	0.0425	20.00	13.21
31	3.668	139.48	0.0453	27.63	14.73
32	4.401	174.75	0.2717	52.40	18.32
34	12.226	432.16	0.1104	24.03	15.24
35	4.646	265.02	0.0863	20.00	23.11

The data set contains 35 events. Rainfall volume ranges from 78790 to 1793090 m³. Runoff volume ranges from 1467 to 534259 m³. The proportion of rainfall which appears as runoff ranges from 1.8% to 29.8%. Initial base flow ranges from 0.0425 to 0.5349 m³/sec. Maximum mean daily streamflow in the data set was 1.7 m³/sec on June 30, 1963. Maximum mean daily base flow of 1.0 m³/sec occurred on the same day. Soil moisture ranged anywhere between the wilting point of 20.0 mm and field capacity, 76.00 mm. Maximum 24-hour rainfall intensity of 87.12 mm/24 hours occurred on June 13, 1970 with a lower limit of 7.11 mm/24 hours on August 7, 1974.

CHAPTER 4

ANALYSIS

The purpose of this chapter is to develop a model which predicts the volume of storm runoff contained in an event. This process involved alternating the development of trial models with parameter optimization until a satisfactory model was produced. The early stages of the analysis process occurred simultaneously with the development and finalization of the data set which was presented in table 3.5.

The models were identified using multiple polynomial regression. Initially, two statistical packages were considered; MINITAB and DAVIS. MINITAB was used for all analysis because it proved to be by far the more versatile package in terms of editing and manipulation of data and in the structure of its commands. It is capable of regressing more than one polynomial at a time, and of performing stepwise regression. It can be used interactively or in batch mode. MINITAB is one of the packages recommended by Draper and Smith (1981) for regression analysis.

The following is a list of parameter abbreviations. Hereafter, each parameter will be referred to by its abbreviation:

Q_V = volume of storm runoff ($\times 1000 \text{ m}^3$)

$Q_{V,est}$ = storm runoff volume estimated by a model ($\times 1000 \text{ m}^3$)

P_V = volume of precipitation ($\times 1000 \text{ m}^3$)

B = baseflow prior to an event (m^3/sec)

S = estimated average soil moisture (mm)

I = maximum 24 hour rainfall intensity during an event (mm/24 hours)

Initially, Q_V was calculated by using the groundwater rating curves (figure 3.5) to separate base flow. This was done to ascertain the general form of the model and to complete the list of parameters which were needed. Q_V was regressed on P_V and B using a linear model. The residual pattern was curved (figure 4.1). This indicates that either a transformation or a higher order model

is required (Draper and Smith, 1981). Attempts were made to fit a model to log transformed Q_v . This was abandoned early in the analysis process because polynomial models were found to produce a better fit and a better r^2 value. Also, log transformations should be avoided if possible because of the large roundoff errors which are incurred when the inverse transformation is applied for predictive purposes.

Once the parameter S had been assessed, it was introduced into the model. In MINITAB, higher order models are fitted to a data set by creating terms up to the desired order in new columns and entering those terms into multiple regression (Ryan, Joiner and Ryan, 1985). For example, if we had variables Y and X and we wished to express Y as a function of a quadratic in X, we would create a third column containing X^2 and regress Y on X and X^2 . Since a second or third order model was indicated, all possible second and third order terms were created and entered into the data file as new columns. These new terms included all squares and cubes of existing parameters, as well as all possible interaction terms. Second order interaction terms are the products of all possible pairs of parameters, and third order terms consist of the products of all

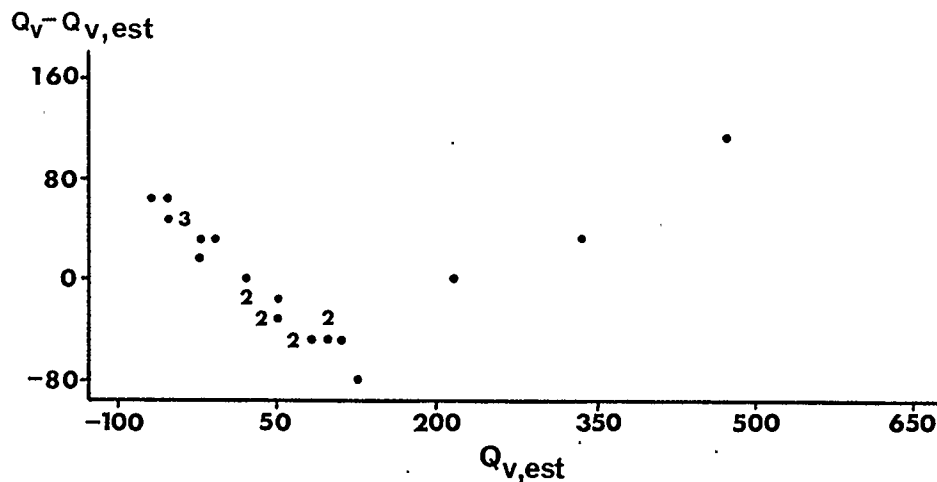


figure 4.1 Residual Plot for a Trial First Order Model

possible triplets of parameters, and of the square of each parameter combined with each other parameter (Draper and Smith, 1981). The parameters Q_v and P_v were converted to units of 1000 m^3 to avoid overflow in the computer.

Stepwise regression was used to select the best possible combination of parameters to be entered into second and third order models. In this procedure, the user selects the list of predictor terms to be considered in the model. The computer package then computes a correlation matrix and first enters the predictor term which is most highly correlated with the response variable (in this case, Q_v). The user specifies an F ratio ($F=t^2$) which the computer uses to judge the significance of each term in the model. At each step, the next best term is entered if it is significant, and the coefficients and t ratios of each term already in the model are re-assessed. Any terms which become insignificant after each step are dropped. This process continues until no more variables are entered or removed. Although critical t ratios for this data set were always greater than 2, the F ratio to remove and enter terms was set at 2 because this was found to produce a better fit. Some of the more significant terms would not have been entered if the default of $F=4$ had been used. The t ratios of each term identified by stepwise regression were examined in light of the critical t ratios for each model which was run and only the significant terms were entered into regression.

Second and third order models were developed to predict Q_v as a function of P_v , B and S. Table 4.1 summarizes the trial models, and figure 4.2 shows the residual plot for each. A general idea of parsimony can be gained by examination of the residual plots for each trial model. The curvature of the residuals in figure 4.2a indicates that a higher order model is needed. The residual plot of the third order model (figure 4.2b) shows no such curvature. This suggests that the third order model is appropriate. An F test, the more precise test for parsimony, will be performed once parameter optimization is complete.

On closer examination of the third order residual plot (figure 4.2b) there appears to be a trend. This indicates that another parameter must be introduced into the data set (Draper and Smith, 1981). The most logical parameter to test at this stage is rainfall intensity. For a given P_v , the more

TABLE 4.1a: TRIAL 2nd ORDER MODEL OF Q_v ON P_v, B AND S
Stepwise Regression of Q_v on 9 Predictors, with N = 32:

STEP	1	2	3	4	5
CONSTANT	-2.615	-18.840	-1.474	8.315	7.410
P _v ²	0.00019	0.00013	0.00015	0.00014	0.00012
T-Ratio	27.78	15.97	13.98	11.04	8.08
P _v B		0.275	0.305	0.423	0.337
T-Ratio		7.93	9.43	6.65	4.44
P _v			-0.056	-0.065	-0.092
T-Ratio			-2.98	-3.56	-4.09
B				-66	-69
T-Ratio				-2.11	-2.31
P _v S					0.00078
T-Ratio					1.90
S	23.6	13.5	12.0	11.3	10.8
R-SQ	96.26	98.82	99.10	99.23	99.32

Regression Analysis:

The regression equation is:

$$Q_{v,est} = 8.32 - 6.52 \times 10^{-2} P_v + 1.39 \times 10^{-4} P_v^2 - 65.63 B + 0.42 P_v B$$

COLUMN	COEFFICIENT	ST. DEV. OF COEFF.	T-RATIO = COEF/S.D.
	8.315	6.567	1.27
P _v	-0.06518	0.01833	-3.56
P _v ²	0.00013949	0.00001264	11.04
B	-65.63	31.12	-2.11
P _v B	0.42292	0.06361	6.65

tcrit=2.052

$$S=11.28, \text{ d.f.} = 27, r^2 = 99.1\%$$

Analysis of Variance

DUE TO	DF	SS	MS=SS/DF	F
REGRESSION	4	443032.4	110758.1	=870.06
RESIDUAL	27	3436.6	127.3	=F(.05,4,27)
TOTAL	31	446469.0		crit =2.73

Further Analysis of Variance:

SS Explained by each Variable when Entered in the Order Given

DUE TO	DF	SS
REGRESSION	4	443032.4
P _v	1	384585.5
P _v ²	1	45175.7
B	1	7645.1
P _v B	1	5626.1

TABLE 4.1a: (continued)

EVENT	P_v	Q_v	PRED. Q_v VALUE	ST.DEV. PRED. Y	RESIDUAL	ST.RES.	
1	1347	365.42	336.04	5.55	29.38	2.99	R
2	337	4.65	27.16	2.93	-22.52	-2.07	R
3	408	60.15	47.37	3.63	12.78	1.20	
4	318	5.01	17.23	2.17	-12.22	-1.10	
5	294	10.17	14.80	2.21	-4.63	-0.42	
6	432	7.09	18.14	3.07	-11.04	-1.02	
7	334	33.62	28.91	3.26	4.71	0.44	
8	119	5.87	0.89	3.41	4.97	0.46	
9	606	42.30	40.07	4.25	2.23	0.21	
10	867	221.53	217.56	9.62	3.97	0.67	X
11	463	66.39	73.66	5.00	-7.28	-0.72	
12	143	23.33	-0.13	5.95	23.46	2.45	R
13	351	7.70	7.31	3.20	0.39	0.04	
14	117	4.99	1.41	3.86	3.58	0.34	
15	642	62.84	55.31	4.02	7.53	0.71	
16	84	1.47	-2.94	3.89	4.41	0.42	
17	172	4.16	1.69	3.54	2.46	0.23	
18	79	1.22	2.03	4.42	-0.81	-0.08	
19	210	5.50	3.15	2.83	2.36	0.22	
20	174	2.54	2.32	2.66	-0.27	-0.02	
21	339	21.88	34.60	4.04	-12.71	-1.21	
22	392	6.46	22.01	2.39	-15.55	-1.41	
23	84	5.72	-1.47	3.53	7.20	0.67	
24	498	16.06	23.22	3.61	-7.16	-0.67	
25	1793	574.85	590.32	10.33	-15.98	-3.52	RX
26	738	53.79	54.29	5.91	-0.50	-0.05	
27	585	37.78	32.34	4.33	4.93	0.47	
28	211	2.42	3.43	2.70	-1.01	-0.09	
29	264	9.54	15.93	3.33	-6.39	-0.59	
30	208	4.40	1.74	3.66	2.66	0.25	
31	139	3.18	1.64	4.11	1.54	0.15	
32	175	2.93	3.43	3.37	-0.50	-0.05	

R DENOTES AN OBS. WITH A LARGE ST. RES.

X DENOTES AN OBS. WHOSE X VALUE GIVES IT LARGE INFLUENCE.

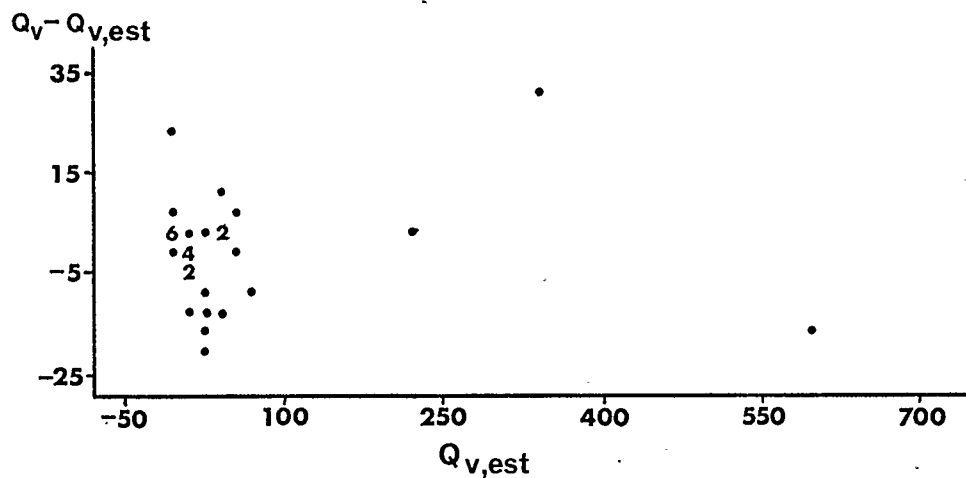


figure 4.2a Residual Plot For Table 4.1a

TABLE 4.1b: TRIAL 3rd ORDER MODEL OF Q_v ON P_v , B and S.
Stepwise Regression of Q_v on 13 Predictors, with $N=32$:

STEP	1	2	3	4
CONSTANT	-2.615	-9.567	-1.148	16.310
P_v2	0.00019	0.00013	0.00015	0.00037
T-Ratio	27.78	18.49	13.80	7.86
P_vBS		0.00247	0.00258	0.00244
T-Ratio		9.57	10.35	12.96
P_v			-0.036	-0.167
T-Ratio			-2.12	-5.58
P_v3				-0.00000
T-Ratio				-4.83
S	23.6	11.8	11.1	8.30
R-SQ	96.26	99.10	99.22	99.58

Regression Analysis:

The regression equation is:

$$Q_{v,est} = 16.31 - .167 P_v + 3.69 \times 10^{-4} P_v2 - 8.78 \times 10^{-8} P_v3 + 2.44 \times 10^{-3} P_vBS$$

COLUMN	COEFFICIENT	ST. DEV. OF COEFF.	T-RATIO = COEF/S.D.
--	16.310	4.975	3.28
P_v2	-0.16700	0.02994	-5.58
P_vBS	0.00036923	0.00004697	7.86
P_v	-8.78262E-08	1.818897E-08	-4.83
P_v3	0.0024377	0.0001881	12.96

tcrit=2.052

$$S=8.298, \text{ d.f.} = 27, r^2 = 99.5\%$$

Analysis of Variance

DUE TO	DF	SS	MS=SS/DF	F
REGRESSION	4	444609.9	111152.5	=1613.2
RESIDUAL	27	1859.1	68.9	=F(.05,4,27)
TOTAL	31	446469.0		=2.73

Further Analysis of Variance:

SS Explained by each Variable when Entered in the Order Given

DUE TO	DF	SS
REGRESSION	4	444609.9
P_v2	1	384585.5
P_vBS	1	45175.7
P_v	1	3282.2
P_v3	1	11566.4

TABLE 4.1b: (continued)

EVENT	P_v	Q_v	PRED. Q_v VALUE	ST.DEV. PRED. Y	RESIDUAL	ST.RES.
1	1347	365.42	365.12	6.68	0.31	0.06 X
2	337	4.65	15.83	1.97	-11.18	-1.39
3	408	60.15	41.87	2.70	18.28	2.33 R
4	318	5.01	8.01	1.88	-3.00	-0.37
5	294	10.17	10.55	1.83	-0.38	-0.05
6	432	7.09	12.41	2.36	-5.32	-0.67
7	334	33.62	17.05	1.99	16.57	2.06 R
8	119	5.87	3.24	2.49	2.63	0.33
9	606	42.30	39.93	3.13	2.37	0.31
10	867	221.53	218.32	6.40	3.21	0.61 X
11	463	66.39	73.15	4.02	-6.76	-0.93
12	143	23.33	14.98	2.30	8.35	1.05
13	351	7.70	2.10	2.13	5.61	0.70
14	117	4.99	3.53	2.52	1.46	0.18
15	642	62.84	51.42	3.18	11.42	1.49
16	84	1.47	8.73	3.05	-7.27	-0.94
17	172	4.16	-0.41	1.96	4.56	0.57
18	79	1.22	6.07	3.15	-4.85	-0.63
19	210	5.50	-0.37	1.78	5.87	0.72
20	174	2.54	2.73	1.91	-0.19	-0.02
21	339	21.88	37.22	2.80	-15.33	-1.96
22	392	6.46	11.79	2.13	-5.33	-0.67
23	84	5.72	7.00	3.06	-1.28	-0.17
24	498	16.06	21.93	2.58	-5.87	-0.74
25	1793	574.85	574.99	8.18	-0.15	-0.10 X
26	738	53.79	66.22	4.31	-12.43	-1.75
27	585	37.78	34.51	3.07	3.27	0.42
28	211	2.42	-0.05	1.77	2.47	0.30
29	264	9.54	20.00	2.09	-10.46	-1.30
30	208	4.40	-2.03	1.81	6.43	0.79
31	139	3.18	0.94	2.25	2.24	0.28
32	175	2.93	8.16	1.93	-5.23	-0.65

R DENOTES AN OBS. WITH A LARGE ST. RES.
X DENOTES AN OBS. WHOSE X VALUE GIVES IT LARGE INFLUENCE.

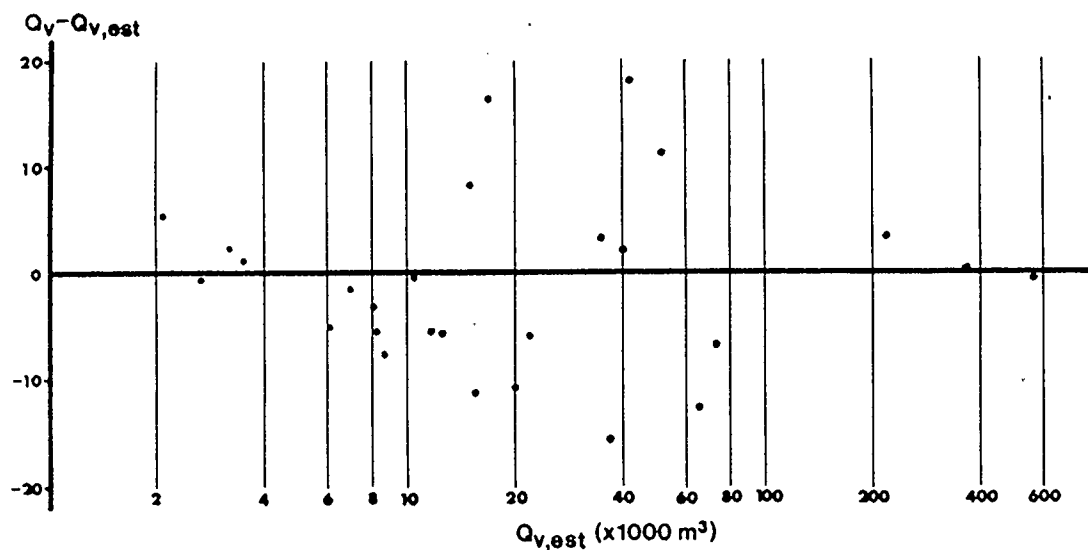


figure 4.2b Residual Plot for Table 4.1b

TABLE 4.1c: TRIAL 3rd ORDER MODEL OF Q_v on P_v , B, S and I
Stepwise Regression of Q_v on 20 Predictors, with N=32:

STEP	1	2	3	4	5	6
CONSTANT	-2.615	-9.567	-8.464	5.710	7.371	7.457
P_v^2	0.00019	0.00013	0.00013	0.00016	0.00019	0.00019
T-Ratio	27.78	18.49	20.76	19.11	9.02	26.56
P_vBS		0.00247	0.00167	0.00148	0.00006	
T-Ratio		9.57	4.51	5.07	0.07	
P_vBI			0.00141	0.00203	0.00260	0.00263
T-Ratio			2.81	4.87	4.77	8.40
P_v^3				-0.059	-0.073	-0.074
T-Ratio				-4.36	-4.58	-5.76
B					269	280
T-Ratio					1.57	5.54
S	23.6	11.8	10.6	8.26	8.05	7.90
r^2	96.26	99.10	99.30	99.59	99.62	99.62

Regression Analysis:

The regression equation is:

$$Q_v \text{ est} = 7.46 - 7.37 \times 10^{-2} P_v + 1.92 \times 10^{-4} P_v^2 + 279.86 B^2 + 2.63 \times 10^{-8} P_v B$$

COLUMN	COEFFICIENT	ST.DEV. OF COEF.	T-RATIO = COEF/S.D.
--	7.457	3.435	2.17
P_v^2	-0.07368	0.01280	-5.76
P_v^3	0.000191890	0.000007226	26.56
B	279.86	50.51	5.54
P_vBI	0.0026331	0.0003136	8.40

$t_{crit} = 2.473$

$$S = 7.895, df = 27, r^2 = 99.6\%$$

Analysis of Variance:

DUE TO	DF	SS	MS=SS/DF	F	
REGRESSION	4	444785.9	111196.5		
RESIDUAL	27	1683.1	62.3	F	=1784.9
TOTAL	31	446469.0		F_{crit}	=F(.05,4,27) =2.73

Further Analysis of Variance:

SS Explained by each Variable when Entered in the Order Given

DUE TO	DF	SS
REGRESSION	4	444785.9
P_v^2	1	384585.5
P_v^3	1	45175.7
B	1	10630.6
P_vBI	1	4394.0

TABLE 4.1c: (continued)

EVENT	P_v	Q_v	PRED. Q_v VALUE	ST.DEV. PRED.Y	RESIDUAL	ST.RES
1	1347	365.42	365.25	6.28	0.17	0.04 X
2	337	4.65	23.14	1.57	-18.49	-2.39 R
3	408	60.15	39.10	2.34	21.05	-2.79 R
4	318	5.01	12.76	1.58	-7.75	-1.00
5	294	10.17	8.19	1.52	1.98	0.26
6	432	7.09	14.28	2.13	-7.19	-0.95
7	334	33.62	21.64	1.93	11.98	1.56
8	119	5.87	1.98	2.30	3.88	0.51
9	606	42.30	37.94	2.98	4.36	0.60
10	867	221.53	221.73	6.28	-0.20	-0.04 X
11	463	66.39	70.23	4.86	-3.85	-0.62 X
12	143	23.33	18.89	2.99	4.44	0.61
13	351	7.70	7.08	1.83	0.62	0.08
14	117	4.99	1.76	2.33	3.22	0.43
15	642	62.84	49.48	2.97	13.36	1.83
16	84	1.47	6.22	2.52	-4.75	-0.64
17	172	4.16	0.86	1.97	3.30	0.43
18	79	1.22	3.02	2.65	-1.80	-0.24
19	210	5.50	1.77	1.80	3.73	0.48
20	174	2.54	3.96	1.87	-1.42	-0.19
21	339	21.88	29.26	3.04	-7.37	-1.01
22	392	6.46	13.49	1.86	-7.03	-0.92
23	84	5.72	4.48	2.55	1.25	0.17
24	498	16.06	20.64	2.49	-4.58	-0.61
25	1793	574.85	575.09	7.69	-0.25	-0.14 X
26	738	53.79	63.68	3.57	-9.89	-1.40
27	585	37.78	32.42	2.96	5.36	0.73
28	211	2.42	1.46	1.78	0.96	0.12
29	264	9.54	14.83	1.71	-5.29	-0.69
30	208	4.40	0.76	1.81	3.64	0.47
31	139	3.18	1.18	2.17	1.99	0.26
32	175	2.93	8.34	1.84	-5.41	-0.70

R DENOTES AN OBS. WITH A LARGE ST.RES.

X DENOTES AN OBS. WHOSE X VALUE GIVES IT LARGE INFLUENCE.

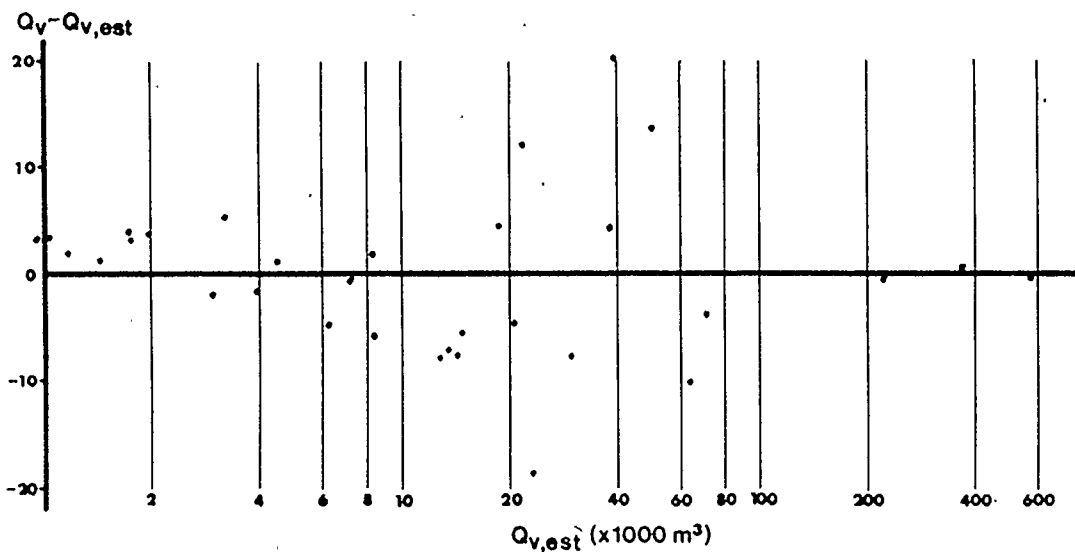


figure 4.2c Residual Plot for Table 4.1c

intense the storm, the more runoff it will tend to produce from throughflow or overland flow (Betson & Marius, 1969). It was decided that the maximum 24 hour rainfall intensity would be used. This quantity is readily available (section 3.2). Also, if the average intensity was used, very low daily rainfall totals would lessen the effect of the high intensities. A graph of Q_v vs I (figure 4.3) illustrates the importance of this parameter. Therefore, I was added to the data set and the list of second and third order terms was re-assessed. This brought the total number of possible predictors up to 32.

A trial third order model was identified (table 4.1c). Figure 4.2c indicates that the residuals are random. Therefore, the parameters which are needed and the order of the model are clear. However, table 4.1c shows that while the model is a significant fit, it is a poor predictor in the case of several events. This problem can be attributed to the values of Q_v since at this stage in the analysis, Q_v was only a first approximation. This led to the development of the base flow separation method discussed in section 3.3.

Once the base flow separation method had been applied and the stormflow volume for each

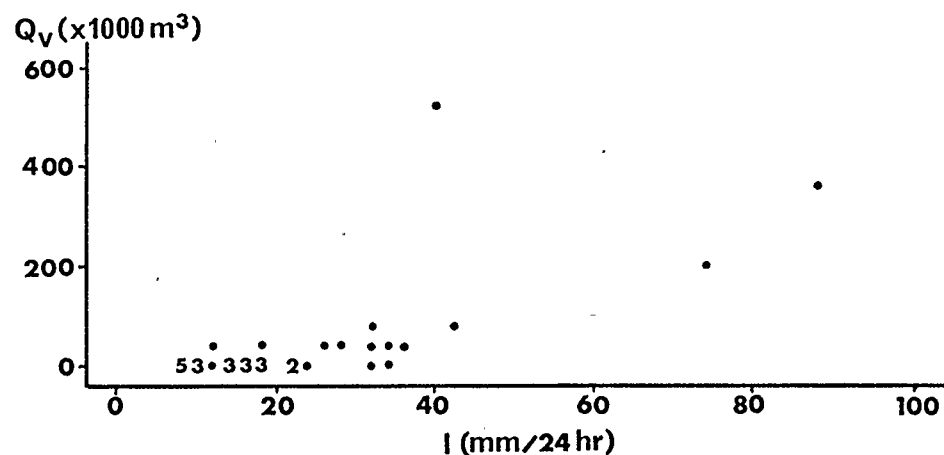


figure 4.3 A Graph of Q_v vs I

event calculated, the parameter optimization was complete. At this time, the data set was finalized (table 3.5). Stepwise regression was used to select the best set of predictors for a second and a third order model, and the two models were identified in the usual way (table 4.2). The purpose of this was to perform an F test to demonstrate which was the most parsimonious model. The terms selected for the second order model were P_V , P_V^2 , I , $P_V I$ and BI . The terms to be entered in the third order model were P_V , P_V^2 , B , B^3 , $P_V I$, $P_V BI$ and BSI . To perform the F test properly, the set of second order predictors must be a subset of the third order set. Therefore, the terms I and BI were added to the set of third order terms, even though they were insignificant when combined with the terms already in the model.

The F test is given as follows:

H_0 : second order is adequate

H_1 : third order is significantly better

$$F = \frac{[SSE(2^{nd}) - SSE(3^{rd})] / [df(2^{nd}) - df(3^{rd})]}{MSE(3^{rd})}$$

$$F = 33.91$$

$$F_{crit} = F(df_{numerator} - df_{denominator})$$

With confidence level at 95%, $F_{crit} = 2.76$

$F > F_{crit}$, therefore reject H_0

Thus, it is demonstrated that the third order model is significantly better than the second order model. The third order model was rerun without the insignificant terms I and BI (table 4.2c). The residual plot for this model is given in figure 4.4. A lack of fit test cannot be performed on this model. Since the data set is not an experimental one, replicates are not available for such a test. Since the residuals are randomly distributed and close to zero, it is safe to assume that there is no significant lack of fit.

At first the model appears to be a good one. The residuals are small, $r^2 = 100\%$, and the standard deviation at 1.847 is 3.9% of the mean stormflow. However, there is a serious problem with the model. This problem becomes apparent when certain pairs of low precipitation events are examined, such as 17&18 and 30&31. The events in each pair have baseflows which are low and

TABLE 4.2a: SELECTION OF SECOND ORDER MODEL FROM OPTIMIZED DATA SET FOR TEST OF PARSIMONY
Stepwise Regression of Qv on 13 Predictors, with N=35:

STEP	1	2	3	4	5
CONSTANT	-3.501	-13.797	6.427	9.042	12.665
P_v^2	0.00018	0.00016	0.00020	0.00020	0.00018
T-RATIO	26.96	39.58	39.09	44.05	31.26
BI		2.84	3.51	3.04	3.34
T-RATIO		9.78	21.52	15.88	17.71
P_v			-0.0911	-0.1018	-0.0822
T-RATIO			-9.64	-11.83	-8.65
$P_v I$				0.00038	0.00076
T-RATIO				3.55	5.16
I					
-0.62					
T-RATIO					-3.32
S	23.1	11.7	5.96	5.08	4.40
r^2	95.66	98.91	99.73	99.81	99.86

Regression Analysis:

COLUMN	COEFFICIENT	ST.DEV. OF COEF.	T-RATIO= COEF/S.D.
--	12.665	2.200	5.76
P_v^2	0.000183261	0.000005862	31.26
BI	3.3380	0.1885	17.70
P_v	-0.082242	0.009507	-8.65
$P_v I$	0.0007599	0.0001472	5.16
I	-0.6189	0.1864	-3.32
			t _{crit} = 2.045

S = 4.40, df = 29, r^2 = 99.8%

Analysis of Variance:

DUE TO	DF	SS	MS=SS/DF	F	F _{crit}
REGRESSION	5	403521.7	80704.3	=4160.0	=F(.05,5,29)
RESIDUAL	29	561.5	19.4		
TOTAL	34	404083.2			=2.55

**TABLE 4.2b: SELECTION OF THIRD ORDER MODEL FROM
OPTIMIZED DATA SET FOR TEST OF PARSIMONY**
Stepwise Regression of Q_v on 32 Predictors, with $N=35$:

STEP	1	2	3	4	5	6	7
CONSTANT	7.0129	-0.5904	5.8003	6.4851	4.3340	7.7167	7.9839
$P_v^2 B$	0.00049	0.00039	0.00037	0.00037	0.00045	0.00047	17.08
T-RATIO	37.70	50.19	45.25	43.12	20.51	23.45	17.08
$P_v I$		0.00112	0.00156	0.00165	0.00181	0.00180	0.00224
T-RATIO		15.78	10.83	11.41	14.80	16.76	8.41
I			-0.48	-0.60	-0.54	-0.52	-0.68
T-RATIO			-3.38	-4.04	-4.52	-4.91	-5.00
$B^2 S$				0.35	2.223.14	2.87	
T-RATIO				2.01	4.73	6.16	5.60
$P_v BS$					-0.00266	-0.00298	-0.00254
T-RATIO					-4.18	-5.23	-4.24
B						-31.0	-27.9
T-RATIO						-3.07	-2.83
$I^2 P_v$							-0.00000
T-RATIO							-1.80
S^2	16.7	5.71	4.96	4.73	3.80	3.35	3.22
r	97.73	99.74	99.81	99.83	99.90	99.92	99.93
STEP	8	9	10	11	12	13	14
CONSTANT	12.40	16.64	16.80	17.60	16.58	15.22	15.27
$P_v^2 B$	0.00041	0.00041	0.00028	0.00025	0.00010	0.00007	
T-RATIO	15.71	16.90	6.15	8.19	1.71	1.38	
$P_v I$	0.00341	0.00366	0.00255	0.00255	0.00125	0.00061	0.00026
T-RATIO	6.08	6.95	4.60	4.58	1.97	2.22	2.36
I	-0.894	-1.047	-0.666	-0.658	-0.349	-0.182	-0.083
T-RATIO	-5.72	-6.64	-3.69	-3.68	-1.90	-1.69	-1.02
$B^2 S$	2.56	1.60	0.50				
T-RATIO	5.20	2.62	0.80				
$P_v BS$	-0.00215	-0.00223	-0.00099	-0.00063	-0.00059	-0.00057	-0.00038
T-RATIO	-3.71	-4.16	-1.65	-1.60	-1.74	-1.68	-1.20
B	-23.7	-64.3	-86.4	-93.6	-85.2	-87.4	-81.7
T-RATIO	-2.54	-3.37	-4.87	-6.19	-6.41	-6.61	-6.39
$I^2 P_v$	-0.00001	-0.00001	-0.00001	-0.00001	-0.00000		
T-RATIO	-2.92	-3.42	-1.87	-1.86	-1.12		
P_v^2	-0.0240	-0.0251	-0.0438	-0.0476	-0.0663	-0.0650	-0.0765
T-RATIO	-2.32	-2.63	-4.35	-5.43	-6.89	-6.77	-15.44
B^2		156	252	291	283	289	277
T-RATIO		2.38	3.96	6.98	7.85	8.12	7.89
P_v^2			0.00005	0.00006	0.00013	0.00015	0.00018
T-RATIO			3.18	4.37	5.12	6.66	36.74
$P_v BI$					0.00223	0.00223	0.00297
T-RATIO					3.12	3.61	9.63
S^2	2.99	2.75	2.36	2.34	2.01	2.02	2.06
r	99.94	99.95	99.97	99.97	99.98	99.97	99.97

TABLE 4.2b: (continued)

STEP	15	16	17	18	19
CONSTANT	14.60	14.22	14.82	12.47	12.04
P_v^2					
T-RATIO					
$P_v I$	0.00021	0.00026	0.00021	0.00029	0.00030
T-RATIO	2.13	3.08	2.52	3.18	3.68
$P_v SI$	-0.00035				
T-RATIO	-1.11				
B	-79.8	-74.5	-87.9	-33.7	-24.3
T-RATIO	-6.31	-6.34	-6.80	-1.05	-4.03
$I P_v^2$					
T-RATIO					
P_v^2	-0.0792	-0.0782	-0.0750	-0.0786	-0.0791
T-RATIO	-18.83	-18.91	-17.74	-17.50	-19.72
B^2	271	245	293	42	
T-RATIO	7.83	9.51	8.66	0.30	
P_v^2	0.00018	0.00018	0.00017	0.00017	0.00017
T-RATIO	39.73	87.34	60.55	62.42	65.61
$P_v BI$	0.00294	0.00269	0.00349	0.00355	0.00355
T-RATIO	9.57	12.75	7.94	8.40	8.54
BSI			-0.0103	-0.0147	-0.0152
T-RATIO			-2.04	-2.72	-2.99
B^3				353	409
T-RATIO				1.84	9.37
S	2.06	2.07	1.96	1.88	1.85
r^2	99.97	99.97	99.97	99.98	99.98

Regression Analysis:

COLUMN	COEFFICIENT	ST.DEV. OF COEF.	T-RATIO= COEF./S.D.
--	13.888	2.028	6.85
P_v^2	-0.078994	0.005086	-15.53
P_v	0.000172695	0.000003593	48.07
B	-30.407	8.888	-3.42
B^3	414.08	44.25	9.36
$P_v I$	0.0004659	0.0001676	2.78
PBI	0.0030782	0.0006569	4.69
BSI	-0.016205	0.005402	-3.00
I	-0.1688	0.1392	-1.21
BI	0.5365	0.6051	0.89

 $t_{crit}=2.06$

$S = 1.863$, $df = 25$, $r^2 = 100\%$
Analysis of Variance:

DUE TO	DF	SS	MS=SS/DF	F
REGRESSION	9	403996.4	44888.5	=12825.3
RESIDUAL	25	86.8	3.5	=F(.05,9,25)
TOTAL	34	404083.2		=2.28

TABLE 4.2c: THIRD ORDER MODEL

Regression Analysis:

The regression equation is:

$$Q_v, \text{est} = 12.04 - 7.9 \times 10^{-2} P_v - 3 P_v^{-3} + 1.73 \times 10^{-4} P_v^2 - 24.28 B + 409.2 B^3 \\ + 2.98 \times 10^{-4} P_v I + 3.55 \times 10^{-3} P_v BI - 1.52 \times 10^{-2} BSI$$

COLUMN	COEFFICIENT	ST.DEV. OF COEF.	T-RATIO COEF/S.D.
--	12.037	1.158	10.40
P_v	-0.079114	0.004013	-19.72
P_v^2	0.000172687	0.000002682	65.61
B	-24.283	6.032	-4.03
B^3	409.20	43.67	9.37
$P_v I$	0.00029794	0.00008103	3.68
$P_v BI$	0.0035488	0.0004157	8.54
BSI	-0.015185	0.005087	-2.99
			$t_{\text{crit}} = 2.052$

$$S = 1.847, \text{ df} = 27, r^2 = 100\%$$

Analysis of Variance:

DUE TO	DF	SS	MS=SS/DF	F
REGRESSION	7	403991.0	57713.0	=16974.4
RESIDUAL	27	92.1	3.4	=F(.05,7,27)
TOTAL	34	404083.3		=2.37

EVENT	P_v	Q_v	PRED. Q_v VALUE	ST.DEV. PRED. Y	RESIDUAL	ST.RES.
1	1347	361.878	361.375	1.733	0.502	0.79 X
2	388	27.874	26.816	0.871	1.058	0.65
3	408	35.308	33.907	0.756	1.401	0.83
4	318	11.419	12.327	0.536	-0.908	-0.51
5	294	5.868	5.333	0.610	0.535	0.31
6	427	12.959	13.083	0.486	-0.124	-0.07
7	334	18.950	20.277	1.081	-1.327	-0.89
8	119	5.624	3.296	0.547	2.328	1.32
9	608	32.276	35.057	0.647	-2.781	-1.61
10	867	218.105	218.872	1.716	-0.767	-1.12 X
11	463	65.162	65.010	1.377	0.152	0.12 X
12	143	18.827	17.163	0.913	1.664	1.04
13	351	7.702	9.656	0.624	-1.954	-1.12
14	117	4.988	3.585	0.623	1.403	0.81
15	642	50.810	47.811	0.711	2.999	1.76
16	84	1.467	5.135	0.707	-3.668	-2.15 R
17	172	4.157	2.849	0.572	1.308	0.74
18	79	3.179	5.646	0.732	-2.467	-1.45
19	210	4.646	2.965	0.435	1.681	0.94
20	174	2.543	3.496	0.516	-0.953	-0.54
21	339	25.796	25.918	0.903	-0.122	-0.08
22	392	9.047	12.066	0.571	-3.019	-1.72
23	84	5.722	4.706	0.610	1.016	0.58
24	498	16.138	18.127	0.624	-1.989	-1.14
25	1793	534.259	534.436	1.836	-0.177	-0.87 X
26	738	60.884	62.489	1.201	-1.605	-1.14
27	585	31.053	28.660	0.728	2.393	1.41
28	211	3.448	1.970	0.447	1.478	0.82
29	264	9.536	9.806	0.907	-0.270	-0.17
30	208	4.157	3.115	0.629	1.042	0.60
31	139	3.668	3.962	0.689	-0.294	-0.17
32	175	4.401	5.175	0.861	-0.774	-0.17
33	683	54.282	52.555	1.004	1.727	1.11
34	432	12.226	11.897	0.575	0.329	0.19
35	265	4.646	4.462	0.436	0.184	0.10

R DENOTES AN OBS. WITH A LARGE ST. RES.

X DENOTES AN OBS. WHOSE X VALUE GIVES IT LARGE INFLUENCE.

similar. In each pair of events, the model assigns the lower $Q_{V,est}$ to the event with the higher P_V . The most significant terms in the model are P_V and P_V^2 . This quadratic is plotted in figure 4.5. Examination of the quadratic reveals the reason for this discrepancy. The value of the quadratic function increases as P_V declines from 250,000 m^3 to 0, causing $Q_{V,est}$ to increase correspondingly for a given B, S and I. This is physically impossible. Clearly, the larger storms, which are statistically more important, are influencing the model to such an extent that the smaller storms are not properly represented. Since the model must be realistic, it is necessary to break the data set into two groups and model each separately.

The data set can be grouped according to either (1) P_V , or (2) B.

1. The obvious dividing line on the basis of P_V is the lowest point on the quadratic (figure 4.5), 250,000 m^3 . The events were divided into two groups, those above and those below that level of P_V . Each group was modeled separately (table 4.3). Plots of Q_V vs P_V , and residuals are presented in figure 4.6. Note that below 250,000 m^3 , P_V does not actually enter into the model. This would suggest that when the volume of precipitation is low, stormflow depends entirely upon antecedent basin storage, and actual differences in the volume of precipitation are negligible.

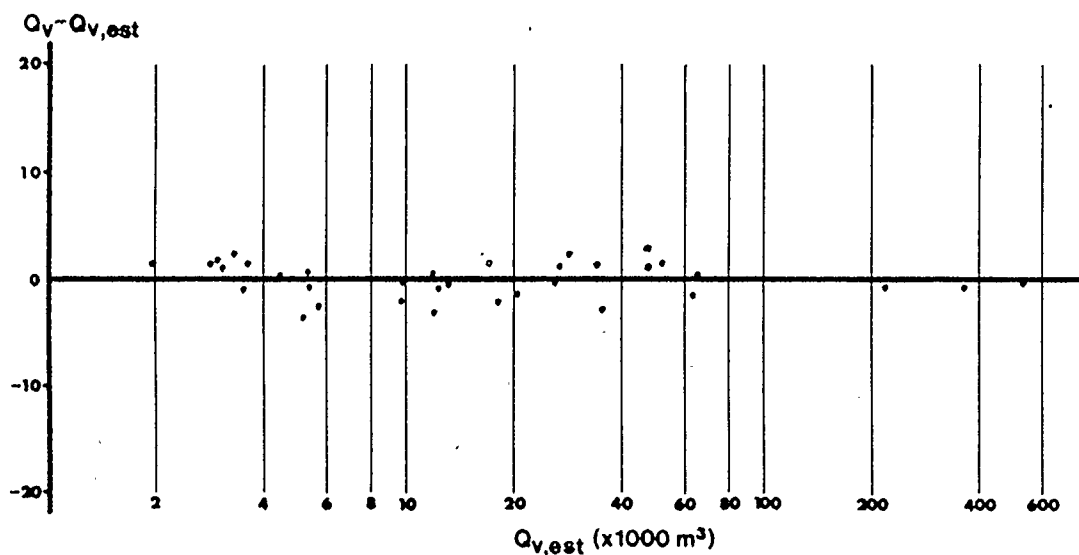


figure 4.4 Residual Plot for Table 4.2c

$$f = 12.04 - 7.91 \times 10^{-2} P_V + 1.727 \times 10^{-4} P_V^2$$

(1000 m³)

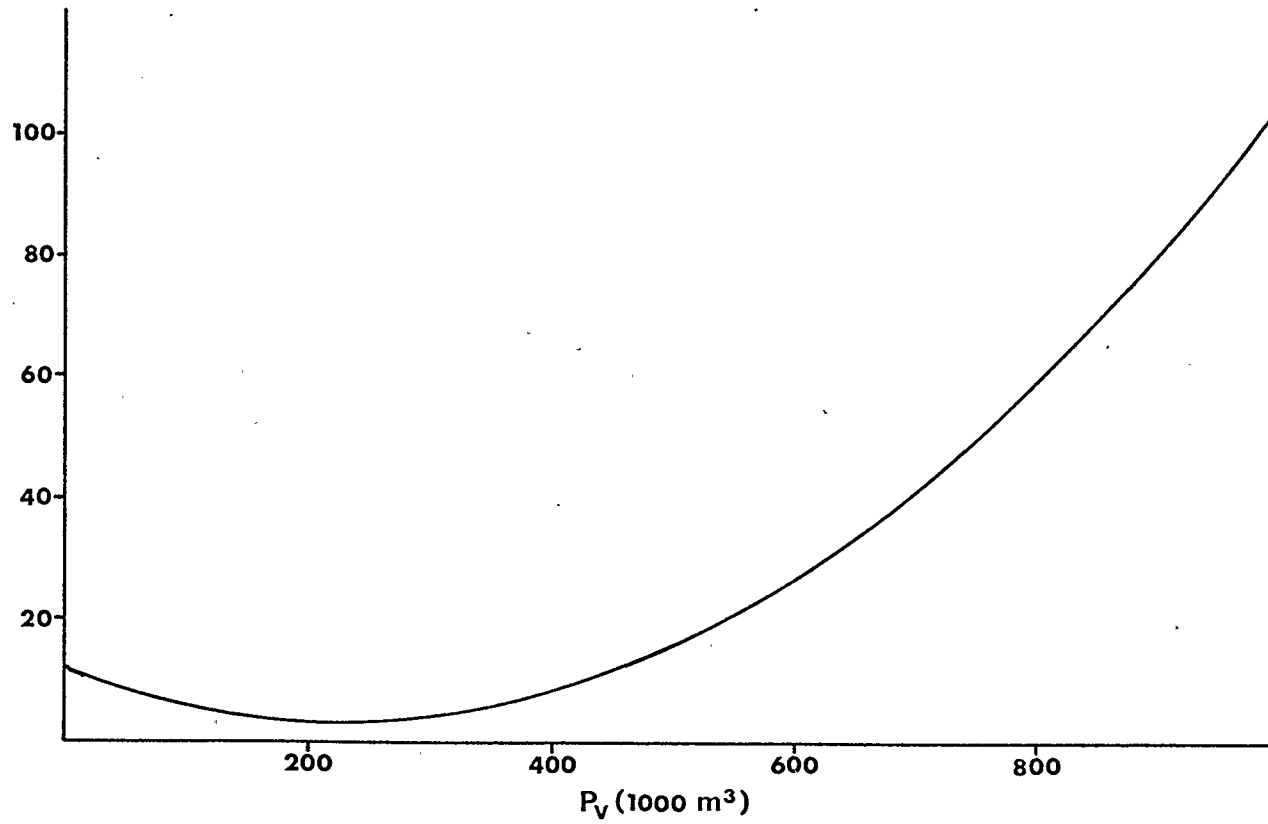


figure 4.5 A Quadratic Function of P_V

TABLE 4.3a: (continued)

Regression Analysis:

The regression equation is:

$$Q_v,est = -8.97 + 1.44 \times 10^{-4} P_v^2 B + 8.21 \times 10^{-7} P_v^2 I + 8.55 \times 10^{-6} P_v^2 + 247.53 B^3 + 1.52 \times 10^{-2} I B - 4.85 \times 10^{-6} P_v SI$$

COLUMN	COEFFICIENT	ST.DEV. OF COEF.	T-RATIO= COEF/S.D.
---	-8.9659	0.9895	-9.06
$P_v^2 B$	0.00014360	0.00001211	11.86
$P_v^2 I$	0.0000008205	0.0000001173	6.99
B^3	247.53	19.46	12.72
P_v^2	0.000085451	0.000005389	15.86
$I B$	0.0151193	0.001856	8.19
$P_v SI$	-0.000004846	0.000002082	-2.33

$t_{crit} = 2.145$

S = 1.740, df = 14, $r^2 = 100\%$

Analysis of Variance

DUE TO	DF	SS	MS=SS/DF	F	
REGRESSION	6	361287.5	60214.6		=20071.5
RESIDUAL	14	42.4	3.0	F_{crit}	=F(.05,6,14)
TOTAL	20	361329.9			=2.85

Further Analysis of Variance:

SS Explained by each Variable when Entered in the Order Given

DUE TO	DF	SS
REGRESSION	6	361287.5
$P_v^2 B$	1	352671.2
$P_v^2 I$	1	7334.3
B^3	1	335.0
P_v^2	1	679.9
$I B$	1	250.7
$P_v SI$	1	16.4

EVENT	$P_v^2 B$	Q_v	PRED. Q_v VALUE	ST.DEV. PRED.Y	RESIDUAL	ST.RES
1	584986	361.878	361.914	1.731	-0.036	-0.21 X
2	48896	27.874	26.528	0.634	1.346	0.83
3	66049	35.308	35.684	0.601	-0.376	-0.23
4	22830	11.419	10.916	0.711	0.503	0.32
5	20017	5.868	5.029	0.676	0.839	0.52
6	18612	12.959	12.518	0.528	0.441	0.27
7	39531	18.950	19.325	0.678	-0.375	-0.23
9	38507	32.276	35.516	0.657	-3.240	-2.01 R
10	401799	218.105	218.316	1.710	-0.211	-0.66 X
11	108068	65.162	64.784	1.341	0.378	0.34
13	6972	7.702	5.917	0.604	1.785	1.09
15	62701	50.810	49.009	0.773	1.801	1.16
21	47818	25.796	26.126	0.880	-0.330	-0.22
22	27338	9.047	12.520	0.602	-3.473	-2.13 R
24	21790	16.138	17.928	0.651	-1.790	-1.11
25	1164534	534.259	534.221	1.738	0.038	0.49 X
26	40061	60.884	61.198	1.365	-0.314	-0.29
27	28093	31.053	28.580	0.712	2.473	1.56
28	22873	9.536	9.615	0.624	-0.079	-0.05
33	83139	54.282	53.641	1.409	0.641	0.63
34	20618	12.226	12.245	0.532	-0.019	-0.01

R DENOTES AN OBS. WITH A LARGE ST. RES.

X DENOTES AN OBS. WHOSE X VALUE GIVES IT LARGE INFLUENCE

TABLE 4.3b: MODEL FOR $P_v < 250$.
Stepwise Regression of Q_v on 32 Predictors, with $N=14$:

STEP	1	2	3
CONSTANT	3.393	5.672	5.709
$B^2 S$	1.15	4.11	3.76
T-RATIO	6.16	5.36	5.23
BS		-1.18	-1.32
T-RATIO		-3.91	-4.66
S^3			0.00002
T-RATIO			1.85
S^2	2.10	1.42	1.28
r	76.00	89.96	92.53

Regression Analysis:

The regression equation is:

$$Q_{v,est} = 5.67 + 4.11 B^2 S - 1.18 BS, \text{ where } P_v < 250$$

COLUMN	COEFFICIENT	ST.DEV. OF COEF.	T-RATIO= COEF/S.D.
--	5.6723	0.7197	7.88
$B^2 S$	4.1120	0.7668	5.36
BS	-1.1752	0.3004	-3.91

$t_{crit} = 2.052$

$$S = 1.417, df = 11, r^2 = 88.1\%$$

Analysis of Variances:

DUE TO	DF	SS	MS=SS/DF	F	
REGRESSION	2	197.913	98.956		=49.31
RESIDUAL	11	22.077	2.007		=F(.05,2,11)
TOTAL	13	219.990		F_{crit}	=3.91

Further Analysis of Variance:

SS Explained by each Variable when Entered in the Order Given

DUE TO	DF	SS
REGRESSION	2	197.913
$B^2 S$	1	167.194
BS	1	30.718

EVENT	$B^2 S$	Q_v	PRED. Q_v VALUE	ST.DEV. PRED.Y	RESIDUAL	ST.RES.
8	0.2	5.624	4.096	0.425	1.528	1.13
12	11.6	18.827	18.450	1.400	0.377	1.74 X
14	0.3	4.988	2.352	0.537	2.636	2.01 R
16	2.4	1.467	2.913	0.928	-1.446	-1.35 X
17	0.1	4.157	4.491	0.490	-0.334	-0.25
18	0.1	3.179	4.527	0.496	-1.348	-1.02
19	0.2	4.646	4.131	0.431	0.515	0.38
20	0.8	2.543	4.270	0.388	-1.727	-1.27
23	0.7	5.722	3.818	0.404	1.904	1.40
28	0.3	3.448	4.065	0.420	-0.617	-0.46
30	0.0	4.157	4.822	0.550	-0.665	-0.51
31	0.1	3.668	4.435	0.488	-0.767	-0.58
32	3.9	4.401	4.847	0.908	-0.446	-0.41
35	0.1	4.646	4.256	0.451	0.390	0.29

R DENOTES AN OBS. WITH A LARGE ST.RES.

X DENOTES AN OBS. WHOSE X VALUE GIVES IT LARGE INFLUENCE

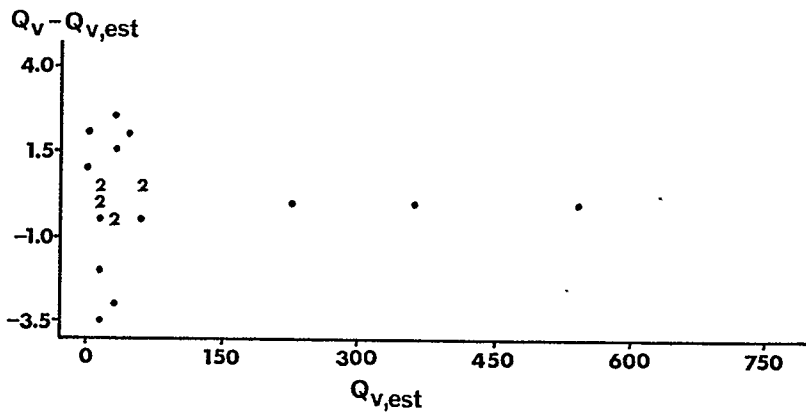
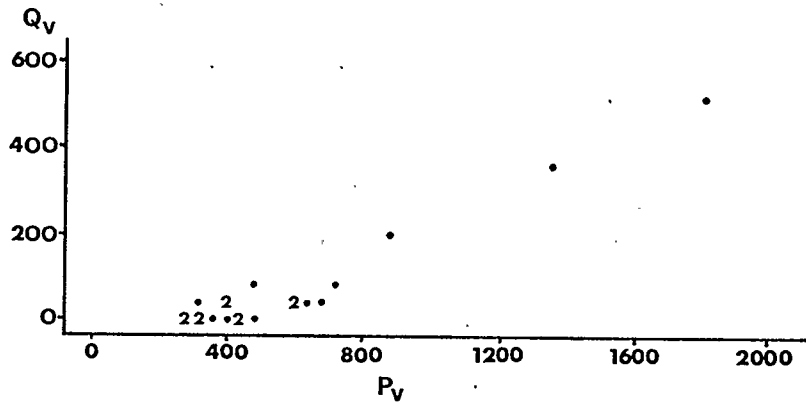


figure 4.6a Plots of Q_v vs P_v and Residuals for Table 4.3a

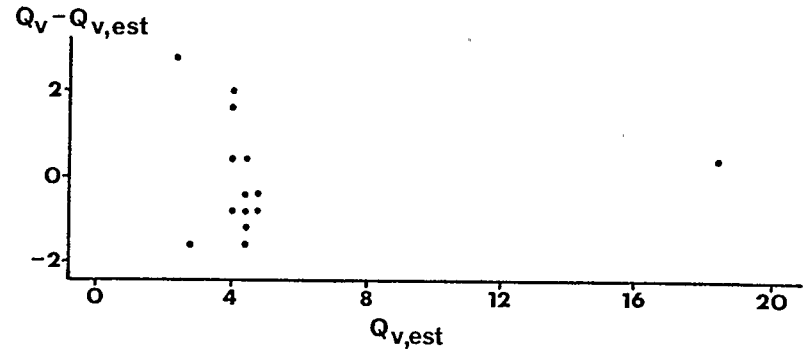
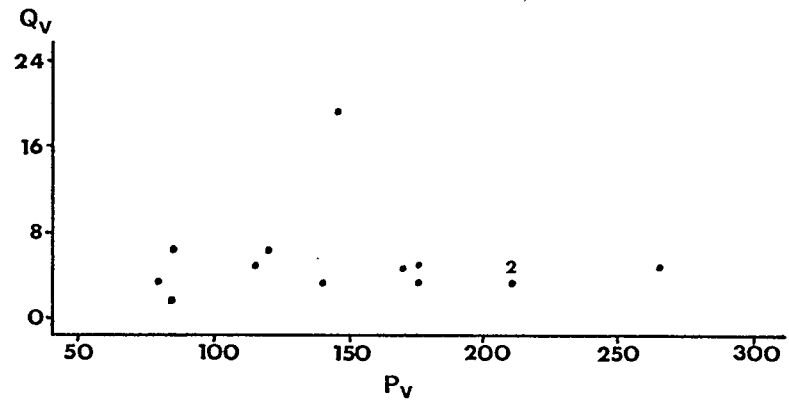


figure 4.6b Plots of Q_v vs P_v and Residuals for Table 4.3b

2. There are two possible ways to group the events according to B . The model in figure 4.3c contains a cubic function in B . This function has been plotted (figure 4.7). The lowest point on this curve is at $B = .14 \text{ m}^3/\text{sec}$. Therefore, this is one obvious choice for a dividing line between the two groups. Another possibility is to use the same base flow class divisions used in section 3.3, that is, to split the events into low flow ($B < 0.2 \text{ m}^3/\text{sec}$) and middle to high flow ($B > 0.2 \text{ m}^3/\text{sec}$) groups. Models were identified for each grouping, and the latter grouping of events provided a better overall fit to the data. The model is shown in table 4.4. Plots of Q_V vs P_V and residuals are also given (figure 4.8). This is an improvement over the model obtained by grouping the events according to P_V (table 4.3). The overall fit is improved for both low and high groups, P_V is an important factor regardless of the base flow, and the model does not appear to contravene any principles of hydrology. Clearly then, it is deemed appropriate to break the events into groups according to their initial base flow. A major advantage to this model is the consistency with procedures established in chapter 2.

To summarize the results of the analysis, an iterative process of model identification and

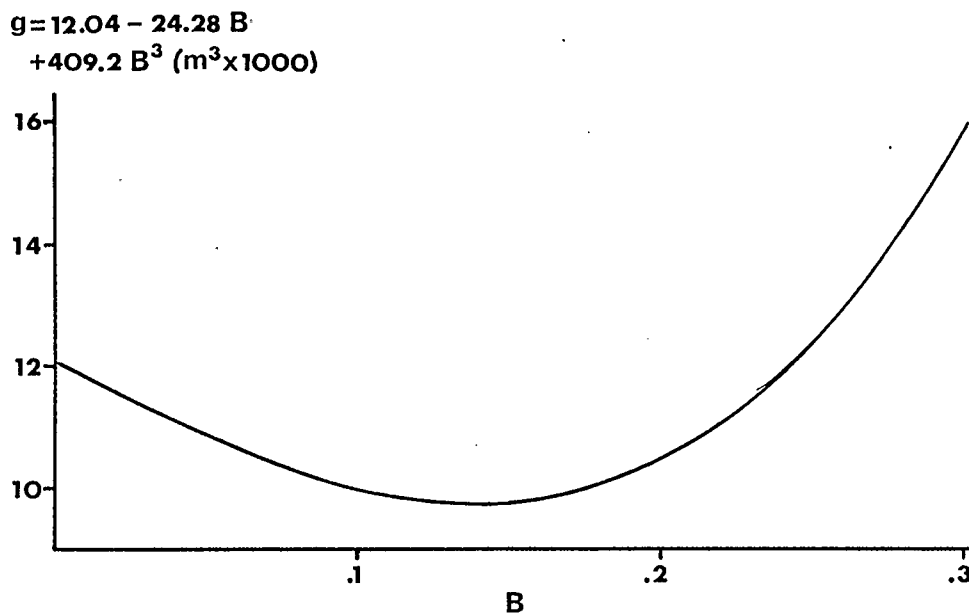


figure 4.7 A Cubic Function of B

TABLE 4.4a: Model for $B < 0.2m^3/sec$
 Stepwise Regression of Q_v on 32 Predictors, with $N=20$:

STEP	1	2	3	4	5	6	7
CONSTANT	2.606	1.888	6.039	7.298	9.233	9.216	9.320
P_v^3	0.00000	0.00000	0.00000	0.00000	0.00000	0.00000	0.00000
T-RATIO	25.97	15.81	15.17	16.34	13.68	32.48	11.15
$I^2 B$		0.052	0.056	0.074	0.196	0.191	0.236
T-RATIO		3.08	4.44	5.11	5.59	8.89	7.99
P_v^2			-0.0216	-0.0176	0.0013		
T-RATIO			-3.83	-3.18	0.19		
I				-0.175	-0.611	-0.591	-0.610
T-RATIO				-2.04	-4.53	-7.48	-8.40
$P_v B^2$					-0.86	-0.83	-1.11
T-RATIO					-3.66	-5.83	-5.81
$P_v^2 I$							0.00000
T-RATIO							-2.02
S^2	3.10	2.56	1.90	1.74	1.29	1.24	1.13
r	97.40	98.33	99.13	99.32	99.65	99.65	99.73
STEP	8						
CONSTANT	10.15						
P_v^3	0.00000						
T-RATIO	6.38						
$I^2 B$	0.230						
T-RATIO	8.07						
P_v^2							
T-RATIO							
I	-0.704						
T-RATIO	-7.63						
$P_v B^2$	-1.00						
T-RATIO	-5.11						
$P_v^2 I$	-0.00000						
T-RATIO	-2.02						
$I^2 P_v$	0.00003						
T-RATIO	1.54						
S^2	1.08						
r	99.77						

TABLE 4.4a: (continued)

Regression Analysis:

The regression equation is:

$$Q_v \text{ est} = 9.22 - 0.59 I + 1.39 \times 10^{-7} P_v^3 + 0.19 I^2 B - 0.83 B^2 P_v$$

where $B < 0.2m / \text{sec}$.

COLUMN	COEFFICIENT	ST.DEV. OF COEF.	T-RATIO= COEF/S.D.
--	9.216	1.042	8.84
P_v^3	1.392746E-07	4.287584E-09	32.48
$I^2 B$	0.19130	0.02151	8.89
I	-0.59067	0.07900	-7.48
$P_v B^2$	-0.8256	0.1415	-5.83
			$t_{\text{crit}} = 2.131$

S = 1.245, df = 15, $r^2 = 99.6\%$ **Analysis of Variance:**

DUE TO	DF	SS	MS=SS/DF	F	
REGRESSION	4	6640.955	1660.239		
RESIDUAL	15	23.247	1.550	F	=1071.1
TOTAL	19	6664.202		F_{crit}	=F(.05,4,15)
				F	=3.06

Further Analysis of Variance:

SS Explained by each Variable when Entered in the Order Given

DUE TO	DF	SS
REGRESSION	4	6640.955
P_v^3	1	6490.921
$I^2 B$	1	62.002
I	1	35.299
$P_v B^2$	1	52.733

EVENT	P_v^3	Q_v	PRED. Q_v VALUE	ST.DEV. PRED. Y	RESIDUAL	ST.RES.
6	78062525	12.959	12.822	0.368	0.137	0.11
8	1701354	5.624	5.154	0.518	0.470	0.42
9	223043364	32.276	32.780	0.559	-0.504	-0.45
13	43235051	7.702	6.786	0.933	0.916	1.11 X
14	1601326	4.988	4.955	0.496	0.033	0.03
15	264937090	50.810	50.001	0.927	0.809	0.97 X
17	5080199	4.157	4.357	0.399	-0.200	-0.17
18	489136	3.179	4.919	0.512	-1.740	-1.53
19	9275428	4.646	4.424	0.404	0.222	0.19
22	60036900	9.047	10.006	0.812	-0.959	-1.02
23	583564	5.722	4.580	0.456	1.142	0.99
24	123847064	16.138	18.101	0.470	-1.963	-1.70
26	401569950	60.884	61.969	1.032	-1.085	-1.56 X
27	200162613	31.053	28.301	0.722	2.752	2.71 R
28	9360313	3.448	4.607	0.394	-1.159	-0.98
30	8962749	4.157	3.771	0.361	0.386	0.32
31	2713596	3.668	2.537	0.373	1.131	0.95
33	318406301	54.282	54.182	0.929	0.100	0.12 X
34	80708940	12.226	12.012	0.483	0.214	0.19
35	18614681	4.646	5.347	0.525	-0.701	-0.62

R DENOTES AN OBS. WITH A LARGE ST. RES.

X DENOTES AN OBS. WHOSE X VALUE GIVES IT LARGE INFLUENCE.

TABLE 4.4b: MODEL FOR $B > 0.2m^3/sec$
Stepwise Regression of Q_v on 32 Predictors, with N=15:

STEP	1	2	3	4	5	6	7
CONSTANT	0.49317	1.05133	1.75497	-3.18007	-2.09171	0.00285	-1.05044
$P_v^2 B$	0.00049	0.00039	0.00036	0.00034	0.00037	0.00040	0.00040
T-RATIO	24.79	45.66	21.89	19.44	25.69	27.26	38.85
$P_v S I$		0.00001	0.00002	0.00003	0.00004	0.00005	0.00004
T-RATIO		14.19	5.45	6.38	8.99	11.75	7.89
$I S^2$			-0.00009	-0.00016	-0.00030	-0.00030	-0.00030
T-RATIO			-2.05	-3.23	-6.30	-8.21	-11.09
B^2				49	128	97	74
T-RATIO				2.19	5.16	4.24	3.87
$P_v S$					-0.00091	-0.00122	-0.00127
T-RATIO					-3.91	-5.58	-7.79
$S^2 B$						0.0042	0.0071
T-RATIO						2.58	4.43
$P_v I$							0.00078
T-RATIO							2.75
S^2	23.7	5.85	5.19	4.48	2.87	2.25	1.87
r	97.93	99.88	99.92	99.94	99.98	99.99	99.99
STEP	8	9	10				
CONSTANT	0.06212	-1.61537	-1.53497				
$P_v^2 B$	0.00040	0.00041	0.00041				
T-RATIO	41.16	51.99	57.85				
$P_v S I$	0.00004	0.00004	0.00004				
T-RATIO	9.13	12.83	13.88				
$I S^2$	-0.00033	-0.00034	-0.00034				
T-RATIO	-12.21	-18.33	-20.08				
B^2	37	8					
T-RATIO	1.44	0.40					
$P_v S$	-0.00131	-0.00053	-0.00047				
T-RATIO	-9.23	-1.83	-2.02				
$S^2 B$	0.0155	0.0208	0.0221				
T-RATIO	3.28	5.68	14.45				
$P_v I$	0.00088	0.00062	0.00063				
T-RATIO	3.51	3.27	3.59				
S^2	-0.00003	-0.00004	-0.00004				
T-RATIO	-1.86	-3.20	-5.57				
$S^2 P_v$		-0.00001	-0.00001				
T-RATIO		-2.88	-3.86				
S^2	1.43	0.963	0.893				
r	100.00	100.00	100.00				

TABLE 4.4b: (continued:)

Regression Analysis:

The regression equation is:

$$Q_v, \text{est} = -3.15 + 4.14 \times 10^{-4} (P_v I + P_v^2 B) + 4.56 \times 10^{-5} P_v SI \\ - 2.06 \times 10^{-5} S^2 P_v + 2.18 \times 10^{-3} S^2 B - 3.68 \times 10^{-5} S^3 \\ - 3.39 \times 10^{-4} I S \text{ where } B > 0.2 \text{m/sec}$$

COLUMN	COEFFICIENT	ST.DEV. OF COEF.	t_RATIO= COEF/S.D.
--	-3.1481	0.8116	-3.88
$P_v I$	0.0004135	0.0001674	2.47
$P_v^2 B$	0.000413650	0.000008187	50.52
$P_v SI$	0.000045554	0.000003278	13.89
$I S$	-0.00033936	0.00002037	-16.66
$S^2 B$	0.021811	0.001829	11.92
S^3	-0.000036763	0.000008489	-4.33
$S^2 P_v$	-0.000020625	0.000001638	-12.59

t_{crit}=2.365

$$S = 1.072, df = 7, r^2 = 100\%$$

Analysis of Variance:

DUE TO	DF	SS	MS=SS/DF	F	
REGRESSION	7	351926.9	50275.3		
RESIDUAL	7	8.0	1.1	F	=45704.8
TOTAL	14	351934.9		F _{crit}	=F(.05,7,7)
				F	=3.79

Further Analysis of Variance:

SS Explained by each Variable when Entered in the Order Given

DUE TO	DF	SS
REGRESSION	7	351926.9
$P_v I$	1	277922.7
$P_v^2 B$	1	73482.7
$P_v SI$	1	120.5
$I S$	1	113.3
$S^2 B$	1	92.7
S^3	1	12.8
$S^2 P_v$	1	182.4

EVENT	$P_v I$	Q_v	PRED. Q_v VALUE	ST.DEV. PRED. Y	RESIDUAL	ST.RES.
1	117316	361.878	361.838	1.072	0.040	1.17
2	12209	27.874	26.807	0.766	1.067	1.42
3	11824	85.308	37.061	0.466	-1.753	-1.82
4	10244	11.419	11.845	0.709	-0.426	-0.53
5	3803	5.868	6.327	0.527	-0.459	-0.49
7	5348	8.950	19.699	0.504	-0.749	-0.79
10	64725	218.105	218.067	1.069	0.038	0.44
11	15058	65.162	64.796	0.870	0.366	0.58
12	1347	18.827	19.099	1.014	-0.272	-0.78
16	743	1.467	1.382	0.595	0.085	0.10
20	2365	2.543	1.280	0.584	1.263	1.40
21	4177	25.796	24.787	0.630	1.009	1.16
25	72871	534.259	534.272	1.072	-0.013	-0.37
29	4107	9.536	9.764	0.925	-0.228	-0.42
32	3201	4.401	4.368	0.434	0.033	0.03

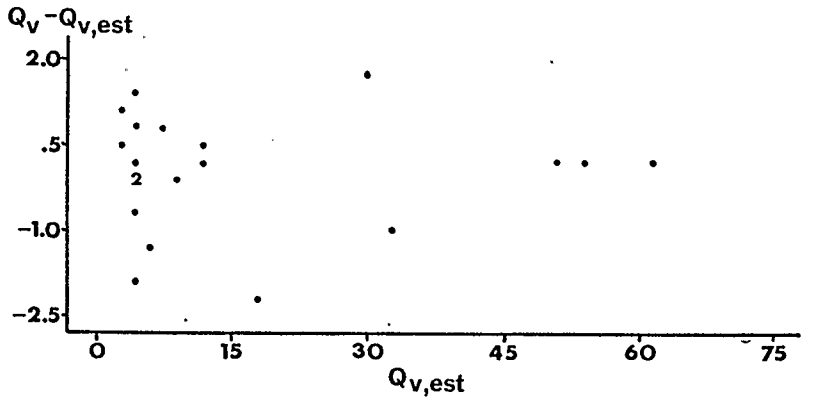
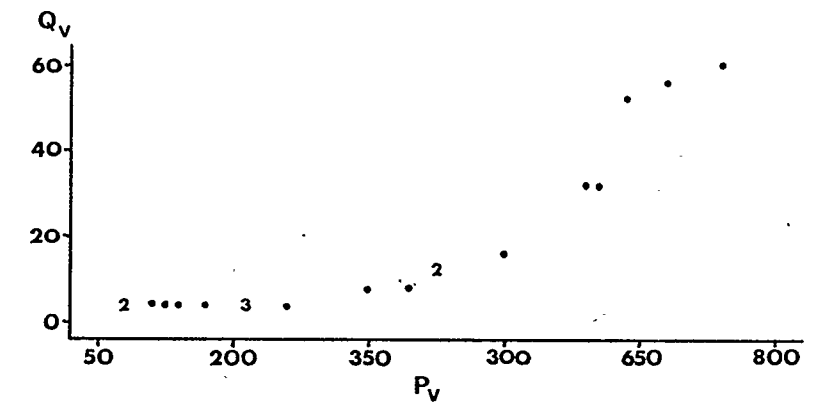


figure 4.8a Plots of Q_v vs P_v and Residuals for Table 4.4a

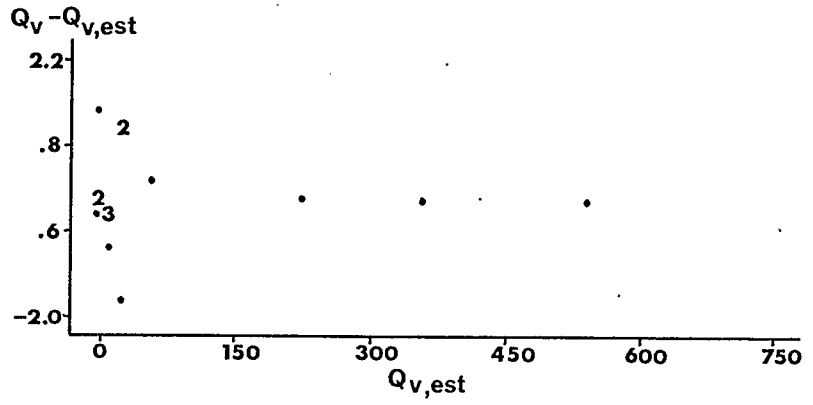
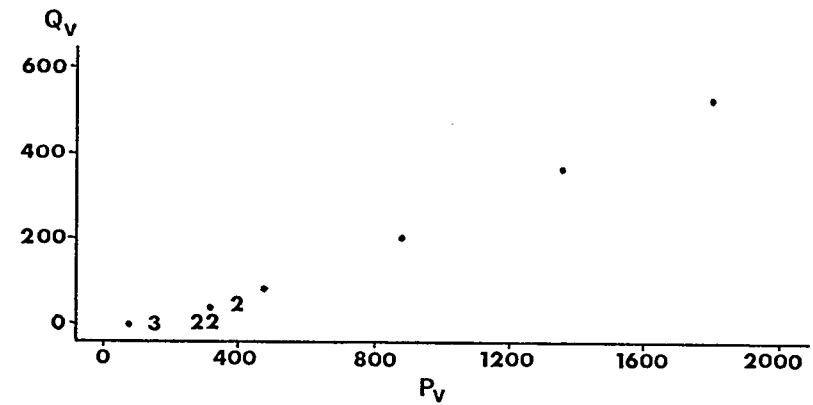


figure 4.8b Plots of Q_v vs P_v and Residuals for Table 4.4b

parameter optimization was used to finalize the data set of 35 events (table 3.6). A third order model of some kind was found to be the most parsimonious. To avoid any discrepancies between the model and basic hydrological principles, the set of events was split into two groups on the basis of initial base flow and each group was modeled separately. The optimum model is given as follows:

Where $B < 0.2 \text{ m}^3/\text{sec}$,

$$Q_{v,\text{est}} = 9.22 - 0.59 I + 1.39 \times 10^{-7} P_v^3 + 0.19 I^2 B - 0.83 B^2 P_v$$

$$\text{standard error} = 1.245 (\times 1000 \text{ m}^3), r^2 = 99.6\%, n = 20 \quad (4.1)$$

Where $B > 0.2 \text{ m}^3/\text{sec}$,

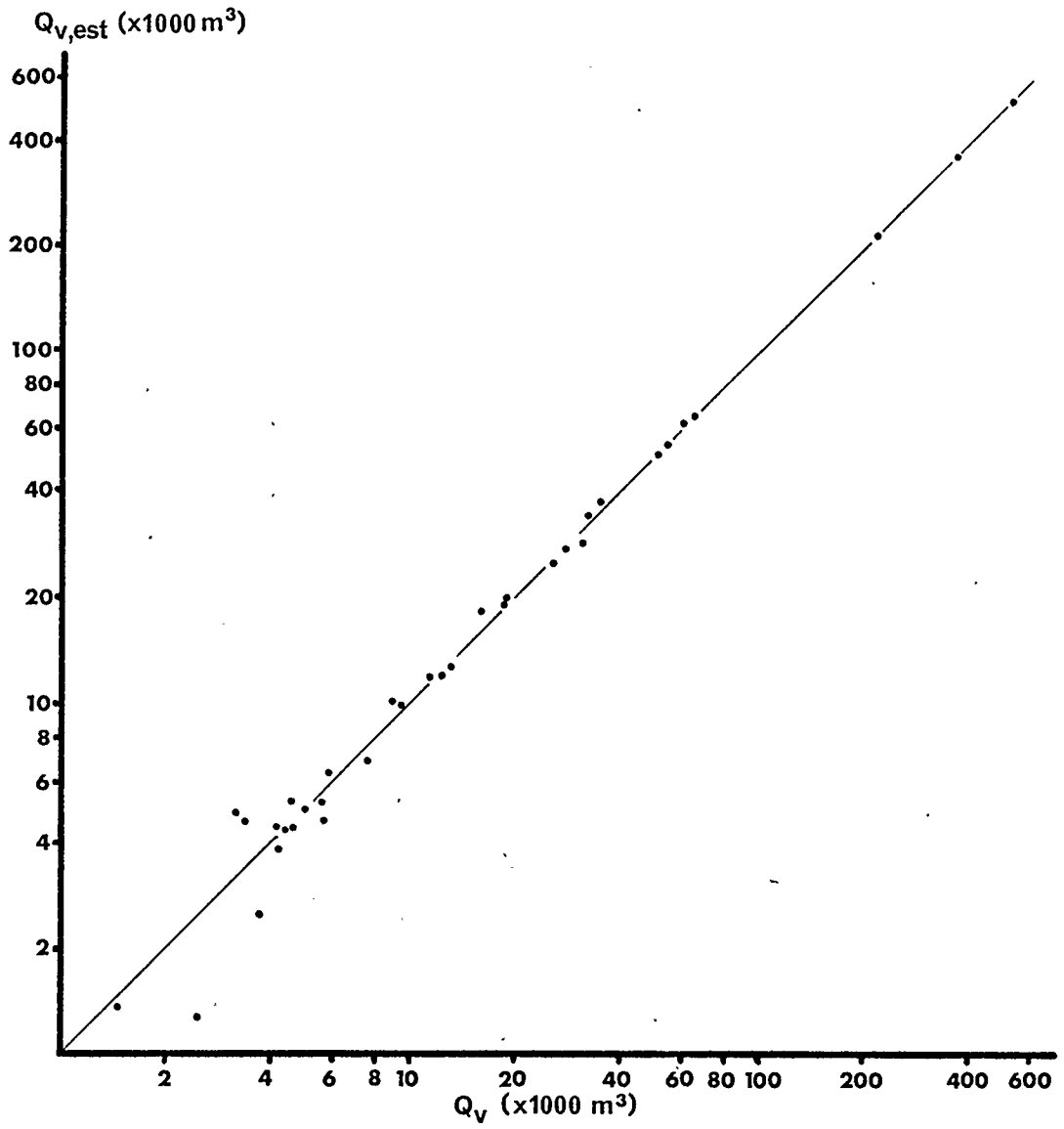
$$Q_{v,\text{est}} = 4.14 \times 10^{-4} (P_v I + P_v^2 B) + 4.56 \times 10^{-5} P_v S I - 2.06 \times 10^{-5} S^2 P_v + 2.18 \times 10^{-2} S^2 B \\ - 3.68 \times 10^{-5} S^3 - 3.39 \times 10^{-4} I^2 S - 3.15$$

$$\text{standard error} = 1.072 (\times 1000 \text{ m}^3), r^2 = 100\%, n = 15 \quad (4.2)$$

The mean error for equation 4.1 is 11.3%, and for equation 4.2 it is 5.9%. A plot of Q_v vs $Q_{v,\text{est}}$ for this model is given in figure 4.9.

This model cannot be extrapolated. It can be used to predict the volume of storm runoff contained in a stormflow event provided that the parameters of the event fall within the range of parameters given in table 3.5. There is a threshold precipitation volume required to produce storm runoff. Because of such factors as interception losses and basin recharge, precipitation which is less than that threshold value may alter the recession limb but will not produce storm runoff. It appears that the threshold precipitation volume is about $80,000 \text{ m}^3$. However, that threshold value will vary inversely with rainfall intensity, for two reasons. As storm intensity increases, the ratio of runoff to basin recharge also increases, and a lower percentage of the rainfall is lost to evaporation. Thus, great care should be used when applying the model to storms where P_v is close to the threshold value.

There is also a threshold intensity required to produce storm runoff. It is possible to have several consecutive days of extremely low intensity rainfall without producing any stormflow. Such

figure 4.9 Q_v vs $Q_{v,est}$

events may cause the hydrograph to rise, but that rise would be due to increased base flow or channel interception. It appears that this threshold intensity is about 3 mm per 24 hours. Both the threshold criteria must be met before stormflow is generated.

A discussion of the model will follow in chapter 5.

CHAPTER 5

DISCUSSION AND CONCLUSIONS

5.1: Discussion

The rainfall-runoff model which is described in chapter 4 was selected because it provided the best fit to the data set. The optimum model is in the form of a pair of equations, 4.1 and 4.2. For any storm event, the volume of direct storm runoff resulting from that event only (Q_v) is predicted as a third order function of the parameters rainfall volume (P_v), maximum 24-hour rainfall intensity (I), and antecedent base flow (B) and soil moisture index (S). The equation to be used is selected according to the value of B for that event.

Since most terms in the model are interactive terms, it is difficult to assess the relative importance of each parameter individually. However, it is possible to state the order of function which each parameter contributes to the overall model. Where B is low (less than $0.2 \text{ m}^3/\text{sec}$), the model contains second order functions of B and I and a third order function of P_v . Soil moisture index is unimportant at this level of base flow. This is perhaps due to two factors:

1. Soil is usually at or near the wilting point at low flow. Low flows tend to occur late in the season when storms tend to be of low volume and far enough apart to allow drying of the soil between events.

2. When the water table is very low, base flow is low. Therefore the volume of unsaturated soil is very large compared to middle or high flow situations, particularly at or near the ridge tops. It is easy to imagine a situation where the soil at the valley bottoms can become saturated and produce storm runoff before the soil in the upper parts of the basin is fully recharged.

Where base flow is in the middle or high range ($B > 0.2 \text{ m}^3/\text{sec}$) the model contains a first order function of B , second order functions of I and P_v and a third order function of S . When the equations 4.1 and 4.2 are considered together, it is shown that the parameters I , B and S all have a significant effect on the relationship between rainfall and runoff at Marmot Creek Basin.

Examination of the residual plots of figures 4.8a and 4.8b indicates that no other parameters are needed in a site specific model.

When the residual plots of figures 4.2c and 4.4 are compared, it is clear that the base flow separation method which was developed for the purpose of this analysis has greatly improved the fit of the model. The author has attempted, apparently successfully, to make this separation method as physically realistic as possible. It seems reasonable to assume that a similar pattern would apply to other mountainous basins with highly permeable surficial deposits. If the same principals were applied to other research basins in the same general area (say, the headwaters of the South Saskatchewan River Basin), a realistic base flow separation method could be found which would be generally applicable to that area. Furthermore, it can be postulated that if statistical modeling procedures were applied to other research basins in the East Slopes, the rainfall-runoff relations which emerged would likely be of a similar form. If this were true, it would be possible to develop a method of predicting model coefficients and the order of parameters based on physical characteristics of the basins. Thus, a generalized rainfall-runoff relation for the East Slopes would emerge. The model would necessarily be simpler than the one presented here with a resultant loss of accuracy for specific basins, but it could be used to predict the volume of storm runoff for ungauged basins. This would ultimately be a highly desirable goal.

The soil moisture index (S) which is used here represents a significant improvement over the API because it is adjusted to account for daily fluctuations of net radiation. However, it could be improved upon by incorporating actual daily values of the Bowen ratio. Unfortunately, measurements of temperature and relative humidity at two levels were not taken at Marmot Creek and consequently, Bowen ratios had to be estimated rather than calculated. The watershed simulators which were discussed in chapter 1 all contain methods of calculating evapotranspiration. For example, the SACRAMENTO model uses the Penman equation which requires the input of a large volume of atmospheric data (Lawson and Shiau, 1977). The regression equations (eq. 3.7 and 3.8) which are employed to estimate daily evapotranspiration are simple to use, require the input of only two parameters and are virtually as accurate as detailed

energy budget calculations. Their accuracy could be greatly improved by the incorporation of actual Bowen ratios. It would be of great value if in future, research basins and perhaps even meteorological stations of the regular national network were equipped to record such measurements.

A major part of all the watershed simulators described in chapter 1 is a rainfall-runoff relation to predict the volume of runoff (Lawson, 1974). The model which is presented here could form part of a watershed simulator if used in conjunction with a snowmelt simulator and a method of reconstructing hydrographs. It is a great deal simpler to use and understand than the methods employed in existing simulators. The advantage of this model is that it condenses the process of predicting stormflow to one step. It requires as input only the four basic parameters, once the threshold values of precipitation volume and intensity are specified. At this stage of development the model is obviously specific to Marmot Creek Basin and cannot be used elsewhere.

There are some drawbacks to the model. Because it is empirically derived, it might not be able to predict accurately the stormflow for an event which involves an 'unusual' combination of parameters, or one for which one or more parameters falls outside the range represented in the data set. Another disadvantage of the data set is that there are so few large volume events. It is natural that the largest events are also the rarest. These events are the most important statistically; they become influentials and therefore it is crucial to the integrity of the model that they be represented accurately. While the author is confident that this was accomplished, it was felt that more high volume events would have been helpful.

The model is quite accurate as discussed in chapter 4. Absolute errors are quite low and appear to be random. It is obvious that percentage errors will increase as runoff volume decreases. Conversely, the percent error decreases for larger events which are most crucial in terms of flood prediction and water resource management. While it is common practice to attribute a small random error to natural variability, there are some sources of error which can be identified:

1. Rain gauges all tend to undercatch, but the error in gauge catch increases with wind speed. There may also be errors in other instruments such as the net radiometer and the automatic stage recorder at the main wier.

2. In establishing a method for estimating daily rainfall it was assumed that the basin was meteorologically homogeneous. While this assumption is reasonable, there is bound to be some spatial variability in the distribution of rainfall intensity, which may lead to a small error in daily rainfall estimates.

3. It was stated in section 3.3 that there still remains some subjectivity in the base flow separation method. This subjectivity concerns the rate at which the base flow hydrograph rises in cases where that rate is assumed to change (eg., event # 26) or where the base flow hydrograph has more than one peak (eg., events #25, #2). To clarify this, it may be possible to determine the rate at which base flow rises as a function, perhaps, of rainfall intensity. This may lead to some error in estimating stormflow volumes.

4. Some errors in estimating soil moisture have been discussed earlier.

5. In section 3.1 it was mentioned that some of the events which occur in June or early July may involve a small but negligible quantity of snow melt. The variability of this snowmelt, although negligible in itself, may add to the error compounded from other sources.

5.2: Conclusions

An empirically derived model is presented which predicts the volume of runoff from rainfall at Marmot Creek Basin. In doing the research which led to the development of this model, the following points were discovered.

1. Base flow was found to rise rapidly in response to rainfall. This led to the development of a site specific base flow separation method which models the rising limb of the base flow hydrograph according to properties of the water table, permeability of the soil and basin morphology, and the falling limb according to a base flow recession curve.

2. A daily soil moisture index was developed using an adaptation of a site specific energy budget method to estimate evapotranspiration.

3. Antecedent base flow and soil moisture index and maximum 24-hour rainfall intensity were found to be significant factors governing the rainfall-runoff relation.

4. The best fit model was found to be a third order model in which the data set is subdivided into two groups on the basis of antecedent base flow.

References

- Atmospheric Environment (1978-1980), *Supplementary Precipitation Data*, Environment Canada, Ottawa
- Beke, G.J. (1969), *Soils of three experimental watersheds in Alberta and their hydrological significance*, unpubl. PhD thesis, U. of Alberta.
- Bernier, P.Y. (1982), *VSAS2: A revised source area simulator for small forested basins*, unpubl. PhD thesis, U. of Georgia.
- Betson, R.P. (1964), What is watershed runoff?, *J. Geophys. Res.*, 69(8), pp. 1541-1552.
- Betson, R.P. and J.B. Marius (1969), Source areas of storm runoff, *Water Res. Res.*, 5, pp.574-582.
- Betson, R.P., R.L. Tucker and F.M. Haller (1969), Using analytical methods to develop a surface-runoff model, *Water Res. Res.*, 5(1), pp. 103-111. .
- Bonell, M., D.A. Gilmour and D.F. Sinclair (1979), A statistical method for modelling the fate of rainfall in a tropical rainforest catchment, *J. Hydrol.*, 42, pp. 251-267.
- Bruce, J.P. and R.H. Clark (1966), *Introduction to Hydrometeorology*, Pergamon Press, London.
- Cheng, T. and W. Nemenishen, (1974), Runoff simulation models for research basins, *Proc. of Alberta Watershed Research Program Symp.*, ed. Logan, P. and R.H. Swanson.
- Chow, V.T. (1964), Runoff, *Handbook of Applied Hydrology*, McGraw-Hill Inc., New York.
- Cook, H.L. (1946), The infiltration approach to the calculation of surface runoff, *Trans. Am. Geophys. Union*, 27(5), pp. 726-747.
- Cote, M. (1984), *Climate of Kananaskis*, unpubl. report for Environment Canada, Atmospheric Environment Service, Edmonton.
- Crawford, N.H. and R.K. Linsley (1966), *Digital simulation in hydrology: Stanford watershed model IV*, Dep't of Civil Engineering, Stanford University, Technical Report #39.
- Davis, J. (1973), *Statistics and data analysis in geology*, John Wiley and Sons, New York.
- DeCoursey, D.G. (1971), The stochastic approach to watershed modeling, *Nordic Hydrol.*, 2, 186-216.
- Department of Forestry of Canada (1965), *Marmot Creek Watershed Research Basin; Forest cover type map*, Information and Technical Services Division, Graphics Section, Ottawa.
- Draper, N.R. and H. Smith (1981), *Applied regression analysis, second edition*, John Wiley and Sons, Toronto.
- Dunne, T. and R.D. Black (1970), Partial area contributions to storm runoff in a small New England watershed, *Water Res. Res.*, 6(5), pp.1296-1311.
- Engman, E.T. (1974), Partial area hydrology and its application to water resources, *Water Res. Bull.*, 10(3), pp. 512-521.
- Engman, E.T. (1981), Rainfall-runoff characteristics for a mountainous watershed in the northeastern U.S., *Nordic Hydrol.*, 12, pp. 247-264.

- Fischera, Z. (1977), Snow accumulation and melt patterns in tree-line stands of Marmot Creek Basin, *Proc. of Alberta Watershed Research Program Symp.*, ed. Logan, P. and R.H. Swanson
- Foth, H.P. and L.M. Turk (1972), *Fundamentals of Soil Science, fifth edition*, John Wiley and Sons, Toronto.
- Gerrard, A.J. (1981), *Soils and Landforms; an Integration of Geomorphology and Pedology*, George Allen and Unwin, London.
- Gupta, V.K., C.T. Wang and E. Waymire (1980), A representation of an instantaneous unit hydrograph from geomorphology, *Water Res. Res.*, 16(5) pp. 855-862.
- Hewlett, J.D. (1982), *Principles of Forest Hydrology*, U. of Georgia Press, Athens, Georgia.
- Hewlett, J.D. and J.m. Bosch (1984), The dependence of storm flows on rainfall intensity and vegetal cover in South Africa, *J. Hydrol.*, 75, pp. 365-381.
- Hewlett, J.D., G.B. Cunningham and C.A. Troendle (1977), Predicting stormflow from small basins by the R-index method, *Water Res. Bull.*, 13(2), pp. 231-253.
- Hewlett, J.D., J.C. Forston and G.B. Cunningham (1977), The effect of rainfall intensity on stormflow and peak discharge from forest land, *Water Res. Res.*, 13(2), pp. 259-266.
- Hewlett, J.D. and A.R. Hibbert (1967), Factors affecting the response of small watersheds to precipitation in humid areas, *Int. Symp. on Forest Hydrology*, Pergamon, Oxford.
- Holtan, N.H., J.P. Ormsby and G.T. Fisher (1977), Applications of a Maryland version of USDAHL-74 to a watershed in Prince George's County, Maryland, *Watershed Research in Eastern North America, Volume II*, ed. Correll, D.L., Smithsonian Institute, Edgewater, Md.
- Holtan, H.N., Stiltner, G.J., Henson, W.H. and Lopez, N.C. (1975), *USDAHL-74 revised model of watershed hydrology*, Technical Bulletin #1518, Ag. Res. Serv., USDA
- Horton, R.E. (1933), The role of infiltration in the hydrologic cycle, *Trans. Am. Geophys. Union*, 14, pp. 446-460.
- Horton, R.E. (1937), Determination of infiltration capacity for large drainage basins, *Trans. Am. Geophys. Union*, 18(2), pp. 371-385.
- Hursh, C.R. (1944), Report of the subcommittee on subsurface flow, *Trans. Am. Geophys. Union*, 25, pp. 743-746.
- Jones, J.A.A. (1971), Soil piping and stream channel initiation, *Water Res. Res.*, 7, pp. 602-610.
- Kirkby, M.J. and R.J. Chorley (1967), Throughflow, overland flow and erosion, *Bull. Int. Assoc. Sci. Hydrol.*, 12(3) pp. 5-21.
- Klemes, V. (1973), Watershed as semiinfinite storage reservoir, *J. of the Irrigation and Drainage Division, A.S.C.E.*, 99, pp. 477-491.
- Lawson, D.W. (1974), *Watershed Modelling and Water Planning and Management*, Environment Canada, Ottawa.
- Lawson D.W. and S.Y. Shiau (1977), *Data Requirements and Reference Documents for the Sacramento Watershed Modelling System*, Environment Canada, Ottawa.
- Lee, R. (1980), *Forest Hydrology*, Columbia U. Press, New York.

- Linsley, R.K. and W.C. Ackermann (1942), Method of predicting the runoff from rainfall, *Trans. A.S.C.E.*, 107, 825-846.
- Linsley, R.K. and J.B. Franzini (1979), *Water Resources Engineering*, McGraw- Hill, New York.
- Linsley, R.K., M.A. Kohler and J.L.H. Paulhus (1982), *Hydrology For Engineers, third edition*, McGraw-Hill, New York.
- Miller, J.F. and J.L.H. Paulhus (1957), Rainfall-runoff relation for small basins, *Trans. Am. Geophys. Union*, 38(2), pp. 216-218.
- Mosley, M.P. (1979), Streamflow generation in a forested watershed, New Zealand, *Water Res. Res.*, 15(4), 795-806.
- Penman, H.L. (1963), *Vegetation and Hydrology. Technical communication #53*, Commonwealth Bureau of Soils Harpenden, England.
- Pilgrim, D.H., D.D. Huff and T.D. Steele (1978), A field evaluation of subsurface and surface runoff, II, Runoff processes, *J. Hydrol.*, 38, pp. 319-342.
- Quick, M. and A. Pipes (1974), *University of British Columbia model mobilization trials*, Streamflow Forecasting: South Saskatchewan River Below Red Deer River (appendix E). PPWB Committee on Hydrology, Water Survey of Canada, Calgary.
- Ryan, B.F., B.L. Joiner and T.A. Ryan (1985), *Minitab Handbook, second edition*, Duxbury Press, Boston.
- Sangal, B.P. (1986), *Recursion Formula for Unit Hydrographs*, N.H.R.I. paper #29, Environment Canada, Ottawa.
- Sherman, L.K. (1942), The unit hydrograph method, *Hydrology*, ed. Meinzer, O.E. McGraw-Hill, New York. repr. 1949, Dover, New York.
- Sittner, W.T., C.E. Schauss and J.C. Monroe (1969), Continuous hydrograph synthesis with an API-type hydrological model, *Water Res. Res.*, 5(5), pp. 1007-1022.
- Sklash, M.G. and R.N. Farvolden (1979), The role of groundwater in storm runoff, *J. Hydrol.*, 43, pp. 45-65.
- Snyder, W.M. (1971), The parametric approach to watershed modeling, *Nordic Hydrol.*, 2, pp. 167-185.
- Stalker, A. MacS. (1973), *Surficial geology of the Kananaskis Research Forest and Marmot Creek Basin region of Alberta*, G.S.C. of Canada paper #72-51, Information Canada, Ottawa.
- Stevenson, D.R. (1967), *Geological and Groundwater Investigations in Marmot Creek Experimental Basin in S.W. Alberta, Canada*, unpubl MSc thesis, U. of Alberta.
- Storr, D. (1974a), *Monthly and Annual Estimates of Evapotranspiration at Marmot Creek Basin by the Energy Budget Method*, Atmospheric Environment Service, Ottawa.
- Storr, D. (1974b), *Relating Subsurface Water Storage to Streamflow in a Mountainous Watershed*, Environment Canada, Ottawa.
- Storr, D. (1977), Some preliminary water balances of Marmot Creek sub-basins, *Proc. of Alberta Watershed Research Program Symp.*, ed. Logan, P. and R.H. Swanson.

Sugawara, M., I. Watanabe, E. Ozaki and Y. Katsuyama (1984), *Tank Model with Snow Component*, National Research Center for Disaster Prevention, #69, Japan.

Thiessen, A.H. (1911), Precipitation for large areas, *Mon. Weather Review*, 39.

Traynor, B.G. (1981), *The Impact of Surface and Subsurface Water on Streamflow and Water Quality in an Actively Mined Watershed*, unpubl. MSc thesis, U. of Calgary.

U.S. Army Engineer Division (1972), *Program Description and User Manual for SSARR: Streamflow Synthesis and Reservoir Regulation*. U.S. Army, Portland Oregon.

Water Survey of Canada, (1962-1980), *Compilation of Hydrometeorological Record, Marmot Creek Basin*, Environment Canada, Calgary.

Weyman, D.R. (1973), Measurements of the downslope movement of water in a soil, *J. Hydrol.*, 20, pp.267-288.

Whipkey, R.Z. (1965), Subsurface stormflow from forested slopes, *Bull. Int. Ass. Sci. Hydrol.*, 10(2), pp. 74-85.

Woolhiser, D.A. (1971), Deterministic approach to watershed modeling, *Nordic Hydrol.*, 2, 146-166.